

https://dspace.org/

Chemical modification of sago beads for suitable application in drug delivery

Masina, Nonhlanhla Precious

2016
http://hdl.handle.net/10539/23113

Downloaded from a DSpace repository. https://dspace.org/

CHEMICAL MODIFICATION OF SAGO BEADS FOR SUITABLE APPLICATION IN DRUG DELIVERY

NONHLANHLA PRECIOUS MASINA



A dissertation submitted to the Faculty of Health Sciences, University of the Witwatersrand, in fulfilment of the requirements a Master of Science in medicine

Supervisors:

Professor Viness Pillay, Department of Pharmacy and Pharmacology, University of the Witwatersrand, South Africa

Co- Supervisors

Associate Professor Yahya Essop Choonara, Department of Pharmacy and Pharmacology, University of the Witwatersrand, South Africa

Associate Professor Lisa Claire du Toit, Department of Pharmacy and Pharmacology, University of the Witwatersrand, South Africa

Johannesburg, 2016

DECLARATION

I, Nonhlanhla Precious Masina declare that this dissertation is my own work and has been submitted for the degree of Master of Science in the field of Pharmaceutics at the Faculty of Health Sciences, University of the Witwatersrand (Johannesburg, South Africa). It has not been submitted before for any degree or examination at this or any other University.

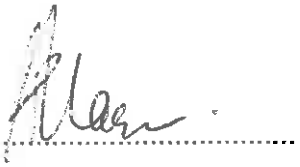

Signature

26/04/2016.

Date

RESEARCH OUTPUTS

A review titled: "*Post-fabrication chemical modification of pre-formed starch-based drug delivery systems*" was prepared for submission and review for the Journal: *Carbohydrate Polymers*

A research paper titled: "*Periodate oxidation of food-grade-pre-formed Sago beads for application in Drug Delivery*" was prepared for submission and review for the Journal: *Carbohydrate Polymers*

Podium presentation at University of the Witwatersrand cross faculty Post Graduate March 2016: The role of post-graduate research in education.

ABSTRACT

Starch is a naturally occurring storage copolymer composed of amylose and amylopectin with unique physicochemical properties that render it an ideal polymer for applications within drug delivery. There are however some key structural properties of starch that can be improved upon to functionalize starch (a natural copolymer) to meet specific requirements in drug delivery system design and applications. Starch chemical modification methods provide a variety of physicochemical benefits, some of which can be used to functionalize pre-formed drug delivery systems further optimizing their application. Of the three main chemical modification methods reviewed, namely: oxidation, esterification and etherification. Surface oxidation evidently is the preferable chemical modification method of pre-formed starch particulates with the greatest potential for further development and application. Surface chemical oxidation of starch introduces physicochemical properties that allow functionalization of pre-formulated delivery systems and in turn increases overall efficacy of drug delivery systems.

This study involved the development and optimization of a surface oxidation method for food-grade Sago starch beads utilizing sodium-meta-periodate ($NaIO_4$). The $NaIO_4$ as an oxidizing agent undergoes a periodate nucleophilic reaction mechanism which was optimized for the development of the S_{ago}-millisphere in this research. One of the key areas of focus in the study was the utilization of naturally occurring and over-the-counter food grade excipients for the sustained release of propranolol. Propranolol has a Narrow Absorption Window (NAW) and requires more frequent doses to exert a therapeutic effect. There is an ongoing decline in patient compliance for oral formulations for propranolol due to the correlation between frequent doses and dosage related side-effects. The S_{ago}-millisphere did not only address the NAW of propranolol formulations currently on the market but yielded a food grade carrier for performance optimization over a twenty-four-hour period.

The produced S_{ago}-millispheres were characterized using a chemical measure of the degree of substitution (DS) for confirmation of $NaIO_4$ surface oxidation. Ammoniacal silver nitrate test was used to confirm specific aldehyde introduction and tested positive on the traditional Tollen's test. The flow properties observed through rheology were indicative of a reduced viscosity and Newtonian flow properties. Fourier Transform Infrared Spectroscopy (FTIR) and Scanning Electron Microscopy (SEM) further confirmed altered physicochemical properties. X-ray diffraction (XRD) profiles also confirmed surface modification with more crystalline physicochemical attributes observed in oxidized derivatives. Crystalline profiles S_{ago}-millisphere with physicochemical techniques confirmed the introduction of di-aldehyde groups via the nucleophilic attack. The S_{ago}-millisphere has shown a sustained release over a twenty-four-hour period, performance superior that the current commercial product in the Large White pig model.

ACKNOWLEDGMENTS

I am thankful and appreciative to everyone who supported and assisted me in completing my research.

To my loving family mom, Themba and Siyabonga who have been patient, supportive and understanding throughout my studies. Ngiyabonga.

To Jay Kloppenberg who has been my cornerstone. Thank you

To the board of trustees and team at African School for Excellence, thank you for all your support and patience during my research.

To the WADDP fellow students: To my fellow students Zamanzima Mazibuka, Khadija Rhoda, Khuphukile Madida Kealega Mokoloba, Mpho Ngoepe, Felix Mashingaidze, Fatima Mia, Derusha Frank and Latavia Sigh. Thank you for your unwavering support during my studies. Research comes with a lot of challenges; your presence and willingness to troubleshoot, problem-solve with me was much appreciated.

To Mr. Pradeep Kumar, having you as a professional mentor has assisted me a great deal in developing my reasoning and research skill. Thank you for always challenging my thinking, providing a safe space for me to problem solve and teaching me what a healthy mentorship looks like.

To my supervisors: Prof Viness Pillay, Prof. Yahya E. Choonara and Prof. Lisa C. du Toit, thank you for your mentorship and patients throughout my research. I have learnt lessons that will continue to shape my career and have grown immensely as an individual. Thank you for resolute mentorship and provision of such an amazing learning environment and experience.

To the National Research Foundation (NRF) of South Africa, the University of the Witwatersrand Financial Aid Office and the Department of Education (DOE) for the funding that enabled this research to be completed.

DEDICATION

In memory of my loving and supportive father, Bhekizizwe Henry Masina, for he continues to inspire me. His efforts and dedication live on through me.

TABLE OF CONTENTS

DECLARATION i
RESEARCH OUTPUTS ii
ABSTRACT iii
ACKNOWLEDGMENTS iv
DEDICATION v
ANIMAL ETHICS xi
LIST OF FIGURES xii
LIST OF TABLES xvi
LIST OF ABBREVIATIONS xvii
List of equations xviii
Chapter 1 1
INTRODUCTION 1
1.1. Aim and Objectives 3
Overview of Dissertation 4
CHAPTER 2 5
LITERATURE REVIEW: CURRENT METHODS FOR STARCH OXIDATION AND APPLICABILITY IN DRUG DELIVERY 5
2.1. Introduction 5
2.2. Chemical modification of starch 6
2.3. Starch oxidation 8
2.3.1 Physicochemical properties of oxidized starch derivatives 9
2.3.2 Application of oxidative methods in pre-formed starch based drug delivery systems 12
2.4. Starch Esterification 13
2.4.1 Physicochemical properties of Esterification derivatives 14
2.4.2 Esterification in drug delivery 14
2.4.3 Esterification of pre-formed drug delivery systems 15
2.5. Aryl Esterification 16
2.6. Etherification methodology and resultant properties 17
2.7. Carboxymethylation 17
2.7.1 Physiochemical properties of carboxymethyl starch 17
2.7.2 Carboxymethylation in drug delivery and applicability to pre-formed systems 18
2.7.3 Hydroxypropylation methods and reaction conditions 19

2.7.4 Physicochemical properties of hydroxypropyl starch 19
2.7.5 Hydroxypropylation in delivery systems 19
2.7.6 Hydroxypropylation applicability to pre-formed drug delivery systems 20
2.8. Hydroxyethylation 20
2.8.1 Hydroxyethylation in drug delivery 20
2.8.2 Hydroxyethylation applicability to pre-formed drug delivery systems 20
2.9. Current advances in drug delivery using starch-based delivery systems 21
2.10. Clinical potential of modified starch 22
2.11. Conclusion 23
CHAPTER 3 25
DEVELOPMENT OF PERIODATE OXIDATION METHOD FOR APPLICATIONS IN THE MODIFICATIONS OF FOOD-GRADE-PRE-FORMED SAGO BEADS IN THE PRODUCTION OF DDS 25
3.1. Introduction 25
3.2. Materials and methods 26
3.2.1 Oxidation methodology: introduction of surface aldehyde groups 26
3.2.2 Ammoniacal silver nitrate (Tollens' reagent test for aldehyde groups) 26
3.2.3 Determination of Degree of carboxyl Substitution (DS) 26
3.2.4 Chitosan crosslinking: Linkage of free reducing aldehyde ends 27
3.2.5 Elucidation of chitosan crosslinking percentage of reducing carboxyl ends 28
3.2.6 Physicochemical characterization of vibrational transitions via Fourier Transform Infrared spectroscopic analysis 28
3.2.7 Viscosity and flow property elucidation for confirmation of altered physiochemical structure 29
3.2.8 Physicochemical characterization of crystallinity via X-ray diffraction 29
3.2.9 Physicochemical characterization of surface morphology via Scanning Electron Microscopy 29
3.2.10 Analysis of thermal properties via Differential Scanning Calorimetry 29
3.3. Results and Discussion 30
3.3.1 Physicochemical characterisation of vibrational transitions via Fourier Transform analysis 32
3.3.2 33

3.3.3 Flow property analysis for confirmation of aldehyde alteration of hydraulic nature. 33
3.3.4 Physicochemical characterization of crystallinity via X-ray diffraction..... 34
3.3.5 Crosslinking percentage analysis of reducing end linkage with chitosan..... 35
3.3.6 Scanning Electron Microscopic evaluation of the Sago beads and the oxidized derivatives 36
3.3.7..... 38
3.3.8..... 38
3.3.9..... 38
3.3.10 Thermal stability and crystallinity evaluation of physicomechanical properties38
3.4. Concluding Remarks 38
CHAPTER 4 40
FACE-CENTERED CENTRAL COMPOSITE DESIGN FOR S_{ago}-millisphere SYSTEM 40
4.1. Introduction..... 40
4.2. Materials..... 41
4.3. Methods 41
4.3.1 Surface oxidation of Sago via optimized method 42
4.3.2 Drug loading of model drug into optimized S_{ago}-millisphere system 42
4.3.3 Quantification of oxidized degree of substitution for oxidized Sago derivatives 42
4.3.4 Aryl chitosan crosslinking by glutaraldehyde..... 43
4.3.5 Thermal gravimetric analysis of the optimized bead system 43
4.3.6 Physicochemical characterization of vibrational transitions via Fourier Transform analysis..... 43
4.3.7 Rheology: viscosity and flow property elucidation..... 43
4.3.8 Physicochemical characterisation of crystallinity X-ray diffraction for optimized derivatives 44
4.3.9 Quantification of chitosan crosslinking percentage of optimized Sago derivatives 44
4.3.10 Maltose standard curve for quantification of amylase sensitivity 44
4.3.11 Optimized formulation amylase sensitivity analysis..... 45
4.3.12 In vitro drug release profiling: standard curve 45

4.3.13 In vitro drug Release Profiling: Dissolution 45
4.4. Results and Discussion 45
4.4.1 Standard curve 45
4.4.2 In vitro drug release characterization of S_{ago}-millisphere Designs 47
4.4.3 Optimized formulation characterization 54
4.5. Concluding Remarks 59
CHAPTER 5 60
IN VIVO PERFORMANCE ANALYSIS AND EVALUATION 60
5.1. Introduction 60
5.2. Materials 61
5.3. Methods 62
5.3.1 Catheter implantation 62
5.3.2 Maintenance of catheter implant 62
5.3.3 Sampling: Aspiration of blood samples via an intra-jugular catheter 63
5.3.4 Sago drug delivery system sample preparation utilizing optimized modification method 63
5.3.5 Dosage administration frequency and sampling methodology 63
5.3.6 Placebo dosage: placebo and safety confirmation 63
5.3.7 Experimental and conventional dosage 63
5.3.8 Plasma sample and standard solution preparation 64
5.3.9 Ultra-performance Liquid Chromatographic analysis for plasma samples 65
5.4. Results and Discussion 65
5.4.1 Surgery: catheter implant to left jugular vein 65
5.4.2 Optimized formulation dosage preparations and characterisation 67
5.4.3 Evaluation of dosage effects, formulation safety and physiological effects 68
5.4.4 Dosage methodology evaluation 68
5.4.5 In vivo performance: Ultra Performance Liquid Chromatographic (UPLC) detection method evaluation 68
5.5. Concluding remarks 72
Chapter 6 73
Conclusion 73
RECOMMENDATIONS 74

REFERENCES 74
Appendix 1 85
Appendix 2 86
Appendix 3 87

ANIMAL ETHICS

I, Nonhlanhla Precious Masina hereby confirm that the study entitled "*In vivo* evaluation of food-grade sago based oral delivery system in large white pigs" received approval from the Animal Ethics Screening Committee (AESC) of the University of Witwatersrand with Ethics Clearance Number: 2013/41/05 (Appendix 1).

LIST OF FIGURES

Figure 2.1*:* Starch copolymer chain with amylase and amylopectin component

Figure 2.2: Schematic summarizing classical chemical methods for starch modification.

Figure 2.3: Starch modification **a**: through the conversion of hydroxyl groups to aldehyde groups and b: Starch oxidation mechanism that yields starch radical (StO) (Pashkuleva *et al.*, 2005).

Figure 2.4: Thrombolytic behaviors of anionic starch nanosphere (A: 24 h; B: 60 h. ■: NP-loaded NK; ●: free NK; ▾: OS-loaded NK; ▲: saline) (Huang *et al.,* 2013).

Figure 2.5: The release of drugs from starch-acetate DS 1.9 films in (a) PBS pH 7.4 without; and (b) with α-amylase (20U/mg of polymer) (mean±S.E.M., *n* =3) (Tuovinen *et.al.*, 2003).

Figure 3.1: Schematic summary of surface oxidation method devised for pre-formed food-grade commercial Sago beads.

Figure 3.2: Tollens' test results for **(a)** negative control Sago beads **(b)** oxidized derivatives and **(c)** positive control; octadecanal.

Figure 3.3: ATR-FTIR spectra of different the three oxidized derivatives. With red spectra for unmodified Sago, Pink spectrum for 30-minute oxidation, Green 60-minute oxidation and orange spectrum for 90-minute oxidation. All ATR-FTIR profiles were obtained from 100 scans at a range of 4000-600cm-1 at a constant pressure of 130psi.

Figure 3.4: Illustrating fingerprint FTIR region for aldehyde groups with the use of octadecanal (darker blue spectra) as a standard. The three oxidation times 30 minutes (red), 60 minutes (lighter blue) and 90 minutes (pink). All ATR-FTIR profiles were obtained from 100 scans at a range of 4000-600cm^{-1} at a constant pressure of 130psi.

Figure 3.5: Rheology profiles of oxidized Sago in comparison to unmodified OTC Sago beads. Unmodified Sago (yellow), 60-minute oxidation (black) and a comparison of oxidized (black) and unmodified Sago (purple).

Figure 3.6: Powdered X-ray Diffraction profiles of Sago and respective derivatives.

Figure 3.7: Scanning electron micrographs were collected for unmodified modified Sago bead derivatives.

Figure 3.8: Dynamic Scanning Calorimetry (DSC) of oxidized Sago derivatives. Heating rate set at 10°C/min between the temperature range of 25°C and 300°C. Each DSC thermogram represents: 30-minute oxidation (black line), 60-minute oxidation (blue line) and 90-minute oxidation (red line).

Figure 4.1: UV-VIS scan from λ 200-600 nm to aid in identifying specific absorption unit peaks for propranolol solution at room temperature. The detection peak was confirmed at 290 nm.

Figure 4.2: Standard curve generated using UV-VIS absorbance units for specified concentrations (mg) at λ 290nm. With Rsq = 0.977164 and equation: y=0.0246+0.26255.

Figure 4.3: Release profiles for design formulation 4; with 90-minute oxidation period and crosslinked with a 0.1% w/v chitosan solution at room temperature. Profile generated utilizing fractionalized released quantifiable by measuring absorption units at λ 290 nm over a 24-hour period. Data processed utilizing DDsolver on Microsoft excel (2010)

Figure 4.4: Release profiles for design formulation 7: with 60-minute oxidation period and crosslinked with a 0.1%$^{w}/_{v}$ chitosan solution at room temperature.

Figure 4.5: Release profiles for design formulation 9; with 30-minute oxidation period and crosslinked with a 0.1% w/v chitosan solution at room temperature. Profile generated utilizing fractionalized released quantifiable by measuring absorption units at λ 290 nm over a 24-hour period. Data processed utilizing DDsolver on Microsoft excel (2010).

Figure 4.6: Release profiles for design formulation 10; with 90-minute oxidation period and crosslinked with a 1.05%$^{w}/_{v}$ chitosan solution at room temperature. Profile generated utilizing fractionalized released quantifiable by measuring absorption units at λ 290 nm over a 24-hour period. Data processed utilizing DDsolver on Microsoft excel (2010).

Figure 4.7: Release profile for design formulation 5 and 6 (average); with 60-minute oxidation period and crosslinked with a 1.05%$^{w}/_{v}$ chitosan solution at room temperature.

Figure 4.8: Release profiles for design formulation 13; with 30-minute oxidation period and crosslinked with a 1.05%$^{w}/_{v}$ chitosan solution at room temperature.

Figure 4.9: Release profiles for design formulation 3; with 90-minute oxidation period and crosslinked with a 2.00%$^{w}/_{v}$ chitosan solution at room temperature.

Figure 4.10: Release profiles for design formulation 1; with 60-minute oxidation period and crosslinked with a 2.00%$^{w}/_{v}$ chitosan solution at room temperature.

Figure 4.11: Release profiles for design formulation 2; with 30-minute oxidation period and crosslinked with a 2.00%$^{w}/_{v}$ chitosan solution at room temperature.

Figure 4.12: Optimised FCCD statistical prediction for the optimised formulation.

Figure 4.13: Release profiles for optimised design formulation generated utilizing fractionalized released quantifiable by measuring absorption units at λ 290 nm over a 24-hour period.

Figure 4.14: Thermogravitational Analysis (TGA) profiles for unmodified Sago (A) and optimised formulation (B). Profiles generated under inert nitrogen conditions 25-700 ^{0}C at heating rate of 10 ^{0} minute $^{-1}$.

Figure 4.15: ATR-FTIR spectra of different the optimised oxidized derivatives (A) and unmodified bead. All ATR-FTIR profiles were obtained from 100 scans at a range of 4000-600cm^{-1} at a constant pressure of 130psi

Figure 4.16: Rheology profiles of optimised formulation in comparison to unmodified OTC Sago beads.

Figure 4.17: Powdered X-Ray Diffraction profiles of optimized formulation and unmodified formulations.

Figure 4.18: Maltose standard curve generated using UV-VIS spectroscopy at λ 540nm.

Figure 5.1: Schematic flow summarizing the sequence of the animal study.

Figure 5.2: Sample preparation for S_{ago}-millisphere system prepared utilizing optimized method parameters with 73.0199 minutes oxidation and 1.5428%$^{w}/_{v}$ chitosan crosslinking in an aryl system with 3:1 glutaraldehyde: hydrochloric acid for every 3g of beads

Figure 5.3: Catheter implantation procedure characterized. (a): Left jugular vein to which a (b): synthetic catheter is joined and looped back to yield two ports as highlighted on and (c) to allow for non-invasive sampling during study period.

Figure 5.4: UPLC derived method parameters: The retention time was found to be 0.832 minutes

Figure 5.5: UPLC calibration curve indicating peak-time curve of plasma standards for C_p: Propranolol concentration detected via UPLC at λ 290nm for samples prepared from placebo plasma samples.

Figure 5.7: AUC and AUMC curves for experimental collated plasma data with final MRT averaged at and 29.71 hours.

Figure 5.8: AUC (a) and AUMC (b) curves for conventional collated plasma data with final MRT averaged at 2.85 hours.

LIST OF TABLES

Table 2.1: Summary of surface chemical modification systems modified via carboxymethylation of granular starch

Table 2: Surface modification applicable to pre-formed drug delivery systems

Table 3.1: Spectroscopic quantification of crosslinking percentage of modified Sago beads

Table 4.1: Design study summary for all 13 face-cantered generated formulation.

Table 4.2: Spectroscopic quantification of chitosan crosslinking efficiency of modified Sago beads

Table 4.3: Estimation of % α -amylase sensitivity of starch

Table 5.1: Data summary for initial observation in intra-jugular catheter implant surgery showing weights pre-surgery and approximate recovery time post-surgery for six subjects involved in the trial.

Table 5.2: Weight tracker for all dosing procedures performed during the animal trial

LIST OF ABBREVIATIONS

AUC Area Under Curve

AUMC Area Under Moment Curve

ATR Attenuated Total Reflectance

ATR-FTIR Attenuated Total Reflectance-Fourier Transform Infrared

CAMs Cell Adhesion Protein Molecules

Cmax Maximum plasma concentration

DS Degree of Substitution

DSC Differential Scanning Calorimetry

DTG Differential Thermal Analysis

MDT Mean Dissolution Time

MTT Maximum Transit Time

NAW Narrow Absorption Window

Nattokinase NK

Potassium Permanganate $KMnO_4$

PXRD Powder X-ray Diffraction

SEM Scanning Electron Microscopy

TGA Thermogravimetric Analysis

Equation 3.1

$$n_{COOH} = 4(V_b - V)C_{HCL}$$

Where:

V_b: is the volume of acid consumed during the titration of the blank.

V: the volume of titration of the sample,

C_{HCl}: the concentration of the acid and 4, the ratio of the total solution volume over the volume sampled for titration (Zhang *et al.*, 2012).

Equation 3.2

$$DS = \frac{162 \times n_{COOH}}{m_{dry} - 58 \times n_{COOH}}$$

In which 162 g/mol is the molecular weight of a gram unit and 58 g/mol is the increase in molecular weight accounted for each carboxymethyl group substitution and m_{dry} is the mass of the dry sample.

Equation 4.1

$A = \varepsilon l\,[C]$

Where:

A: Absorbance

ε: Absorptivity

l: Path length

c: Concentration

Parameters for characterizing drug release curve:

AUC: Area Under the dissolution Curve

MRT: Mean Residence Time of the drug substance molecules in the dosage form

MDT: Mean Dissolution Time

DE: Dissolution Efficiency

AUMC: is the Area Under the Moment Curve,

Equations used to elucidate parameters:

The AUC and AUMC were determined during all studies for this research assumed the non-compartmental analysis to determine the mean residence time (MRT) within the trapezoid rule. Utilizing the following equations;

Equation 4.2

$$AUC_{t_0}^{t_\infty} = \frac{Cp_{last}}{\lambda}$$

Equation 4.3

$$AUMC_{t_0}^{t_\infty} = \left(\frac{t_{last} \times Cp_{last}}{\lambda}\right) + \frac{Cp_{last}}{\lambda^2}$$

Equation 4.4

$$AUC_b^a = \int_a^b C(t)dt$$

Equation 4.5

$$AUMC_b^a = \int_a^b C(t)tdt$$

Equation 4.6

$$MRT = \frac{AUMC}{AUC}$$

Where *MRT* is the mean residence time, *AUMC* is the area under the moment curve; *AUC* is the area under the curve and of λ (elimination rate constan

CHAPTER 1
INTRODUCTION

Starch is one of the most abundant and inexpensive naturally occurring polymers. It consists of two components, a linear α-amylose component with α 1-4 glycosidic links and a branched amylopectin component with additional α1-6 glycosidic links between the D-glucopyranosyl units. The polymer can be obtained from a variety of plant sources with varied amylose and amylopectin proportion. This difference with genetic origin has implications on microstructure details of the starch. However, most commercially available starches have average percentage composition of 80-90:10-20 amylose and amylopectin respectively. Due to the biodegradable and biocompatible nature of starch, it has been explored widely as a polymer for controlled drug delivery for various orally administered formulations, which is the most accepted administration route.

Pharmaceutical use of starch and/or other polymers in drug delivery is employed in the matrix system. The drug dispersed in a porous matrix network that is either swellable or non-swellable and the active is released in response to stimuli such as pH, charge or an enzymatic reaction (Huang and Brazel, 2001). The primary objective of such systems is the provision of controlled drug release mechanisms that reduce oscillations of drug concentrations in plasma. This aids in controlled drug concentrations in the circulatory system keeping it within the optimal range required for therapeutic action (Huang and Brazel, 2001). This both maximizes the efficacy of the drug and reduces dosage related side-effects as it negates frequent doses. A few orally administered formulations have a Narrow Absorption Window (NAW) and thus the objective for most matrix network formulations is to prolong the presence of the delivery system in the gastrointestinal tract (Huang and Brazel, 2001).

To maximize application of starch in drug delivery and other industries the physiochemical and physicomechanical properties can be modified. There are four basic types of starch modifications namely: 1. chemical, 2. physical, 3. enzymatical and 4. genetical (Kaur *et al.*, 2011). Chemical modification of starch involves esterification, etherification or oxidation of the available hydroxyl groups, the extent of which varies based on the genetic origin of the starch (Das *et al.*, 2010) and nature of the reaction. Depending on the nature of the chemical reagent used in starch modification, it can be classified as a monofuctional or difunctional reagent. Monofunctional reagents provide an anionic, cationic, hydrophobic or covalently reactive substituent group (BeMiller, 2007). Such modifications alter the gelatinization and pasting properties of starch. This results in a more stabilized form of starch within which associations

between the amylose and amylopectin are blocked. Common examples of monofuctional modifications include hydroxypolpropalation and acetylation. Difunctional reagents can allow for crosslinking of polymers since they can react with more than one hydroxyl group and can reinforce starch granules (Be Miller, 2007). The most common crosslinking agents include trimetaphosphates, phosphoryl chloride and adipic-acetic amongst others. Such reagents also stabilize starch by reducing the swellability solubility and mobility (Be Miller, 2007).

Chemical surface modification methods aid in starch functionalization making applicable to systems that it otherwise would not. An example of such modifications the utilization of an oxidizing system in which potassium permanganate is used to either introduce di-ketones or form starch radicals (Gao *et al.*, 1998 and Pashkuleva *et al.*, 2005). This modification can yield an increased drug encapsulation potential for nanoparticles (Thielamans *et al.*, 2006). The formation of radicals suggests crosslinking functionality which shows great prospects for oral formulations targeted for controlled drug release. The self-crosslinking potential has also been shown and produced from oxidative methods that used potassium permanganate ($KMnO_4$) (Pashkuleva *et al.*, 2005). In addition, the introduction of the di-ketones, the $KMnO_4$ introduces the possibility of hydrogen bond formation possibly within the polymer and polar drugs. This could contribute to enhanced retention of the imbibed drug within the GIT.

One of the main limitations for chemical surface modifications is the requirement for homogeneous mixture for the reaction to occur. This is not always possible when working with intact particles or granules. To overcome this, some modification methods utilize regioselective enzyme-catalysed reactions, this was attempted in this study. In such modifications, the enzyme is incorporated in a reverse micelle using an anionic surfactant aerosol-OT (AOT). The AOT forms a thermodynamic water droplet surrounded by a surfactant monolayer in oil. The enzyme is thus able to collide with substrate in a non-polar environment and display optimum activity (Chakraborty *et al.*, 2005). Depending on the type of enzyme used, various modifications are possible and for this study, enzymes such as lipase were considered. The primary focus of the study was the chemical modification of the surface of Sago beads to render them more suitable for pharmaceutical application whilst preserving the structural integrity of the beads.

Metroxylon species (Sago starch) is isolated from sago palm. There are different species widely utilized in Sago starch production includes M. longispinum, M. sylvestre, M. microcanthum, M. sagu and M. rumphii. Sago palm is an important resource; it has various uses especially in the production of starch either as Sago flour or Sago pearl. The commercially available Sago pearl was utilized for this study. Furthermore, surface

modification of the beads can yield delivery systems suitable for the delivery of NAW drugs (such as propranolol). This is due to high self-crosslinking potential that may yield systems with increased GIT retention potential of the buoyant systems due to the multi-matrix system that have altered chemical composition and can deter amylase and other enzyme activity.

For this study, surface chemical modification of commercially available Sago beads via a periodate oxidative method was explored and optimized to produce the S_{ago}-millispheres. The developed periodate method produced a delivery system that proved suitable for controlled release over a 24-hour period for model drug propranolol in Large White pigs. The S_{ago}-millisphere also showed prolonged drug delivery by increasing GIT retention potential of the buoyant system due to quantified oxidation alterations and chitosan crosslinkage.

The novelty of this delivery system is based on a single-excipient formulation proven to have extended GIT retention and can reduce the chances of dosage related side-effect associated with excipients in most NAW formulations. Furthermore, the use of limited chemical grade reagents during production render the S_{ago}-millisphere more cost effective. This combined with the fact that Sago can compete economically on yield and price compared to other crops for example the estimated yield for Sago starch is 2000–3000 kg/HaYr compared to cassava 2000 kg/HaYr and maize 1000 kg/HaYr (Stantan, 1992).

1.1. Aim and Objectives

The aim of this study was to chemical modify of the surface Sago beads to enhance drug retention thus render the S_{ago}-millisphere more suitable for application drug delivery. This aim was achieved through the following objectives:

1. Evaluation of the physiochemical and physicomechanical properties of the commercially available Sago beads.
2. Development of a novel oxidative method that can be applicable to pre-formed starch particles targeted for drug delivery.
3. Optimization of S_{ago}-millisphere for the sustained release of the NAW drug propranolol.
4. Physiochemical and physicomechanical characterization of modified S_{ago}-millisphere to gauge stability and superiority of S_{ago}-millisphere in relation to commercial equivalent.
5. Performance evaluation and optimization of *in vitro* drug release studies to determine the system performance of S_{ago}-millisphere and to inform further modification required to the system before *in vivo* analyses.

6. S_{ago}-millisphere *in vivo* performance evaluation and comparison with *in vitro* performance in a Large White pig model.

OVERVIEW OF DISSERTATION

Chapter 1 briefly introduces starch. The challenges associated with starch functionalized platforms are also explored briefly for their relevance in the development of drug delivery system design. The aims and objectives of the study are outlined as well as the implications and outcomes of surface oxidation are summarized.

Chapter 2 is an in-depth literature review and extension of chapter 1. It provides comprehensive analysis of currently explored and understood oxidation methods with a focus on the resultant functionality imparted on starch-based derivatives. The chapter also explores the applicability of the different modification methods to pre-formed starch particles.

Chapter 3 describes in detail the development of an oxidative method that is applicable to pre-formed starch particles utilizing commercially available Sago food-grade beads. The produced S_{ago}-millispheres were further evaluated for any alteration or improvement in the physicochemical properties to aid in the quantification of the functionalization due to surface modification. Synchronously, the physicochemical and physicomechanical nature of the food grade Sago bead characterization are detailed in this chapter.

Chapter 4 details the optimization of the oxidation method and a Face Centered Central Composite Design (FCCCD) design for the development of S_{ago}-millisphere. The FCCD studies also detail the physicomechanical characterization and dissolution studies utilized when generating an optimized formulation for S_{ago}-millisphere delivery system for propranolol.

Chapter 5 details the *in vitro* analysis for the optimized S_{ago}-millisphere in the Large White pig model.

Chapter 6 details the recommendations and conclusion for the study with further description of a potential scientific direction for extension.

CHAPTER 2
LITERATURE REVIEW: CURRENT METHODS FOR STARCH OXIDATION AND APPLICABILITY IN DRUG DELIVERY

2.1. INTRODUCTION

Traditionally, in oral delivery systems, excipients have been viewed as inert substances that function, amongst others, as binders, disintegrants, adhesives and sweeteners. However, in the past decade there has been a greater focus on the effects of excipients and the potential reduction of synthetic and chemical-grade agents within pharmaceutical formulation to increase patient compliance, and in some cases, the biocompatibility and efficiency of formulations (Singh, Kaur, and McCarthy, 2007; Averous, 2013). Studies have shown that excipients can in fact influence the rate and extent of drug release, in turn affecting the efficiency of the system and the absorption of the active. There is thus a great trend toward the use of natural excipients that are sometimes referred to as "herbal excipients" (Ražem and Katušin-Ražem, 2008).

The view that excipients are inert and have no effect on formulation performance has therefore changed and it is now recognized that they have a significant influence on the efficacy of the delivery system. Furthermore, there is a continued focus on natural versus synthetic excipients in formulation design. A large proportion of the excipients used are natural polymers because of their biocompatible nature, inexpensiveness and accessibility. This class of polymers is generally highly stable, hydrophilic and gel forming (Beneke, Viljoen, and Hamman, 2009). Within this class of polymers, starch is the most abundant storage polymer, found in a variety of plant organs and is widely explored in the pharmaceutical and other industries. This co-polymer consists of two macromolecular complexes: amylose and amylopectin, the proportions of which vary with botanical origin (Dimantov, Greenberg, Kesselman, and Shimoni, 2004). Amylose, a linear polysaccharide of glucose units linked through α-1-4 glycosidic bonds, on average accounts for 20-30 % of starch composition (Dimantov *et al.*, 2004). Amylopectin, the more branched macromolecular component, has additional α-1-6 links and accounts for 70-80 % of starch composition (Tharanathan, 2005).

The pharmaceutical application of starch and other polymers in drug delivery is mostly applicable in the matrix-assisted system approach. In this approach, a drug is dispersed in a porous matrix network that is either swellable and/or non-swellable and is released in response to stimuli such as pH, charge or enzymatic reaction (Huang and Brazel, 2001). The primary objective of such systems are the provision of controlled drug release mechanisms

that reduce oscillations of drug concentrations in the blood, thus maintaining drug plasma concentrations within an optimal range required for therapeutic action (Huang and Brazel, 2001; Nabais *et al.*, 2007). This both maximizes the efficacy of the drug and reduces dosage related side effects in some formulations (Pal, Singhal, and Kulkarni, 2002).

In order to maximize the application of starch in drug delivery and other industries, the physiochemical and physicomechanical properties can be tailored to fit the required properties of the produced system. There are four basic types of starch modifications, namely; chemical, physical, enzymatic and genetic, all of which target the three available hydroxyl groups of the starch co-polymer (Figure 2.1). Chemical modification is the most widely explored modification method due to the non-destructive nature of a select few of the processes and potential increases in the functionality of the modified starch. Modification thus enables enhancement and/or introduction of key properties that may be required for specific pharmaceutical applications (Jamzad, Tutunji, and Fassihi, 2005). The three available hydroxyl groups (at position: C2, C3 and C6) can be chemically modified through esterification, etherification and oxidation (Khan and Ahmad, 2013). The degree of modification of the three available groups typically varies with the genetic origin of the starch and the reaction conditions (Pu *et al.*, 2011). Such modifications in native starch alter the gelatinization, swelling, solubility properties, pasting and retrogradation characteristics (Tharanathan, 2005). These newly formed properties therefore allows for the modified starch matrices to be functionalized for pharmaceutical applications with more appreciable physicochemical and biodegradation properties when compared to its native form. This article therefore reviews the chemical modification methods utilized in the preparation and synthesis of modified starch co-polymers with emphasis given to their applications in drug delivery system design and formulation, which has not been notably reviewed previously.

2.2. CHEMICAL MODIFICATION OF STARCH

Chemical reagents used for starch modification can be classified as a monofunctional or bi-functional reagents based on their chemical properties (Wolf, Bauer, and Fahey, 1999). Monofunctional reagents provide a non-ionic, cationic, hydrophobic or covalently reactive substituent group (Sui and BeMiller, 2013). Such modifications generally alter the gelatinization and pasting properties of starch, resulting in a more stabilized starch derivative in which associations between amylose and amylopectin are blocked (Jeon, Viswanathan, and Gross, 1999). A common example of a modification method that uses monofunctional reagents is hydroxypropylation, an etherification modification method (Pal *et al.*, 2002). Bi-functional reagents allow for crosslinking of polymers since they can react with more than one hydroxyl group and can thus reinforce starch granules (Wang & Wang, 2003; Tharanathan,

2005). Common crosslinking agents such as tri-meta-phosphates and phosphoryl chlorides can also stabilize starch by modifying its swellability, solubility and mobility (Xiao, 2012). In the past few years there has been great focus on the chemical modification of starch with a variety of different starch molecules synthesized, each with its own chemical properties and functionality. There are very few methods applicable to preformed starch particles as most reactions require the sample to be in solution or a slurry (Anwunobi & Emeje, 2013) and the reagents tend to be too harsh for application in preformed particles (Chakraborty, Sahoo, Teraoka, Miller, and Gross, 2005). The three main chemical modifications for starch and their variations are summarized in Figure 2.2.

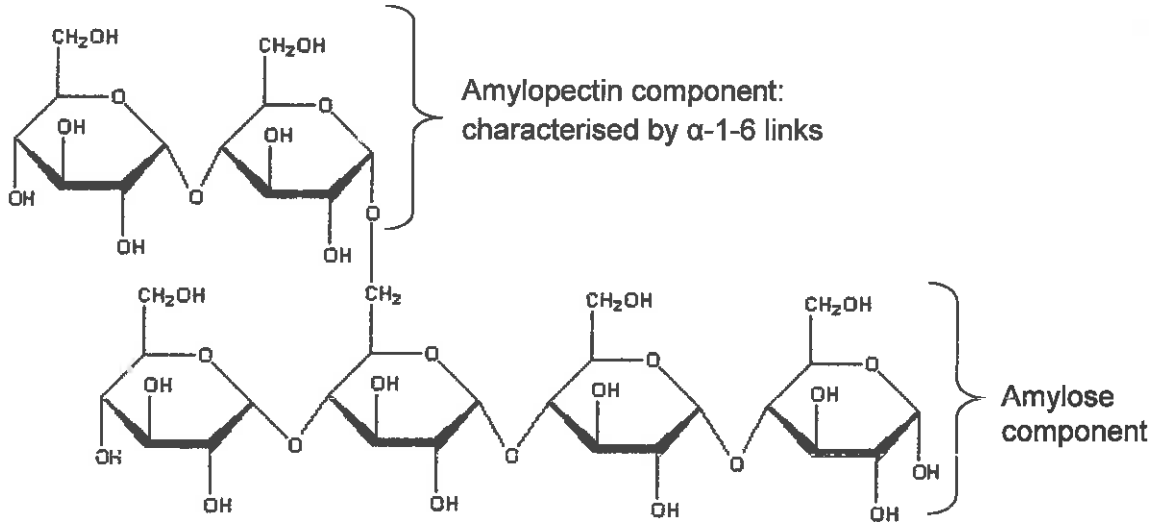

Figure 2.1: Starch copolymer chain with amylase and amylopectin component.

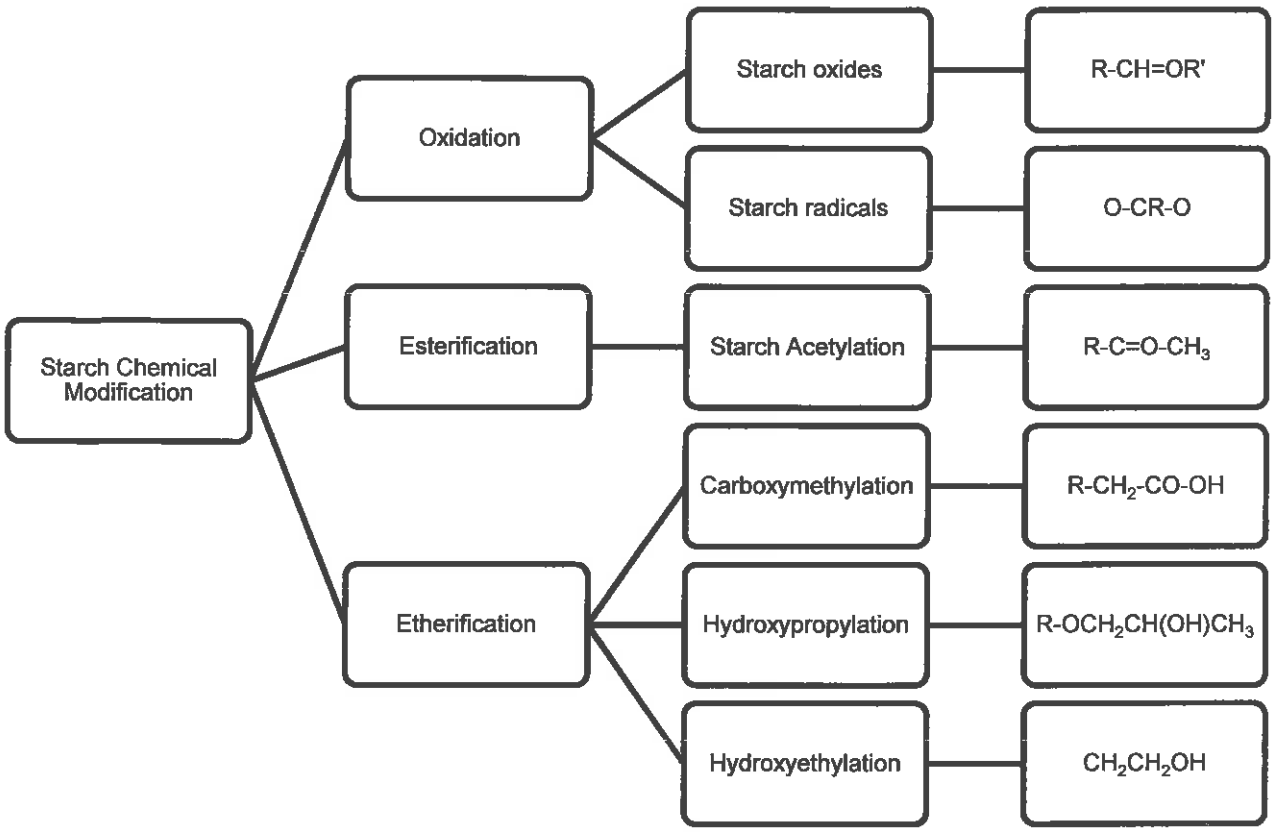

Figure 2.2: Schematic summarizing classical chemical methods for starch modification.

2.3. STARCH OXIDATION

Oxidized starches have been shown to have improved physiochemical properties such as film formation and adhesivity in some formulations, promoting a controlled release of active agents in drug delivery systems (Onofre, Wang, and Mauromoustakos, 2009). The starch derivative is typically produced by reacting starch slurry with an oxidizing agent under controlled temperature and pH (Yaacob, 2011). During the oxidative process, the three available hydroxyl groups are targeted for oxidation to yield new starch derivatives. The nature and properties of the oxidized starch derivative is dependent on the nature of the oxidative method and reagents utilized, resulting in improved physicochemical properties of the native starch particles (Sangseethong, Termvejsayanon, and Sriroth, 2010). This results in various alterations to the molecular structure of starch that functionalizes the co-polymer to the required properties for the derivative and a more efficient application in drug delivery.

Physicochemical properties of the oxidized derivatives generally include reduced viscosity, high clarity and low temperature stability resulting in greater applications in the food, biotechnology and pharmaceutical industries (Singh *et al.*, 2007). The surface morphology of the oxidized starch matrices is also variable, dependent largely on the chemical reaction time

(Sangseethong, Termvejsayanon, and Sriroth, 2010). Particularly in biotechnology and pharmaceutical applications, modifications of viscosity and thermal stability have greater implications and functionalization potential. Modification of surface morphology also has a significant effect on matrix functionalization as changes in this property can result in the controlled biodegradation of the starch matrix. This is of increased significance in polymeric drug delivery systems in which the release of the active agent is controlled or sustained over a specified period with predictable release kinetics (Beneke *et al.*, 2009). This reduces the frequencies of dosing, increases patient compliance and allows for the production of superior systems. Improved viscosity and altered thermal properties due to oxidation furthermore has implications on the swellability properties of the starch derivative affecting the water uptake ability, rendering derivatives ideal for applications in most oral formulations such as hydrogels, tablets and various other devices (Nabais *et al.*, 2007; Onofre, Wang, and Mauromoustakos, 2009; Shalviri, Liu, Abdekhodaie, and Wu, 2010; Kittipongpatana and Kittipongpatana, 2013).

Chemical oxidation of starch is typically targeted at the three available hydroxyl groups which can be substituted through oxidative and/or substitutive mechanisms which typically involve a series of reactions (Balakrishnan and Jayakrishnan, 2005; Li *et al.*, 2011). One such example includes the introduction of aldehyde groups to native starch particles where there is a series of at least two reactions that occur (Gao, Liu, Chen, Jin, and Chen, 2009). The first reaction is the oxidation of hydroxyl groups to carbonyl or carboxyl groups, which is followed by the depolarization of chains by cleaving the α-(1-4) links between the glucopyronose units (Zhang, Liu, Wang, and Gao, 2011; Zhang, Wang, Zhao, and Wang, 2012). Depolarization can thus be correlated to oxidation efficiency, which can be affected by a number of factors including the nature of the reaction and reagents used, starch molecular structure and organization (Kuakpetoon and Wang, 2001).

2.3.1 *PHYSICOCHEMICAL PROPERTIES OF OXIDIZED STARCH DERIVATIVES*

There are two possible products from the oxidative process with distinguishable physiochemical properties. One potential outcome is the formation of carboxyl groups which has been reported to increase the hydrophilic nature of resultant starch derivatives in some studies (Rinaudo, 2010; Zhang *et al.*, 2011). The increased hydrophilic property correlates to reduced linearity of the molecule and/or introducing an anionic charge that limits retrogradation and improves water solubility (Tharanathan, 2005). Furthermore, the increased hydrophilic nature of carbonyl-starch allows somewhat tailored applications in matrix drug delivery systems that are required to swell and control the release of active agents in oral systems and the improve the delivery of poorly water soluble drugs or actives i.e. enzymes and hormones (Vieira, Ferreira, Coelho, and Gil, 2008 ; Mahkam, 2010; Li *et al.*, 2011).

In addition, the introduction of dialdehydes can increase interactions with other biological macromolecules such as proteins due to potential reactions with amino and imino groups (Alves et al.,2007; Zhang *et al.*, 2011; Xiao, 2012). This distinct property of dialdehyde-starch derivatives renders them good candidates for application in biotechnology for enzyme immobilization and in delivery of macromolecules used in disease treatment (Fang *et al.*, 2010). These derivatives can also form hemiceacetyls/acetyls crosslinked derivatives that can yield reinforced systems with controllable swellability such as bioplastics and hydrogels (Singh *et al.*, 2007). Various reagents can be used in the chemical oxidation of starch but the most frequently used include; permanganate, nitrogen dioxide, sodium hypochlorite, periodate and chromic acid (Balakrishnan and Jayakrishnan, 2005). Unlike common oxidizing agents $NaIO_4$ is selective in its reaction and only targets the C2-C3 glycosidic link thus enabling the oxidation method to occur at a specific site (Rinaudo, 2010). Potassium permanganate ($KMnO_4$) is a strong oxidizing agent and a classic example of a commonly used oxidation method with great potential for applications in preformed starch-based systems. The strong oxidant is normally used in conjunction with a reducing agent such as nitric acid (HNO_3) for an oxido-reductive starch modification system (Pashkuleva, Marques, Vaz, and Reis, 2005). The $KMnO_4/HNO_3$ system is a widely explored combination, frequently used as an initiator for graft polymerization of some vinyl monomers onto starch cellulose and other polymers.

Work by Pashkuvela and co-workers (2005) showed surface modification in three starch based films without monomers. This particular study produced derivatives that showed increased adhesion of osteoblast-like cells to biomaterials, such as starch, further showing the application of starch in tissue engineering scaffolds (Pashkuleva *et al.*, 2005). This is one of very few studies that explored the use of the $KMnO_4$ oxidation method without any application of a monomer treatment. In this case, the $KMnO_4/HNO_3$ modification system was shown to be non-invasive and increased the hydrophobic nature of pre-formed starch-based systems. Interestingly, this study produced derivative films that were more hydrophilic and showed increased attachments of osteoblast-like cells when compared to unmodified/native-starch films.

There are two possible proposed reaction mechanisms for the $KMnO_4/HNO_3$ system (Figure 2.3), one yielding di-ketones and the other, starch active radicals (Sánchez-Rivera, García-Suárez, Velázquez del Valle, Gutierrez-Meraz, and Bello-Pérez, 2005). There are different propositions in regard to which mechanisms presides over the other. However, the rate and efficacy is largely affected by reaction conditions such as the reactive group on the targeted polymer, the concentration of $KMnO_4$ and the pH, like most chemical reactions (Pashkuleva

et al., 2005). In addition, the introduction of the di-ketones introduces the possibility of hydrogen bond formation within the polymer. The radical formation allows for grafting of polymers and a potential of self-crosslinking of modified starches (Liu & Sun, 2008). Although FTIR data from Pashakuleva and co-workers (2005) was not significantly different, they did show increased intensities around 1700 cm^{-1} implying an increase in the C=O proportions. Furthermore, surface interaction for the osteoblast-like cells showed enhanced surface interactions, which are governed by calcium-oxygen bonds. The modified films also showed and increased polar dispersity, which is correlative to an increased hydrophobicity with great potential in the treatment of bone fractures and other bone injuries. The non-invasive nature of the modification system renders it a potential method in the chemical oxidation of other preformed starch-based delivery systems, such as nanoparticles, starch granules and grains, without loss of structural integrity or requirement to be in a solution or slurry.

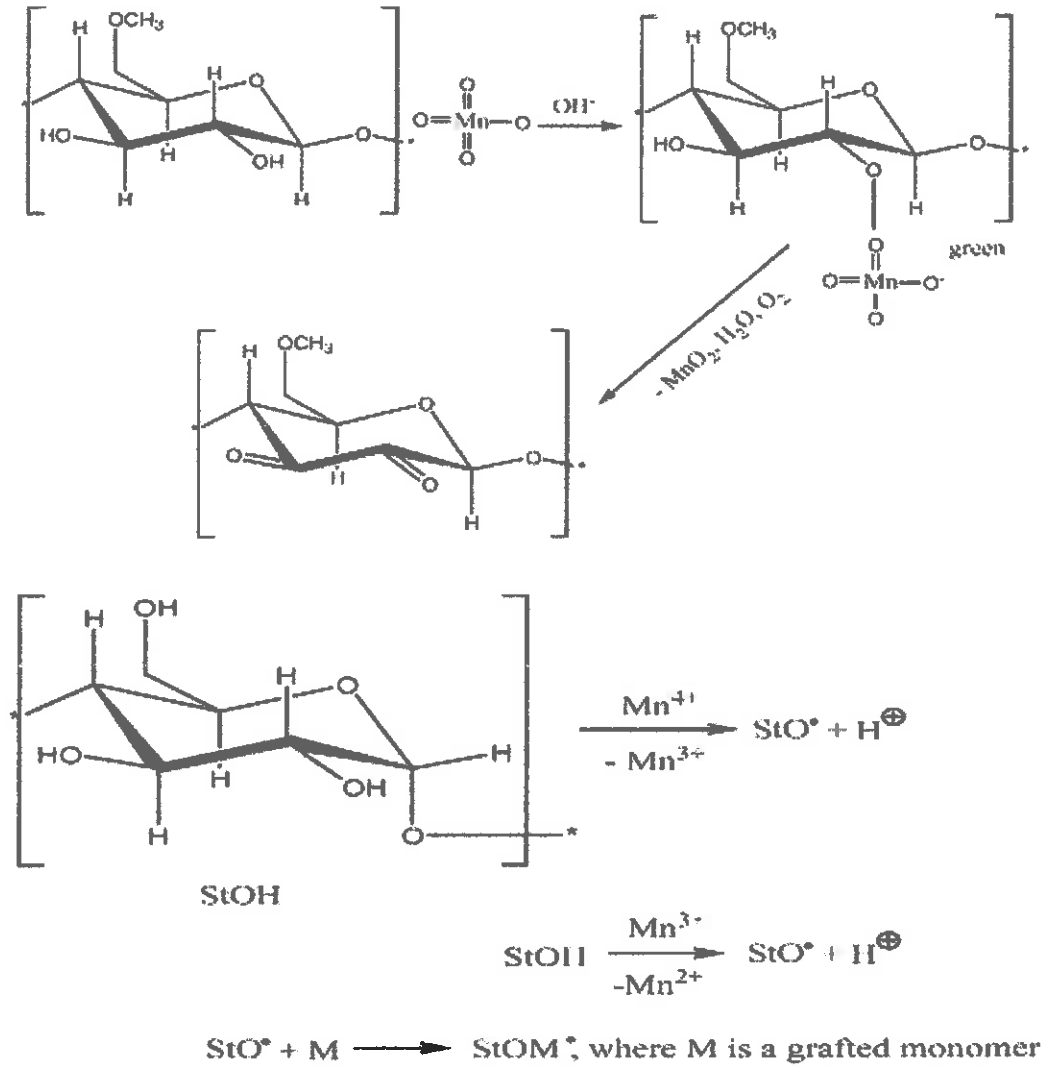

Figure 2.3: (a) Starch modification through the conversion of hydroxyl groups to aldehyde groups and (b) starch oxidation mechanism that yields starch radical (StO) (reproduced with permission from Pashkuleva et al., 2005).

Similar to $KMnO_4$, hypochlorite is also a strong oxidizing agent. Whilst, hypochlorite is not always a preferred reagent, as it results in the production of high salt and chloride by-products, the method is largely employed in the industrial production of oxidized starch (Kuakpetoon and Wang, 2001; Pashkuleva *et al.*, 2005). One of the most widely explored uses of hypochlorite oxidation is its inert capability to target the amorphous starch polymer regions, which is largely the amylopectin portion of starch (Marinich, Ferrero, and Jiménez-Castellanos, 2009). Physiochemical properties of derivatives from hypochlorite oxidation vary based on the pH of the reaction i.e. under acidic conditions, carbonyl groups are produced in larger quantities (Sánchez-Rivera et al., 2005; Sangseethong *et al.*, 2010), whereas in more alkaline conditions, carboxyl derivatives, which have greater commercial use, are produced in larger quantities (Sangseethong *et al.*, 2005). The mechanism of hypochlorite oxidation and the nature of derivatives are fairly similar to that of $KMnO_4/HNO_3$ reaction, in that it also involves a series of two reactions which can be altered such that one reaction presides over the other for the required derivative to be produced (Pashkuleva *et al.*, 2005).

2.3.2 *APPLICATION OF OXIDATIVE METHODS IN PRE-FORMED STARCH BASED DRUG DELIVERY SYSTEMS*

Production of an anionic starch derivative such as carboxyl-starch from a hypochlorite chemical oxidation method largely functionalizes the co-polymer, enabling chemical reactions with other macromolecules such as cationic amino acids (Sangseethong *et al.*, 2005). In the study undertaken by Huang and co-workers (2013) nattokinase (NK) starch-based nanospheres targeted for thrombolytic disease treatment were investigated. This study reported a high drug entrapment efficiency, which can prove to be a challenge in drug delivery system design (Figure 2.4). The anionic starch analyzed in the study made for a more efficient active entrapment as NK has a net positive charge, typical for kinases, in which the NK entrapment efficiency was enhanced due to weak ionic interactions.

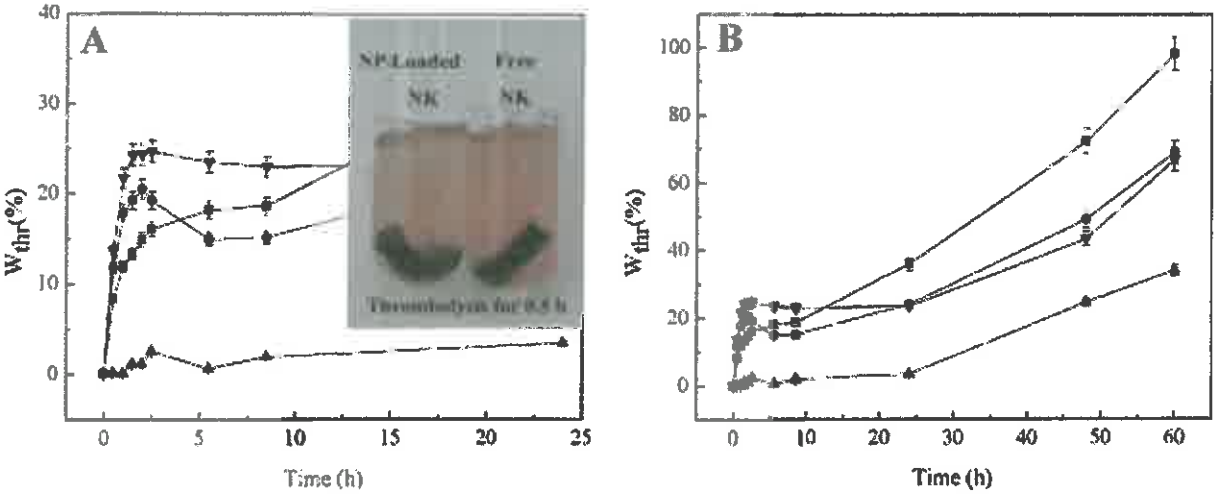

Figure 2.4: Thrombolytic behaviors of anionic starch nanosphere [(A) 24 h; (B) 60 h. ■: NP-loaded NK; ●: free NK; ▼: OS-loaded NK; ▲: saline] (reproduced with permission from Huang *et al.*, 2013).

Oxidized starch derivatives also allow for the conjugation and crosslinking of starch with other polymers due to the reactivity of the resultant groups such as dialdehydes and ketones. This has recently been employed in the formulation of an oxidized-starch-chitosan hydrogel (Baran, Mano, and Reis, 2004). Key property analyses from hydrogel studies further confirmed the reduced viscosity of oxidized starch derivatives as the swellability of the hydrogel increased with increased oxidized starch (Sangseethong *et al.*, 2010; Xiao, 2012). Properties of these hydrogels highlighted though one of the main disadvantages of chemical oxidation of starch, as the tensile strength was reported to decline with increased oxidized starch percentage.

2.4. STARCH ESTERIFICATION

Esterification of starch involves the conversion of the three available hydroxyl groups to alkyl or aryl derivatives. This modification typically alters the retrogradation properties of starch and translates to limited intra-amylase chain interactions, as well as interactions with the outer amylopectin chains (Jeon *et al.*, 1999). There are various methods that fall into this category, the most common and basic being acetylation, which is widely used in the food, biotechnology and textile industries (Horchani, Chabouni, Gargouri, and Sayari, 2010). There are three types of acetylated starches; each based on the degree of substitution (DS) i.e. low, medium and high DS starch. Low DS starch is the most common type of acetylated starch, with DS values between 0.01 and 0.2 DS and is cold water-soluble (Elomaa, 2004). Low DS starch acetates are commonly produced by using acetic anhydride as a reactant and an alkaline, typically sodium hydroxide, as the catalyst (Paulos *et al.*, 2016). The native starch is activated with the alkaline to form an alkoxide, a more reactive starch derivative that reacts with the hydroxide (OH^-) to form an acetylated derivative (Tharanathan, 2005). Medium DS starch has DS values between 0.3 and 0.1 and is generally water-soluble but not to the extent of the low DS starches

(Pu *et al.*, 2011). The high DS starches (2-3) are not water-soluble but are soluble in organic solvents. The efficiency and extent of acetylation depends on the ultrastructure of the starch type which varies with botanical origin and the specific reaction conditions (Singh *et al.*, 2007). In most cases high DS is observed in low amylose starches because acetylation has been shown to occur in the amorphous regions and because there is less hindrances with low amylopectin branches for the C=O incorporation (Tuovinen *et al.*, 2004).

2.4.1 *PHYSICOCHEMICAL PROPERTIES OF ESTERIFICATION DERIVATIVES*

The acetyl group ($COCH_3$) is much larger in size with more expansive electron clouds when compared to OH^-. As a result, individual chains repel each other due to steric hindrance as the modified starch derivatives attempt to exist in the lowest, more stable, energy state (Wiberg and Rablen, 1993). The repulsion between the chains not only increases the swelling capability of starch as water uptake is increased, but also enhances amylose leaching, thus increasing starch solubility (Muljana *et al.*,2010). The extent to which swellability is increased depends on the nature of starch and the DS (Angellier, Molina-boisseau, Belgacem, and Dufresne, 2005). Furthermore, the substitution of the hydroxyl groups with larger substituent groups show reduced retrogradation, transition temperatures and gelatinization temperatures (Paulos et al., 2016). Structural morphology is also altered by acetylation to varying extents for different starches and thus so is DS (Raatikainen, Korhonen, Peltonen, and Parone, 2002). In some cases, minor surface alteration is observed where starch acetate surfaces are rougher and tend to aggregate (Muljana, Picchioni, Heeres, and Janssen, 2010). Surface gelatinization could possibly occur due to the presence of bases such as NaOH required for acetylation reactions (Singh *et al.*, 2007). Furthermore, a physical change in the native molecular structure has implications in the natural degradability of the starch derivative. This resultant resistant property renders the derivatives highly useful in sustained release formulations, with a controlled biodegradation, as it can increase GIT residence time for some oral formulations (Beneke *et al.*, 2009; Pu *et al.*, 2011).

2.4.2 *ESTERIFICATION IN DRUG DELIVERY*

Acetylated starch (AS) has shown sustained drug release in some polymeric systems due to the increase in swellability and decreased enzyme sensitivity during gastrointestinal digestion (Shirwaikar, Prabu, Lakshmana, and Kumar, 2008). In some cases, AS has also been linked to improved biovalabity of macromolecular treatments like insulin (Minimol and Sharma, 2013). The increased C=O proportions assist in site-directed drug delivery because the carboxyl group has a high affinity for amino groups and will thus be attracted to sites which have amino containing ligands as well as increased interactions with lysine (Tuovinen *et al.*, 2004). To test for controlled drug release from starch acetates (Figure 2.5), it was shown that

acetylation of potato starch films and microparticles have a much more retarded drug release profile when compared with native starch (Tuovinen *et al.*, 2004).

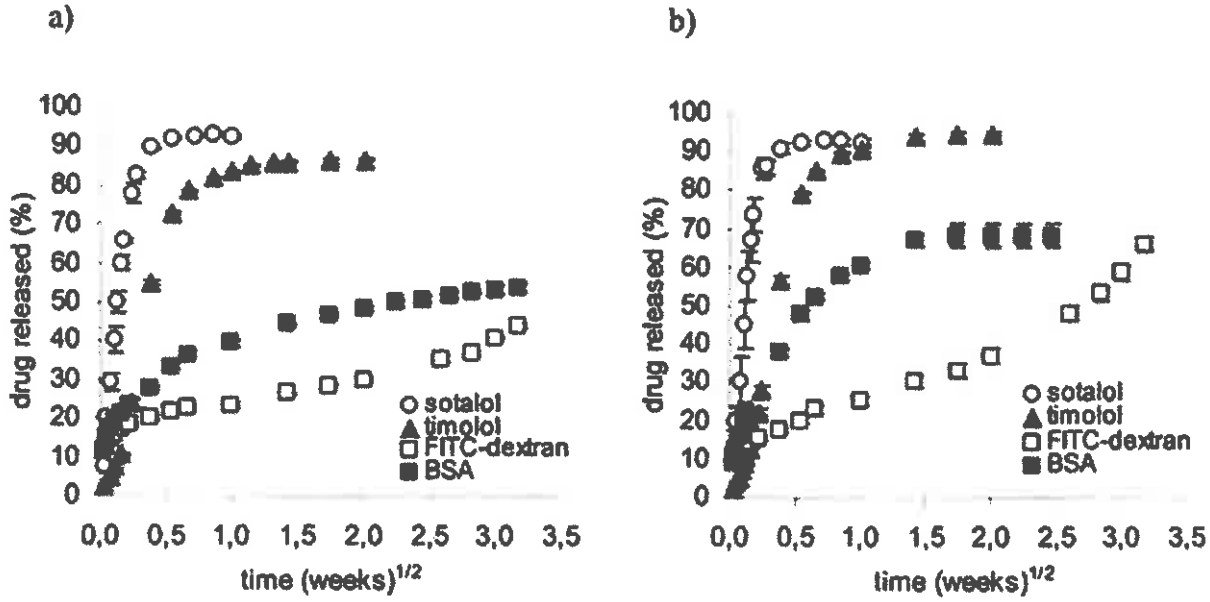

Figure 2.5: The release of drugs from starch-acetate DS 1.9 films in (a) PBS pH 7.4 without; and (b) with α-amylase (20 U/mg of polymer) (mean±S.E.M., *n* =3) (Tuovinen *et al.*, 2003).

The retarded drug release has also been observed in tableting, in which the use of acetylated starch showed decreased drug release due to reduced wettability of the tablet (Chen *et al.*, 2004). Acetylated starches furthermore shows greater amylase degradation thus are applicable when targeting delivery systems to the colon, where the starch acetates are hydrolyzed by esterase enzymes (Ahmad, Tester, Corbett, and Karkalas, 2006; Pu *et al.*, 2011).

2.4.3 *ESTERIFICATION OF PRE-FORMED DRUG DELIVERY SYSTEMS*

Classical acetylation has been investigated utilizing preformed systems such as granules, nanoparticles and microparticles. In most cases the surface is not altered to a great degree especially for starch granules (Raatikainen *et al.*, 2002). However, in some cases chemical acetylation requires the use of organic solvents and is overall more costly, with results that are not always reproducible. There is however, continued interest in the use of biocatalysts as a means of acetylation; this methodology not only has the potential of solvent free acetylation, but also has region-specificity and sterio-specificity due to the nature of enzyme activity (Chakraborty *et al.*, 2005). Utilization of these biocatalysts thus increases acetylation efficiency and tend to be more cost effective and reusable. The enzymes commonly utilized for his type of modifications are lipases and proteases which catalyze the esterification of

starch with various organic acids that are selected based on the physicochemical properties targeted (Horchani *et al.*, 2010). The resulting derivatives tend to be hydrophobic and are widely used as thermoplastics (Simi and Abraham, 2007). To achieve a region-selective enzyme catalyzed esterification, Charkraborty and co-workers (2005) used a lipase enzyme to catalyze the esterification of vinyl stearate onto the starch molecule. The enzyme was incorporated in a reverse micelle using an anionic surfactant, aerosol-OT (AOT). The AOT forms a thermodynamic water droplet surrounded by a surfactant monolayer in oil. The enzyme is thus able to collide with the substrate in a non-polar environment, yet still shows optimum activity (Chakraborty *et al.,* 2005). The rate of such reaction can easily be controlled through enzyme concentration and the temperature (Najafi *et al.*, 2016) of reacting apparatus and thus tends to have a higher efficiency and reproducibility. In a similar study, Horchani and co-workers (2010) modified starch surface with oleic acid. Although the acids for the studies differed, in both cases hydrophobicity was increased, the sensitivity towards amylase decreased and it was reported to show complete resistance to amylase (Horchani *et al.*, 2010). Esterification using lipase enzymes generally results in a decreased hydrophilic character, which in some cases is one of the limitations of native starch. Furthermore, the reduced swelling also implies an increased retention time for oral starch-based delivery systems, prolonging the residence time of the system in the stomach (Amass, Amass, and Tighe, 1998). This is highly applicable for drugs that have narrow absorption windows and low pH stability, as it constitutes a more controlled drug delivery system. The resistance to the amylase enzyme also contributes to the potentially increased residence time.

2.5. ARYL ESTERIFICATION

Similar to the lipase catalyzed esterification methods, the addition of an aryl group also increases the hydrophobicity (Minimol and Sharma, 2013) of starch and thus increases the interactions with non-polar polymers. To enhance starch application, some modifications employ mechanisms that introduce an aryl to the surface of preformed starch based systems. In a study by Angellier and co-workers (2005), the surface of waxy maize starch was modified by the addition of alkenyl succinic anhydride and phenyl isocyanate without altering the morphology and crystallinity of the formed nanocrystals (Angellier *et al.*, 2005). Other studies used oxazoline maleate and obtained similar results (Kosan, Meister, Liebert, and Heinze, 2006). This modification mechanism has also been successful in the derivation of thermoplastics (Carvalho, Curvelo, and Gandini, 2005). Unlike acetylation, the swelling properties will not be enhanced, yet interactions with non-polar polymers used as matrixes for composite material are possible. This is a more promising method of esterification, which involves chemical grafting (Namazi and Dadkhah, 2010).

2.6. ETHERIFICATION METHODOLOGY AND RESULTANT PROPERTIES

Esterification is a modification method in which the hydroxyl groups are substituted with carboxymethyl, hydroxypropyl, and/or hydroxyethyl group through the formation of an ether link (R-OR). Although the etherification methodology may vary, they typically require an alkaline catalyst to initiate the chemical substitutions; where sodium hydroxide is commonly used (Heinze, Liebert, Heinze, and Schwikal, 2004).

2.7. CARBOXYMETHYLATION

One of the most common methods of etherification is carboxymethylation (CM), preferred due to its simplicity and rapidness. CM is an etherification process that substitutes hydroxyl groups with anionic carboxymethyl groups which are less polar (Lawal *et al.*, 2009). CM improves hydrophilicity, thus facilitating water absorbance. Increased water absorbance has significant implications in drug delivery system development, particularly in the matrix assisted approach (Massicotte, Baille, and Mateescu, 2008). CM is derived from native starch that goes through a two-step reaction, in which an activated starch complex (commonly activated with NaOH) is reacted with monochloroacetic acid or its salt derivative via the Williamson ether synthesis, yielding a CM starch derivative (Heinze *et al.*, 2004).

2.7.1 *PHYSIOCHEMICAL PROPERTIES OF CARBOXYMETHYL STARCH*

The carboxymethyl group is bulkier with a larger electron cloud than the OH^- of native starch and thus reduces the tendency of starch re-crystallization (Chen and Wang, 2006). This in turn decreases heat and bacterial sensitivity due to steric hindrances. The carboxymethyl group also introduces the possibility of increased pH responsiveness, rendering the derived polymer excellent for controlled drug delivery application (Lee *et al.*, 2010). The solubility properties are also altered as the hydrophobic character is increased, due to an increase in crosslinking potential, accompanied by reduced swelling properties (Chen and Wang, 2006). Other biotechnological applications of carboxymethyl starch include the extraction of toxic metals due to the increased cation exchange capacity introduced by the carboxyl group, which increases with DS (Kim and Lim, 1999). Although carboxymethyl starch is used in numerous delivery systems, due its pH sensitivity and crosslinking potential, it is not that widely used in surface modification of preformed systems, due to the bulky carboxymethyl group that would destruct/ deform such structures. Furthermore, the methodology in which carboxymethyl starch is derived alters the morphology of native starch particles.

2.7.2 *CARBOXYMETHYLATION IN DRUG DELIVERY AND APPLICABILITY TO PRE-FORMED SYSTEMS*

CM starch has been widely explored as a disintegrant due to the pH responsiveness imparted by the carboxymethyl group. In a gastric medium, carboxymethyl starch has been proven to improve tablet stability through dimerization and hydrogen bond formation, resulting in retarded disintegration, providing a controlled, and in some cases a sustained, drug release profile (Mulhbacher, Ispas-Szabo, and Mateescu, 2004). In a more neutral pH, CM starch has been proven to have a positive swelling effect on polymers in matrices. The carboxymethyl group facilitates a proton exchange as it can function as a zwitterion (Assaad, Wang, Zhu, and Mateescu, 2011). Notably formulations that are swellable have been largely explored in drug delivery, especially in the oral formulation design field as they may be modified to show some gastro-retentive properties, allowing for the development of more superior products (Assaad and Mateescu, 2010). CM starch has also been widely explored for application in various hydrogel applications as it provides an added advantage for sustained release due to poly-anionic behavior that imparts swellability properties (Assaad and Mateescu, 2010). Other novel applications of CM starch include CM derived using dextran sulphate in the site-specific delivery of reactive oxygen species in carcinogen treatment regiments (Saboktakn *et al.*, 2010). Due to the harsh chemical treatment required with a strong alkali, based on the Williamson's ether synthesis, chemical carboxymethylation has not been typically preferred for surface in the modification of preformed starch particles in drug delivery (Besheer *et al.*, 2007; Doan, Hong, Duy, Duoc, and Dieu, 2012). However, there have been studies that have explored the use of various organic solvents to help maintain structural integrity of starch derivatives (Table 2.1). Although these have not yet been explored within drug delivery, they however have potential for application of surface application of both micro and nano-structures.

Table 2.1: Summary of surface chemical modification systems modified via carboxymethylation of granular starch

Starch	Medium	Water (wt %)	DS	RE	References
Corn	Isopropyl alcohol	24	0.53	0.3	Jingwu *et al.*,1993
Potato	Isopropyl alcohol	12	0.9	N/A	Jingwu *et al.*,1993
Corn	Isopropyl alcohol	20	0.22	0.13	Bhattacharyya *et al.*, 1995
Amaranth	Isopropyl alcohol	10	0.24	0.11	Heinze et al.,*2004*
Corn	Cyclohexane	20	0.24	0.14	Kosan *et al.*, 2006
Amaranth	Cyclohexane	10	0.34	0.15	Kosan *et al.*, 2006

DS: Degree of Substitution, wt%: percentage weight per unit-volume and RE: Reaction Efficiency (%monomer bonded to starch).

2.7.3 *HYDROXYPROPYLATION METHODS AND REACTION CONDITIONS*

Another common etherification method for starch is hydroxypropylation, which is derived through treatment of starch with propylene oxide in the presence of a strong alkaline catalyst (Singh *et al.*, 2007). A reaction typically requires starch to be in slurry and is carried out at temperatures of 40°C. The hydroxyl groups are substituted, through a nucleophilic substitution reaction mechanism, with hydroxypropyl groups. The resulting hydroxypropyl starch (HPS) derivatives are physicochemically similar to those of the carboxymethylation method; however, the hydroxypropyl group is bulkier and thus can disrupt the inter- and intra-molecular forces in starch. As a result, the hydrogen bonds are broken and weakening the starch granules, leading to increased rotational flexibility of starch amorphous regions, allowing in an increased water uptake and thus an increase in the swellability (Ju, Yan, and Zhang, 2012).

2.7.4 *PHYSICOCHEMICAL PROPERTIES OF HYDROXYPROPYL STARCH*

The bulky hydroxypropyl group reduces the internal hydrogen bond strength and quantity in starch. This substantially decreases the ability of starch to re-crystallize, which reduces the retrogradation property of starch, yielding a derivative that is stable at high temperatures (Pal *et al.*, 2002). In addition, this disruption in the ordered structure of the copolymer renders the HPS more accessible to water molecules and thus increases the hydrophilic character of HPS derivative (Chen, Hob, and Sheu, 2010). When combined with the innate hydrophilic property of the hydroxypropyl group, HPS derivatives have improved swellability and viscosity. This renders these starch derivatives applicable as excipients in formulations that require long-term freeze-thaw, cold storage stability or improved general shelf-life (Pal *et al.*, 2002).

2.7.5 *HYDROXYPROPYLATION IN DELIVERY SYSTEMS*

Due to the high hydrogen content of HPS, it is typically applied as pH-dependent excipient that allows for the development of a self-regulated system. This is one of the most important physiochemical properties of HPS, as the dissolution of the pH-sensitive polymers is usually highly dependent on the surroundings and thus has been used widely in oral formulations for targeted drug delivery to different parts of the gastrointestinal tract. HPS has been widely utilized as an excipient but very seldom is it explored as a stand-alone system or for approaches centered on its functionality. There are, however, many studies that have explored HPS as a co-polymer or an activated complex for copolymerization or grafting. An example of such an application is the development of nanoparticles used for the sustained release of insulin by Zhang and co-workers (2012). In this study, the reducing ends of the HPS derivative were used to impart hydrophilic character which preserving the polymers ability to swell. Furthermore, the produced particles showed high levels of amylase resistance and thus aided in targeting the particles for colon specific drug delivery (Zhang *et al.*, 2012).

2.7.6 *HYDROXYPROPYLATION APPLICABILITY TO PRE-FORMED DRUG DELIVERY SYSTEMS*

It is generally accepted that HPS derivatives are much more stable when compared to native starch. However, the harsh reaction conditions required in HPS methods have not yet been applied to pre-formed systems or any starch granules, as the structural integrity for systems will not be preserved.

2.8. HYDROXYETHYLATION

Similar to the aforementioned modification systems, hydroxyethylation (HES) also targets the three available hydroxyl groups for substitution with hydroxyethyl groups in a mechanism that is very similar to that detailed for starch oxidation (Chen *et al.*, 2010). The derivative is produced using ethylene oxide in a strong alkaline. However, the distinct characterization of these derivatives is that they tend to be highly water soluble, due to the hydrophilic hydroxyethyl groups, yielding a starch derivative that is both water soluble and has stabilized solubility (Besheer *et al.*, 2007). Furthermore, the fairly large hydroxyethyl group renders the derivative resistant towards amylase degradation, making it a good candidate for sustained release applications in drug delivery (Kenawy, Kamoun, Eldin and El-Meligy, 2013).

2.8.1 *HYDROXYETHYLATION IN DRUG DELIVERY*

There are various potential applications of this soluble naturally-derived polymer which has an increased *in vivo* half-life and lacks immunogenic properties due to its structural resemblance to collagen (Chen *et al.*, 2010). The HES derivative properties correlates to the DS exhibited by a derivative, if there are more hydroxyethyl groups substituted for hydroxyl groups, then the increased solubility and resistance towards enzymatic degradation becomes more pronounced (Besheer *et al.*, 2007). Due to the high hydrophilic nature of the HES derivative, there has been a large application of hydroxyethyl starch in the formulation of hydrogels. To obtain a recognizable HES derivative, a very high proportion of amylopectin is required, as the chemical reaction used to introduce HES-type property targets the amorphous regions of the co-polymer (Narayanan *et al.*, 2015). By definition, HES is in fact a synthetic polymer mostly derived from purified amylopectin.

2.8.2 *HYDROXYETHYLATION APPLICABILITY TO PRE-FORMED DRUG DELIVERY SYSTEMS*

Similar to the chemical modification method of the derivation of HPS, the modification method requires very harsh reaction conditions that have not yet been optimized for preformed delivery systems or granule-type starch targeted for surface modification. Based on reviewed modification methods, it is evident that not all methods are applicable to pre-formed systems. Table 2.2 summarizes the methods that have been applied to preformed systems and the respective active agents targeted for delivery.

Table 2.2: Surface modification applicable to pre-formed drug delivery systems

Modification Type	Yield	Reaction Requirement	Active Agent	Starch	Reference
Chemical oxidation	Anionic nanoparticles	Reverse micro-emulsion	Nattokinase	Anionic	Huang et al (2013)
Esterification (Enzyme based region-specific)	Nanoparticles	Dry enzyme catalyzed	N/A	Standard	Chakrabrorty et al (2005)
Esterification	Tablet	Organic solvent solution	N/A	starch acetate	Raatikainen et al. (2002)
Esterification (Aryl)	Nanocrystals	Aromatic	N/A	waxy maize	Angellier et al. (2005)

2.9. CURRENT ADVANCES IN DRUG DELIVERY USING STARCH-BASED DELIVERY SYSTEMS

Recent studies have focused on the modification of starch for application in drug delivery systems. These include starch nanoparticles synthesized from maize starch (modified and un-modified) used to formulate 2 different types of nanoparticles used in a transdermal drug delivery system (Santander-Ortega *et al.*, 2010), to successfully bypass the skin without interference to the skin's integrity. Produced through emulsification-diffusion, higher yields of nanoparticles with controllable particle size and degree of polydispersity were achieved (Anwunobi and Emeje, 2011). The modified starch nano-particles, by the addition of propyl groups, were shown to be non-toxic. Permeation data for the delivery of flufenamic acid using the nano-particles was enhanced by about ten-fold as compared to caffeine and testosterone for nano-encapsulated and free drugs when used in excised skin from female Caucasian patients.

Research by Paulos and co-workers (2016) produced nanoparticles from acetylated dioscorea starch, synthesized by reacting native dioscorea starch with acetic anhydride. Acetylated starch nanoparticles were then fabricated by spontaneous emulsification and solvent evaporation method under high speed homogenization. It was determined that the process variables: solvent type; surfactant type and concentration; homogenization speed; and time significantly influence the polydispersity and size of the nanoparticles. Using a central composite design, nanoparticles of particle size less than 200 nm and a polydispersity index (PDI) of < 0.2 was achieved. In contrast to the work of Paulos and co-workers (2016), Minimol and Sharma (2013) produced amphiphilic PEGylated starch acetate nanoparticles that when in contact with insulin, self-aggregated into particles of 32mm. Due to the highly appreciable bioadhesivity of the PEGylated nanoparticles, an application in protein delivery is plausible.

Yang and co-workers (2014) produced 5-aminosalicylic acid- loaded starch nanoparticles of 40 nm utilizing starch amount, surfactant amount and oil/water ratio as process variables. N,N-bisacryloylcystamine cross-linked nanoparticles were degraded into oligomers through the cleavage of the disulfide linkages by dithiothreitol. From the results, accelerated drug release was achieved through the use of dithiothreitol as the reducing agent. In addition, excellent biodegradability and biocompatibility showed promising results in the application of drug delivery.

Najafi and co-workers (2016) delivered ciprofloxacin via acetylated corn starch nanoparticles. Synthesized by the reaction of native corn starch using acetic anhydride and acetic acid varying degrees of substitution particles of 312 nm diameter were achieved. Varying the degree of substitution varied the entrapment efficiency from 67.7 to 89.1%. Xiao and co-workers (2016) also by varying the degrees of substitution, developed a nanoparticulate system using broken rice. The particles were loaded with doxorubicin hydrochloride for cancer therapy. Since the safety of nanomaterial is of great concern in biomedical applications, through toxicity analysis using rat hepatocytes as well as HeLa human cervical carcinoma cells, were shown to be a suitable carrier for cancer chemotherapeutics (Sun, 2015; Xiao *et al.*, 2016).

Methoxy poly (ethylene glycol)/starch grafted copolymers (MPEG-g-S), synthesized through bromoacetylation of potato starch followed by substitution of methoxy poly (ethylene glycol) (Movagharnezhad and Moghadam, 2016) highlights the specialized applications of carboxymethylation and the nature of derivatives produced. Loaded with the antibiotic, ceftizoxime, the reaction conditions require usage of sulfuric acid which may prove challenging to implement in pre-formed systems yet results from this study have indicated the that grafted co-polymers are well suited for drug delivery.

2.10. CLINICAL POTENTIAL OF MODIFIED STARCH

There have been a few clinical trials undertaken to evaluate the use of chemical starch as drug delivery systems. A study undertaken by Vandenbossche *et al.*, (1992) detailed the use of modified hydrophilic starch matrices for the delivery of theophylline compared to a commercially available product. The results of this determined that there was no significant improvement in the sustained-release profile when compared to the commercial product at all ratios evaluated. The use of intravenous starch has also been noted to have unwanted side-effects. A review conducted by Wiedermann, (2008) detailed the use of hydroxyethyl starch in fluid management in patients suffering from sepsis. The focus of this article was to review randomized clinical trials where hydroxyethyl starch was used over traditional infusions such

as colloids and gelatin. It was noted in this review that the administration of hydroxyethyl starch increased the risk of acute renal failure in patients requiring fluid replacement during sepsis and the use this modified starch in these patients should be avoided. The use of hydroxyethyl starch in parental formulations can however be beneficial. A recent study undertaken by Narayanan *et al.*, (2015) noted that hydroxyethyl starch nanoparticles, prepared via cross-linking precipitation, has the potential to be a successful carrier for drugs with varying hydrophobicities. These nanoparticles were furthermore noted to be potential controlled-release platforms upon administration with the release profile determined on the chemical nature of the modified starch in addition to the drug-matrix interaction.

Other studies have also shown the benefits of using modified starch based delivery systems. Modified tapioca starch has been noted previously to be a potential adjunctive treatment in diarrhea with successful results seen in rats (Wingertzahn *et al.*, 1999). Additionally, a randomized, double-blind pilot study undertaken by Correia et al., (2008) noted the improved therapeutic effectiveness of modified corn starch over its native form for the treatment of Glycogen Storage Disease Types Ia and Ib. In this study, it was determined that the modified starch maintained blood glucose concentrations significantly longer than the cornstarch therapy, possibly removing the need for additional dosing, primarily at night. The use of modified starch can therefore be seen as advantageous in various clinical outcomes dependent largely on the type of modification used in the preparation of these platforms as well as the type of patients being treated.

2.11. CONCLUSION

Among all three major chemical modification methods explored, surface oxidation and esterification, evidently seem to be methods that have the highest potential for further developments. The physicochemical properties introduced through these methods allow for functionalization of pre-formulated delivery systems and has the potential to increase the overall efficacy of starch-based systems. Based on the research reviewed, there is an obvious requirement for a solvent-free reaction or mild reagent for application in pre-formed particles for drug delivery. Considering sample preparation and time method complexity within drug delivery, pre-formed modifications for starch-based particles evidently have increased potential but have only been explored by few researchers. Solvent-free and solid state modification can vastly change the landscape of the drug delivery design approach. The functionalities introduced through chemical modification offer a significant improvement to starch-based systems, enabling the production of starch-based systems in a much less time consuming, yet extremely efficient approach. Furthermore, there is a growing patient base that has greater concerns about chemical grade substrates used in pharmaceutical -formulations.

Cost-effective and efficient functionalization of starch has great potential in addressing dwindling patient compliance numbers and obvious escalating costs of design and manufacturing. Post-fabrication modification methods that also preserve the structural and functional integrity of formulations have increased potential. This is especially true in the applications of natural pre-formed starch particles, enhancing the application of non-synthetic polymers in drug delivery. Whilst unmodified starch has its many advantages, the pitfalls can be addressed through surface modifications that enable leveraging on, further improving its physicochemical properties.

CHAPTER 3
DEVELOPMENT OF PERIODATE OXIDATION METHOD FOR APPLICATIONS IN THE MODIFICATIONS OF FOOD-GRADE-PRE-FORMED SAGO BEADS IN THE PRODUCTION OF DDS

3.1. INTRODUCTION

Oxidized starches have been shown to have improved physiochemical properties (Onofre and Wang 2010) such as film formation and improved adhesive properties in some formulations, promoting a controlled release of active agents in drug delivery systems (Onofre et al. 2009). The starch derivative is typically produced by reacting starch slurry with an oxidizing agent under controlled temperature and pH (Yaacob, 2011). During the oxidative process, the three available hydroxyl groups are targeted for oxidation to yield new starch derivatives with altered properties. The nature and properties of the oxidized starch derivative is dependent on nature of the oxidative method and reagents utilized, resulting in improved physicochemical properties of native starch particles (Sangseethong et al., 2010).

In polymeric drug delivery systems, altered flow properties have a significant role in the improvement of release kinetics (Beneke et al., 2009). Oxidized starch is traditionally utilized as an excipient in several controlled and/or sustained release formulations such as tablets, hydrogels and others (Kittipongpatana and Kittipongpatana, 2013). Improved viscosity and altered thermal properties due to oxidation can improve the swellability of starch derivative affecting the water uptake ability, rendering derivatives ideal for applications in most oral formulations such as hydrogels, tablets and various other devices (Te Wierik et al., 1997; Nabais et al., 2007; Shalviri et al., 2010). The extent of any altered physiochemical property (i.e. viscosity and others) is however dependent on the nature of the reaction and/or the oxidizing agent utilized.

Frequently utilized oxidation reagents include; permanganate, nitrogen dioxide, sodium hypochlorite, periodate and chromic acid amongst others (Balakrishnan and Jayakrishnan, 2005). Like potassium permanganate, hypochlorite is also a strong oxidizing agent which yields different derivatives depending on the reaction condition. In starch modification, hypochlorite oxidation tends towards the production of anionic derivatives. Production of an anionic starch derivative such as carboxyl-starch in hypochlorite chemical oxidation method, functionalizes the co-polymer and enables chemical reaction with other macromolecules such as cationic amino acids (Sangseethong et al., 2005).

In this study, a periodate oxidation method utilizing sodium(meta)periodate (NaIO4) was developed for the surface chemical modification of commercially available Sago beads to produce S_{ago}-millisphere system. The physichochemical properties of the resulting S_{ago}-

millispheres were evaluated via: chemical degree of substitution (DS), Fourier Transform Infrared Spectroscopy (FTIR), Scanning Electron Microscopy (SEM) and X-ray diffraction (XRD).

3.2. MATERIALS AND METHODS

Food-grade Sago starch beads were purchased over-the-counter (OTC), food-grade chitosan (Warren Chem Specialities, batch number:WA200703003), 99%$^{w}/_{w}$ sodium (meta) periodate ($NaIO_4$), Hydrochloric acid (HCL) 37% $^{w}/_{w}$, Glutaradehyde 50%$^{v}/_{v}$ solution, Dimethylfoxyde 50%$^{v}/_{v}$ were purchased from Sigma-Aldrich (St. Louis, Missouri, USA) at reagent grade and were utilized with no further purification or alterations, ethanol absolute (≥99.8 purchased from Merck, Halfway House, Gauteng, South Africa) at reagent grade.

3.2.1 *OXIDATION METHODOLOGY: INTRODUCTION OF SURFACE ALDEHYDE GROUPS*

To prepare the S_{ago}-millispheres, a 0.02M $NaIO_4$ solution with 1.27% $^{v}/_{v}$ HCL and 42.37% $^{v}/_{v}$ ethanol. Oxidized samples were prepared using three different time points: 30, 60 and 90 minutes for oxidation reaction duration. The oxidative reactions were carried out in sealed amber 250mL flask. To ensure that there were no further side-reactions, samples were thoroughly rinsed with distilled and deionized sterile water (one liter for rinsing every 6g of oxidized beads). Excess water was then carefully removed using filter paper and the S_{ago}-millispheres dried under the fume hood in an amber container.

3.2.2 *AMMONIACAL SILVER NITRATE (TOLLENS' REAGENT TEST FOR ALDEHYDE GROUPS)*

Freshly prepared Tollens' reagent was used to test for the successful introduction of aldehyde groups to the Sago beads. *Tollens' reagent*: to prepare the reagent test-tubes were thoroughly cleaned using 3M sodium hydroxide. To the clean vial, 2mL of a 0.2M silver nitrate solution was added and 1 drop of the 3M solution added to the vial. To this resultant solution, 3mL of a 2.8%$^{w}/_{v}$ ammonia solution was added drop-wise with constant shaking.

Tollens' test: 0.5mg of unmodified starch was added to a test-tube, to this 1mL of freshly prepared Tollens' reagent was added and incubated at room temperature for 10 minutes. This was also done for a positive control octadecanal as well as the S_{ago}-millisphere.

3.2.3 *DETERMINATION OF DEGREE OF CARBOXYL SUBSTITUTION (DS)*

To determine the degree of oxidation, the number of carboxyl and carbonyl group was estimated using a titration method adapted from Zhang *et al.* (2012) with a few modifications: 0.1g of the S_{ago}-millispheres was crushed into a fine powder using pestle and mortar. The powder was then dispersed in 50mL of sterilized deionized water. To this resultant solution, 10mL of a 0.1M NaOH was added. The resulting slurry was heated and stirred until the starch

was fully dissolved. Once the solution had cooled, the 0.15M HCL solution was then use to back titrate to phenolpthalein end-point. Phenolphathalein dye was freshly prepared to 10%$^{w}/_{v}$ in 50% ethanol solution.

Equations used for DS determination:

$$n_{COOH} = 4(V_b - V)C_{HCL} \qquad \text{Equation 3.1}$$

V_b was recorded as the volume of acid consumed during the titration of the blank. V was recorded as the volume of titration of the sample, C_{HCl} recorded as the concentration of the acid and 4, the ratio of the total solution volume over the volume sampled for titration (Zhang *et al.*, 2012).

$$DS = \frac{162 \times n_{COOH}}{m_{dry} - 58 \times n_{COOH}} \qquad \text{Equation 3.2}$$

In which 162g/mol is the molecular weight of a gram unit and 58g/mol is the increase in molecular weight accounted for each carboxymethyl group substitution and m_{dry} is the mass of the dry sample (Zhang *et al.*, 2012).

3.2.4 *CHITOSAN CROSSLINKING: LINKAGE OF FREE REDUCING ALDEHYDE ENDS*

A 2% $^{w}/_{v}$ of chitosan in 0.5% $^{v}/_{v}$ hydrochloric acid was prepared. For the crosslinking reaction; 1.5g of dried S_{ago}-millisphere were pre-treated with 1mL of ethanol to prevent swelling. A 2.5mL of the 2%$^{w}/_{v}$ chitosan was added to the pre-treated beads and allowed to stand at room temperature for eight hours. To ensure efficacy of the crosslinking reaction, chitosan-crosslinked S_{ago}-millisphere were further crosslinked with a very dilute glutaraldehyde in a vaporized system (see Figure 3.1). For the glutaraldehyde solution usage for oxidation-crosslinking step (3:1 glutaraldehyde: hydrochloric acid) 1mL of solution was utilized for every 3g of S_{ago}-millispheres. The solution was evenly dispensed in a desiccator and the chitosan-coated S_{ago}-millispheres were then placed in the closed system and crosslinked for exactly 12 hours.

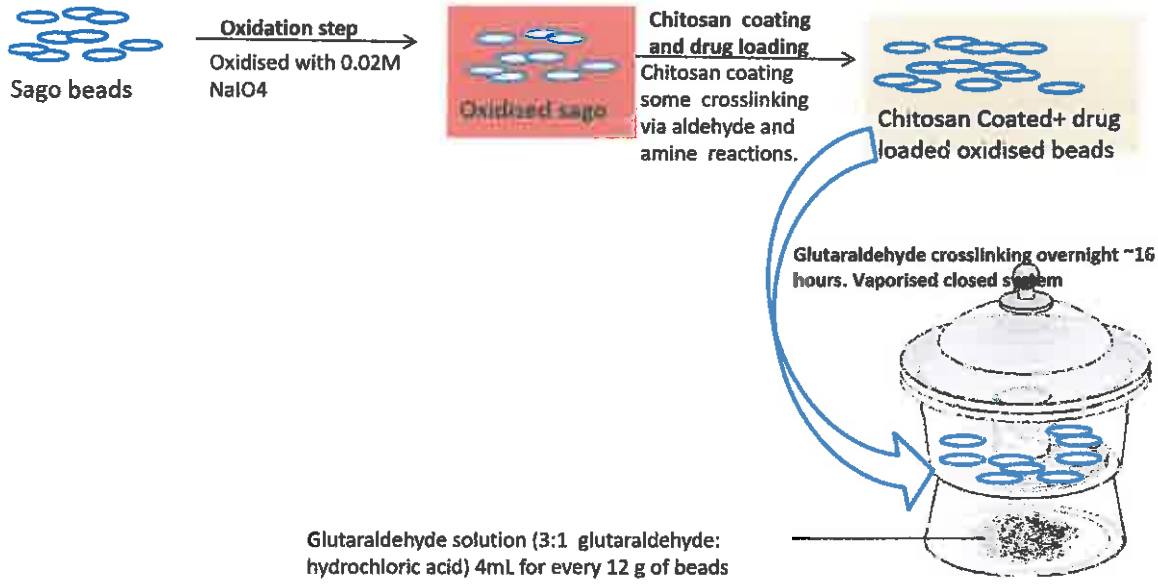

Figure 3.1: Schematic summary of surface oxidation method devised for pre-formed food-grade commercial Sago beads.

3.2.5 *Elucidation of chitosan crosslinking percentage of reducing carboxyl ends*

A method adapted from study by Ping He and peers (1998) was used to quantify chitosan crosslinking percentage via interactions between mucin and final S_{ago}-millisphere and crosslinked derivative ($Sago_{NaIO4}$) solution. A 0.5M mucin solution was prepared and the absorbance of the solution measured at 280nm, this was recorded as A_{muc}. $Sago_{NaIO4}$ (1g) was exposed to 1mL of the mucin solution for 15 minutes and the absorbance of the resultant mucin solution measured at 280nm. This was recorded as A_{syst} and the difference (A_{muc}-A_{sys}) between the 2 absorbance values ΔA was recorded as the fraction of chitosan that had not been crosslinked successfully. Thus, higher ΔA values correlate with low efficiency of the crosslinking method and vice versa.

3.2.6 *Physicochemical characterization of vibrational transitions via Fourier Transform Infrared spectroscopic analysis*

S_{ago}-millisphere were crushed using a coffee grinder and further ground into a fine powder with a pestle and mortar to ensure that the beads were fully crushed. FTIR spectrometer (Nicolette Impact 400 D FT-IR Spectrometer, ThermoFisher Scientific, UK) was used to observe the ATR profile of the ten samples and the additional S_{ago}-millispheres (crushed). The FTIR spectrometer allows detection of vibrational frequencies of chemical functional groups in response to infrared radiation. Analysis was repeated in triplicate and interferograms translated via the mathematical technique of Fourier Transformation before being presented as an infrared spectrum, which plots transmittance versus wave number.

3.2.7 *Viscosity and flow property elucidation for confirmation of altered physiochemical structure.*

To aid in characterization of the flow property of the commercial Sago beads and S_{ago}-millisphere, the rheological properties were analyzed with reference to the ten amylose/amylopectin 5%$^{w}/_{v}$ samples dissolved in a 0.1M sodium hydroxide. The Haake Modular Advanced Rheometer System (ThermoHaake MARS 69Modular Advanced Rheometer, Thermo Electron, Karlsruche, Germany) was used to generate rheograms and determine the viscosity (η) of the solutions. The instrument operating software (Haake RV20 version 2.3) evaluated Rheograms and aided in determining the viscosity of the solutions. Parameters used to collect data were: cone and plate gap 0.0051m, driver version 0.29, inertia 89051.00PA, A-factor 1.721x10-6Kg.m^2, M-factor 57.01rad/s, temperature 10°C, 25°C, 40°C damping 30.00 and utilized a C35/1° Ti sensor.

3.2.8 *Physicochemical characterization of crystallinity via X-ray diffraction.*

X-ray diffraction (XRD) is fundamental in comprehensive understanding of structure for both polymers and polymer composites. Based on the XRD profile, a polymer can be classified as crystalline, semi-crystalline, amorphous polymeric and composite materials, a key physicochemical property that affects the functionalization and applications possible. To collect XDR spectra (benchtop Miniflex 600 Rikagu, Japan) both un-oxidized and oxidized samples were ground into fine powder and a very thin layer placed in the XDR sample holder. Optical devices were fixed with a soller slit at 2.5°. Data was collected from 9^0 to 90° with a 2° step at 5° per minute.

3.2.9 *Physicochemical characterization of surface morphology via Scanning Electron Microscopy*

Both oxidation and crosslinking have an effect on the surface morphology of the OTC food-grade Sago beads. Scanning Electron Microscopy (SEM) imaging was performed to determine and prove any alterations in the overall surface of the bead. Each sample was placed sample holder and sputter-coated with gold for a period of no longer than 90 seconds. Coated and secured samples were then placed in a FEI Phenom™ Desktop Scanning Electron Microscope (Eindhoven, The Netherlands) to acquire SEM images.

3.2.10 *Analysis of thermal properties via Differential Scanning Calorimetry*

Differential scanning calorimetry (DSC) was used to determine thermal properties of the S_{ago}-millispheres. Accurately weighed finely crushed samples (10±0.4mg) were placed in a 40µL aluminum crucible pan. Crucibles were then sealed and pricked with a sterile needle (approximately 0.2mm opening) to obtain an open system. Powders from all three oxidation

time points were analyzed to determine any changes in thermal properties within the temperature range: 25 to 270°C using a Differential Scanning Calorimeter (Mettler Toledo DSC1 STARe System, Switzerland), method adapted from Fukuoka *et al.,* 2002.

3.3. RESULTS AND DISCUSSION

To detect if the aldehyde groups had been introduced, Tollen's reagent was used. Positive test using Tollens reagent resulted in silver Ag (s) precipitating out and forming a mirror-like coating around the test-tube, see Figure 3.2. The modified Sago beads showed a positive result for the test (see Figure 3.2). For positive reaction silver nitrate acts as an oxidizing agent which is reduced to form a silver precipitate at per equation: $(C_5H_{11}O_5)$ $-CHO + 2[Ag\ (NH_3)_2]\ OH \rightarrow (C_5H_{11}O_5)-COOH + 2Ag + 4NH_3 + H_2O$ (Sangsuck, 2010). The positive control (prepared using octadecanal) strongly correlates with the positive introduction of aldehyde groups to the Sago bead surface without any major loss to structural integrity.

Data from DS determination also correlated with preliminary Tollens' reagent data in suggesting successful oxidation method for the 30, 60 and 90-minute oxidation time periods. This was clearly observed through the formation of silver deposits on the experimental test-tube surface as seen on Figure 3.2a and b. This supports the assertion of the presence of surface aldehydes (Montazer *et al.*, 2012) on the Sago beads, the comparative control on Figure 3.2c showed a negative result for the test. The S_{ago}-millispheres also showed an increase in substituted carboxyl groups 0.119, 0.267 and 0.311 respectively for DS quantification values. Each S_{ago}-millisphere trial tested positive for aldehydes on the Tollens' test. Furthermore, increased DS with increased oxidation time correlated with the increases of aldehyde groups and thus a reduced percentage of carboxymethyl groups since they are chemically transformed via nucleophilic substitution (Rinaudo, 2010).



Figure 3.2: Tollens' test results for **(a)** negative control Sago beads **(b)** oxidized derivatives and **(c)** positive control; octadecanal.

3.3.1 *Physicochemical characterisation of vibrational transitions via Fourier Transform analysis*

Physicochemical modifications are further confirmed by the ATR-FTIR spectra comparing different oxidation profiles to the unmodified bead profile (see Figure 3.3). Increases in oxidation time results in the reduction of the O-H bond stretch within 3000-3500cm^{-1} (Jacobsen and Dickison , 1974) correlating to a positive di-aldehyde introduction by periodate reaction (Pu *et al.*, 2011). Sodium *meta*-periodate ($NaIO_4$) is a mild and specific oxidant that can convert cis-glycol groups in carbohydrates to reactive aldehyde groups. Unlike common oxidizing agents $NaIO_4$ is selective in its reaction and only targets the C2-C3 glycosidic links thus enabling the oxidation to occur at a specific site (Rinaudo, 2010). It is for the same reason that the 1500-2000cm^{-1} region (Zhang *et al.*, 2011) becomes more characteristic as this is the classic footprint region for aldehyde groups as also evident in the octadecanal spectrum (see Figure 3.4). Similarly, aldehydes groups are also associated with aromatic stretching in the region: 2500-3000cm^{-1}. This characterizes the hemiacetal aromatic structures that aldehydes can form when in high concentration (Kim *et al.*, 2000) as is the case with increased DS.

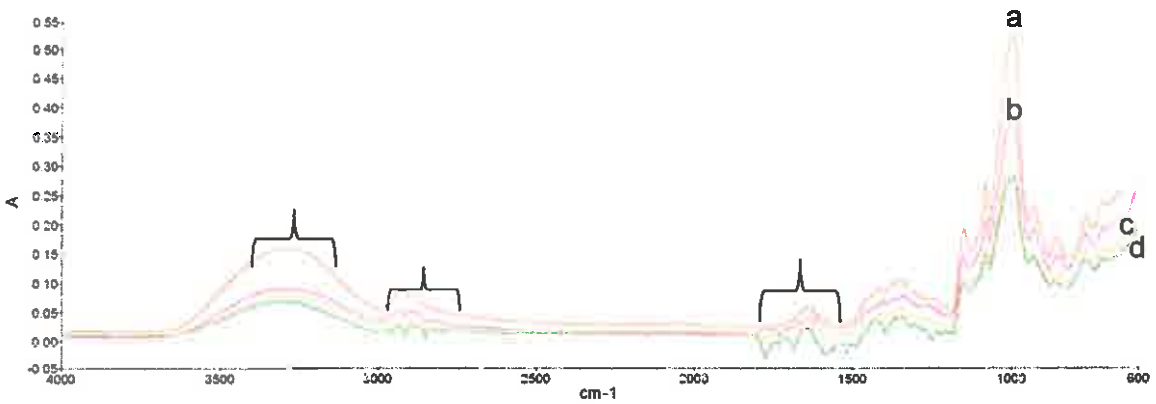

Figure 3.3: ATR-FTIR spectra of the three oxidized starch derivatives, a: for unmodified Sago, b:30-minute oxidation, d: 60-minute oxidation and c:90-minute oxidation tie trial samples. All ATR-FTIR profiles were obtained from 100 scans at a range of 4000-600cm^{-1} at a constant pressure of 130psi.

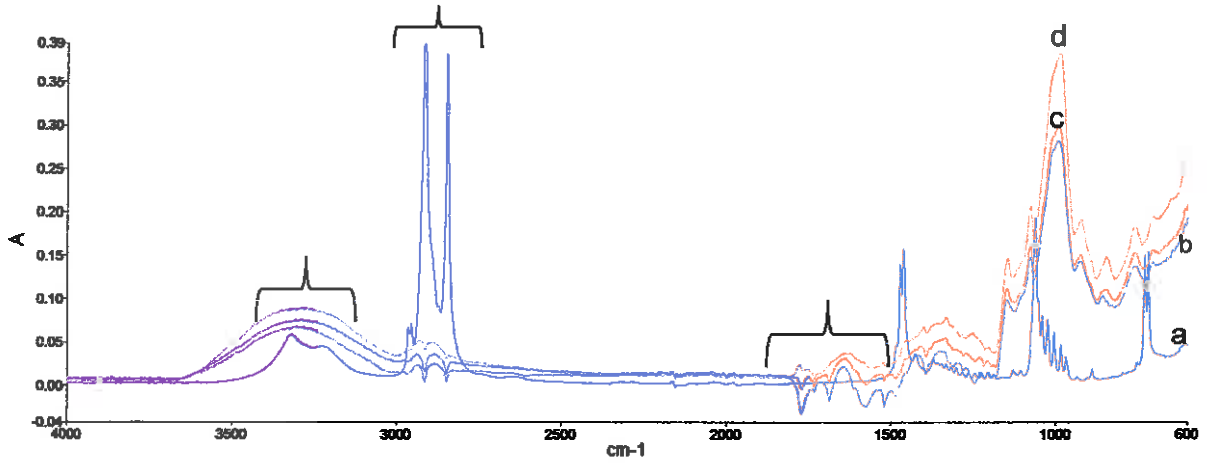

Figure 3.4: Fingerprint FTIR region for aldehyde groups with the use of a: octadecanal as a standard. The three oxidation time trials at d: 30 minutes, b:60 minutes and c: 90 minutes. All ATR-FTIR profiles were obtained from 100 scans at a range of 4000-600cm^{-1} at a constant pressure of 130psi.

3.3.3 *FLOW PROPERTY ANALYSIS FOR CONFIRMATION OF ALDEHYDE ALTERATION OF HYDRAULIC NATURE.*

Similarly, the rheology results also correlate with FTIR spectra. There is an evident increase in stability and linear flow properties observed in flow profile when comparing derivative and un-modified beads. As previously discussed by Chen and co-workers, reducing sugars have a stabilizing role in polymers due to the reducing ends reactivity and can display the stabilizing effect of water aiding in the linear polymer flow (Chen *et al.*, 2010). This can be expected if the introduction of aldehydes is successful since the overall reducing sugar percentage theoretically doubled due to successful surface oxidation. There is an overall reduction of viscosity (G) as observed in Figure 3.5 comparing unmodified and oxidized Sago with increasing oxidation time and thus the DS causes the change in flow properties. When polymers are chemically functionalized, the viscosity is altered which affects the dissolution (Molekul *et al.*, 2010), diffusion and ultimately the bioavailability of a drug in any polysaccharide-based delivery system (Singh *et al.*, 2007).

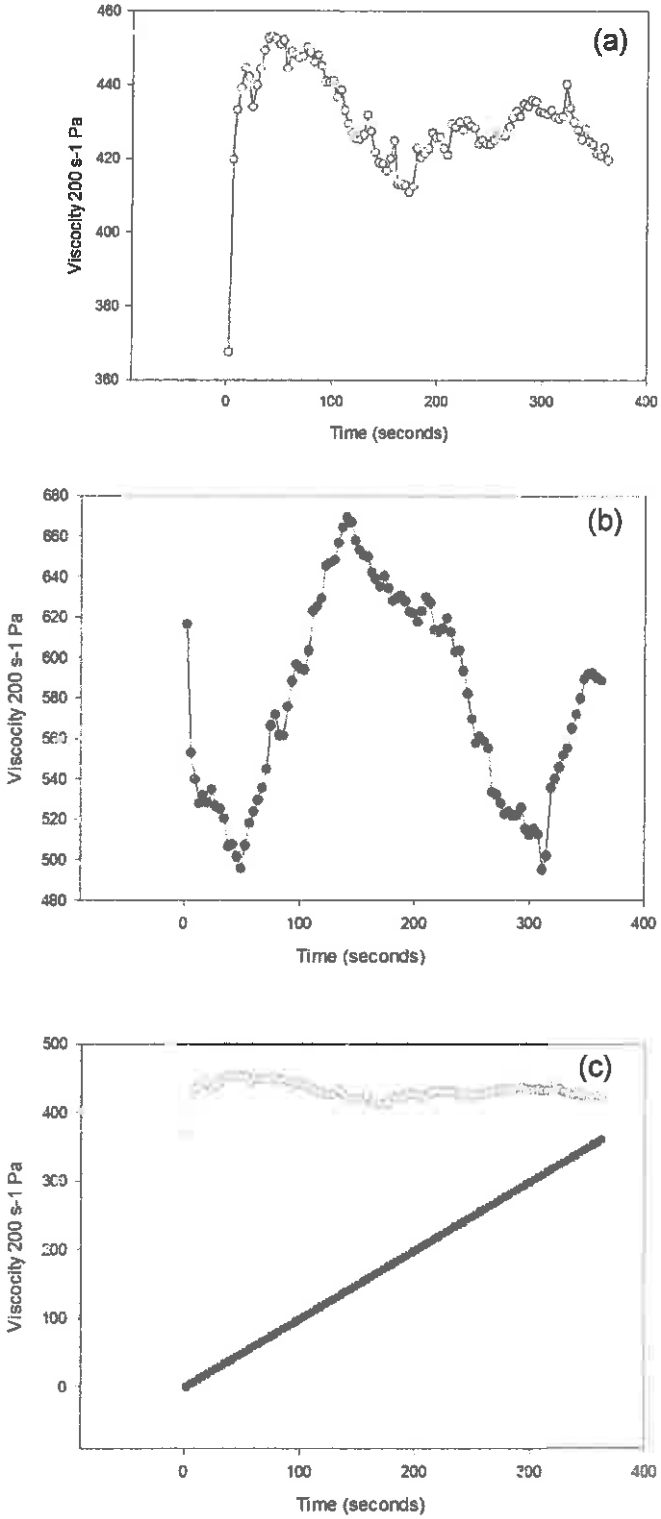

Figure 3.5: Rheology profiles of oxidized Sago in comparison to unmodified OTC Sago beads. Unmodified Sago: (a), 60-minute oxidation: (b), and (c): a comparison of oxidized and unmodified Sago.

3.3.4 *PHYSICOCHEMICAL CHARACTERIZATION OF CRYSTALLINITY VIA X-RAY DIFFRACTION*

The XRD profiles show a complete transformation of an amorphous polymer to a more crystalline structure as observed on the XRD diffracting pattern (see Figure 3.6). This can be

seen by the clear periodic peaks observed in the oxidized profile when compared to unmodified Sago beads. This is in line with and supports data from preliminary tests confirming the introduction of aldehyde groups to the surface. When aldehydes are specifically introduced to the Sago at C2 and C3 carbons, the dialdehydes introduced can interact to form a hemiacetyl (Kim *et al.,* 2000). This results in a more crystal lattice-type morphology that is more stable and much more organized as shown by analysis. XDR data correlates to rheology and FTIR data, confirming that the surface modification method does not disrupt the structural integrity of the commercial food-grade Sago bead but in fact readers the derivatives more stable with a much more lattice crosslinked structure.

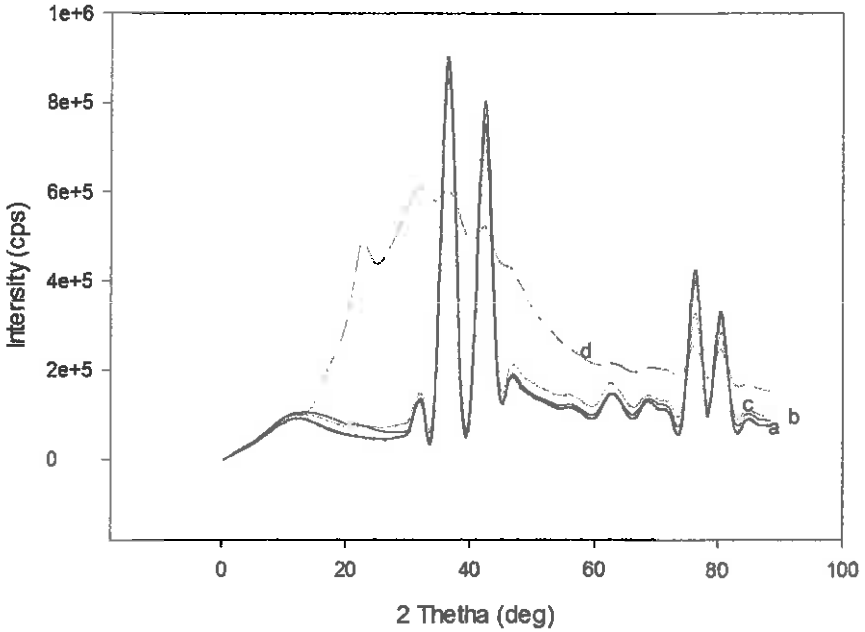

Figure 3.6: Powdered X-ray Diffraction profiles of d: unmodified Sago and modified derivatives a: 30-minute oxidation, b: 60-minute oxidation and c: 90-minute oxidation.

3.3.5 *CROSSLINKING PERCENTAGE ANALYSIS OF REDUCING END LINKAGE WITH CHITOSAN*

The absorbance-difference (ΔA) between the measured and theoretical values for the mixture of mucin/Sago system was calculated (see Table 3.1). The absence of any interaction is thus represented by a zero value for ΔA. The absorbance differences, measured between the pure mucin solution and the one that was exposed to the delivery systems, were close to zero. This result suggests that there was a very close to no interaction between chitosan and mucin (Deacon *et al.,* 1999). The absorbance differences obtained from the mucin/Sago system were very precise as the calculated differences of the value for the individual solutions, $\Delta A \approx 0$. Based on this observation, it is correct to assume little interactions between mucin solution and chitosan-crosslinked beads suggesting that the crosslinking reaction for the S_{ago}-millispheres was a complete success. Successful crosslinking allows for application in controlled and/or sustain drug release (Calinescu *et al.,* 2007). Furthermore, interactions with mucin provide for

muco-adhesive future application of the developed system for exploration (Coucke *et al.*, 2009). The dual nature of the applied modification system amplifies the benefits of the dual modification method as seen in most dual-type modification methods for starch (Karim *et al.*, 2008).

Table 3.1: Spectroscopic quantification of crosslinking percentage of modified Sago beads

A_{muc}	A_{sys}	ΔA
0.205	0.203	0.002
0.206	0.203	0.003
0.205	0.203	0.002
0.205	0.203	0.002
0.20525	0.203	0.002

A_{syst}: Absorbance at λ500 nm for the oxidized and crosslinked derivative
A_{muc}: Absorbance at λ500 nm for the standard mucin solution
A_{muc}-A_{sys}: ΔA unsuccessfully crosslinked chitosan fraction.

3.3.6 *Scanning Electron Microscopic evaluation of the Sago beads and the oxidized derivatives*

Scanning electron micrographs were collected for commercial, oxidized, and S_{ago}-millisphere beads to further illustrate and confirm data that there is in fact an alteration in surface structure (see Figure 3.7). The oxidized samples showed a slightly more porous surface compared to the unmodified and even less so the crosslinked S_{ago}-millispheres. If the oxidation method is successful, it is expected that there will be some repulsion between the electronegative oxygen atoms that have been introduces. Thus, it after oxidation, when the bead surface will be more porous. This aids in both drug loading and provision of reducing ends for crosslinking reaction. Subsequently, the crosslinked S_{ago}-millispheres should in fact be less porous, as observed, if the crosslinking method which links the di-aldehyde groups is in fact successful. This correlated to XRD and crosslinking percentage data further confirming successful physicochemical modification without disrupting the spherical oval structure of the commercial beads.

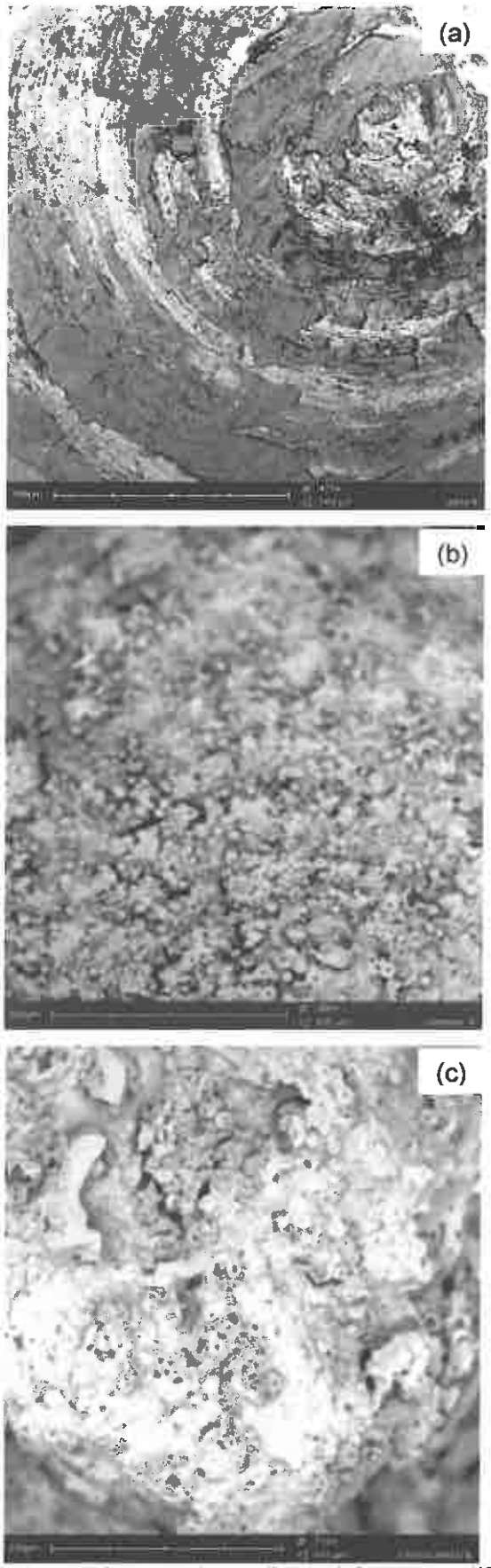

Figure 3.7: Scanning electron micrographs collected for unmodified (a) oxidized (b) and oxidized and crosslinked (c) Sago bead derivatives.

3.3.10 *THERMAL STABILITY AND CRYSTALLINITY EVALUATION OF PHYSICOMECHANICAL PROPERTIES*

Like XRD, rheology, SEM and DSC profiles for oxidized derivative yield a profile indicative of a more crystalline structure. From the profiles, as the oxidation period increases, the heat flow decreased (see Figure 3.8). This correlates with the proposed chemical crystallinity imparted by the introduction of aldehyde groups (Cava *et al., 2012)*. When profiles for all three derivatives were compared, the 30-minute oxidation trial properties exhibited a first order transition (Thielemans *et al. 2006*) indicative of a melting transition temperature (T_m) at 100°C. Whereas the 60 and 90-minute oxidation profiles exhibit a second order transition indicative of a glass transition temperature (T_g) at 30°C characteristic of crystalline polymers (LeCorre *et al.*, 2012). This further supports claims and observations on successful surface introduction of aldehyde groups to Sago bead surface.

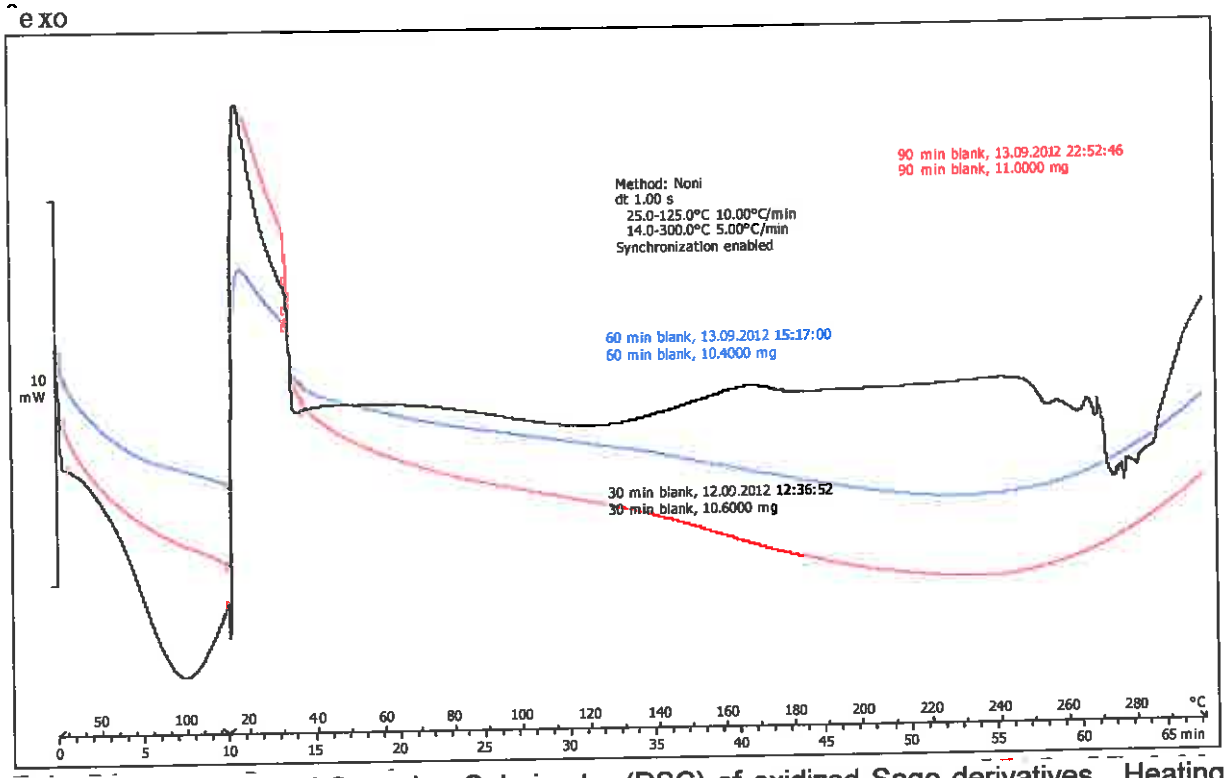

Figure 3.8: Differential Scanning Calorimetry (DSC) of oxidized Sago derivatives. Heating rate set at 10°C/min between the temperature range of 25°C and 300°C. Each DSC thermogram represents: 30-minute oxidation (black line), 60-minute oxidation (blue line) and 90-minute oxidation (red line).

3.4. CONCLUDING REMARKS

Periodate surface oxidation was proven to be a suitable method for oxidation of pre-formed starch particles. For this work, stabled-aldehyde S_{ago}-millispheres were produced at oxidation times 30,60 and 90-minutes to yield DS 0.119, 0.267 and 0.311 respectively. Results show a preserved and reinforced structural integrity and overall increased crystallinity. Furthermore,

S_{ago}-millisphere can be functionalized for application in pharmaceutical delivery of active agents. There is also a notable reduction in chemical grade excipients that could have a positive effect on patient compliance as the use of "herbal" (more natural) formulations is the rise as patients become more informed about formulation composition. Furthermore, there is an upward trend in the development of lifestyle diseases which must be treated most likely through orally administered formulations, as it continues to be the preferred route. This reality makes formulations such as the S_{ago}-millisphere potentially very cost effective due to limited chemical grade excipients required during production. The innate reduction to amylase sensitivity and increased crystallinity makes the S_{ago}-millispheres good candidates for colon targeting therapies as well as actives that may exhibit a narrow absorption window for therapeutic action.

CHAPTER 4
FACE-CENTERED CENTRAL COMPOSITE DESIGN FOR S_{AGO}-MILLISPHERE SYSTEM

4.1. INTRODUCTION

To maximize pharmaceutical applications of starch, the physiochemical and physicomechanical properties are modified to yield superior derivatives that render the copolymer more applicable for specific drug delivery platforms (Onofre et al., 2009). Chemical modification methods for starch are grouped into four types (Kaur et al., 2012). The chemical methods involve various reactions targeted at the three available hydroxyl groups and the degree of modification varies based on the genetic origin of the starch and the modification method (Sangseethong et al, 2005). Modification products tend to have properties that allow for enhanced drug loading in some systems (Huang et al., 2013), improved swellability in some hydrogels (Dragan and Apopei, 2011) and classically act as stabilizers that improve formulation shelf-life (Thakur et al., 2013). The focus for this study was the use of food grade material in the development of a gastro-retentive controlled release system for the delivery of propranolol. Oxidized derivatives have been previously shown to possess greater drug entrapment efficiencies and promising stabilizing properties in some anionic starch particles (Huang et al., 2013).

In this study, a bi-reagent modification method was employed in the development of the novel Sago system with an aim of functionalizing the food-grade starch and increasing efficacy of propranolol delivery. Very limited research has been undertaken on the solid-state chemical modification of pre-formed starch particles as well as the reduced excipient formulation targeted at control release of propranolol as has been set out in this study. The pharmaceutical performance of the produced S_{ago}-millispheres was evaluated and characterized for application in drug delivery. The chemical modification of the physiochemical properties rendered the beads more suitable for the delivery of oral formulations. There was a keen interest in increasing the gastro-retentive character of the beads and increasing the efficacy of propranolol having a narrow absorption window while reducing chemical grade reagents used in the formulation.

The *in vitro* testing was designed to test for performance of the designs to allow for the selection of the best performing system to progress to preclinical trials. Furthermore, in vitro drug release studies- allow for the simulation of *in vivo* environment to allow the elimination of non-suitable formulation and select for superior design. Utilizing the one-variable-at-a-time approach the designs was initially narrowed down to 3 formulations with varying oxidation

times (30, 60 and 90 minute of oxidation). The chitosan and glutaraldehyde concentrations were kept constant and the DS, drug loading efficiency and structural integrity used as measurable responses. The combination of these excipients was then utilized to generate formulations using a strong statistical Design of Experiment (DOE).

The design process simultaneously considered all design variables, constants as well as the possible effect of each component/process and potential effect to design thereof (Pongstabodee et al., 2012). After the one-variable-at-a-time screening process (Pabari and Ramtoola, 2012), three factors, i.e. chitosan concentration, oxidation time and drug loading efficiency were evaluated. A face-cantered central composite design (FCCCD) response surface methodology (RSM) was then applied to optimise the responses for sustained release. Each formulation was prepared in triplicate and subjected to drug dissolution studies, physicomechanical analysis to determine optimal design for sustained release and structural integrity (Balachandran et al., 2012). Once the formulations were developed and optimized, the physicochemical properties of the optimized characterized and the degree of oxidation (DS), drug loading efficiency, performance efficiency as well as molecular structure were analysed.

4.2. MATERIALS

Food-grade sago starch was purchased over-the-counter (OTC) at Shoprite Checkers, food-grade chitosan (Warren Chem Specialities, batchno:WA200703003), chemical grade Sodium (meta) Periodate, Propranolol hypochloride (≥99% pure), sodium chloride (≥99 pure),(±)-1-Isopropylamino-3-(1-naphthyloxy)-2-propanol hydrochloride (≥99% pure), Sodium phosphate, Dinitrosalicylic acid, sodium potassium tartrate tetrahydrate, water soluble starch, α-Amylase (≥99% pure), DL-Propranolol hydrochloride (≥99% pure), absolute ethanol (≥99% pure), Hydrochloric acid (HCL) (≥32% pure), Glutaradehyde 50% wt solution, Dimethylfoxyde (≥99% pure), Sodium phosphate monobasic salt and other chemicals were of analytical grade and purchased at Sigma Aldrich, through the South African distributor.

4.3. METHODS

The inclusion of the excipient within these formulations was designed to optimize the properties of a physical oral dosage form and to enhance the bioavailability/release of propranolol. Fractional dissolution is a measure of the amount of drug released at a specific set-time point. The fractional dissolution was assessed over a 24-hour period hours because most, if not all, the effective loaded propranolol should be released from the dosage form during this period. The formulations that achieved the highest drug loading and fractional

dissolution were highly desirable. The fractional dissolution analysis indicated that a high concentration of chitosan and moderate oxidation period is beneficial to the formulation.

4.3.1 *Surface oxidation of Sago via optimized method*

To prepare the oxidized beads, a 0.02M $NaIO_4$ solution with 1.27%$^{v}/_{v}$ HCL and 42.37%$^{v}/_{v}$ ethanol was prepared. Oxidized samples were prepared at three different time points: 30, 60 and 90 minutes for oxidation reaction duration. The oxidative reactions were carried out in sealed amber 250mL flask. To ensure that there were no further side-reactions, samples were thoroughly rinsed with distilled and deionized sterile water (one litre for rinsing every 6g of oxidized beads). Excess water was then carefully removed using filter paper and beads dried in the fume hood in an amber container.

4.3.2 *Drug loading of model drug into optimized S_{AGO}-millisphere system*

Oxidized derivatives were dried in a sterile fume hood for 4 hours. A 2%$^{w}/_{v}$ of chitosan in 0.5%$^{v}/_{v}$ hydrochloric acid and 15mg/mL propranolol solution was prepared; this was named referred to as: DC (drug loading +crosslinking solution) solution. For the drug loading-crosslinking reaction; 1.5g of dried oxidized beads were pre-treated with 1mL of ethanol to prevent swelling and 2.5mL of the DC solution was added to the pre-treated beads and allowed to stand at room temperature for up to 8 hours.

4.3.3 *Quantification of oxidized degree of substitution for oxidized Sago derivatives*

To determine the degree of oxidation, the number of carboxyl and carbonyl group was estimated using a titration method that quantifies the degree of substitution (DS) adapted from Zhang *et al.* (2012) with a few adaptations: 0.1g of the oxidized sago starch was crushed into a fine powder using pestle and mortar. The powder was then dispersed in 50mL of sterilized deionized water. To this resultant solution, 10mL of 0.1M NaOH was added. The resulting slurry was heated and stirred until the starch was fully dissolved. Once the solution had cooled, the 0.15M HCL solution was then use to back titrate to phenolpthalein end-point. Phenolphathalein dye was freshly prepared to 10% $^{w}/_{v}$ in 50% ethanol solution.

Equations used for DS determination:

$$n_{COOH} = 4(V_b - \mathrm{V})C_{HCL}$$

V_b was recorded as the volume of HCL consumed during the titration of the blank. V was recorded as the volume of titration of the sample, C_{HCL} is the concentration of the HCL and 4 is the ratio of the total solution volume over the volume sampled for titration.

$$DS = \frac{162 \times n_{COOH}}{m_{dry} - 58 \times n_{COOH}}$$

In which 162g/mol is the molecular weight of a GU and 58g/mol is the increase in molecular weight accounted for each CM group substitution and m_{dry} is the mass of the dry sample.

4.3.4 *ARYL CHITOSAN CROSSLINKING BY GLUTARALDEHYDE*

To ensure efficacy of the crosslinking reaction, chitosan-crosslinked beads were further crosslinked with a very dilute glutaraldehyde in a vaporized system. For glutaraldehyde solution (3:1 glutaraldehyde: hydrochloric acid), 1mL was used for every 3g of beads. The solution was evenly dispensed in a desiccator and the chitosan-coated oxidized beads were then placed in the closed system and crosslinked for exactly 12 hours.

4.3.5 *THERMAL GRAVIMETRIC ANALYSIS OF THE OPTIMIZED BEAD SYSTEM*

Thermal gravimetric analysis (TGA) of the optimized formulation was carried out with the utilization of a Thermogravitational Analysis System-4000 (Perkin Elmer, Waltham, MA, USA) under constant nitrogen atmosphere. Accurately weighed samples (9.5mg i.e. average S_{ago}-millisphere) were placed within the crucible. The weight percentage, the rate of degradation, onset of degradation and the end-point of degradation was determined. The TGA was run with at heating rate of 10°C/min at range: 30°C -700°C.

4.3.6 *PHYSICOCHEMICAL CHARACTERIZATION OF VIBRATIONAL TRANSITIONS VIA FOURIER TRANSFORM ANALYSIS*

Sago beads were crushed using a coffee grinder and further crushed with pestle and mortar to ensure that the beads were powdered. Fourier Transition Infrared Red spectrometer (Nicolette Impact 400 D FT-IR Spectrometer, ThermoFisher Scientific, UK) was used to observe the ATR profile of the ten samples and the additional Sago beads (crushed). The FTIR spectrometer allows detection of vibrational frequencies of chemical functional groups in response to infrared radiation. Analysis was repeated in triplicate and interferograms translated via the mathematical technique of Fourier Transformation before being presented as an infrared spectrum, which plots transmittance versus wave number.

4.3.7 *RHEOLOGY: VISCOSITY AND FLOW PROPERTY ELUCIDATION*

To aid in characterisation of the flow property of the optimized formulations, the rheological properties were analyzed with reference unmodified Sago, 5% $^{w}/_{v}$ samples dissolved in a 0.1M sodium hydroxide were prepared. The Haake Modular Advanced Rheometer System (ThermoHaake MARS 69 Modular Advanced Rheometer, Thermo Electron, Karlsruche, Germany) was used to generate rheograms. The instrument operating software (Haake RV20 version 2.3) evaluated Rheogrm with parameters: cone and plate gap 0.0051m, driver version 0.29, inertia 89051.00PA, A-factor 1.721x10-6Kg.m2, M-factor 57.01rad/s, temperature 10°C, 25°C, 40°C damping 30.00 and utilized a C35/1° Ti sensor. The resulting data was processed

using Sigma plot SigmaPlot (Systat Software, San Jose, CA). The assumption for the dissolved macromolecule is based on the permanent physiochemical change associated with successful chemical crosslinking.

4.3.8 *Physicochemical characterisation of crystallinity X-ray diffraction for optimized derivatives*

As described in previous chapter, X-ray diffraction (XRD) is fundamental in comprehensive understanding of structure for both polymers and polymer composites. Based on the XDR profile, a polymer can be classified as crystalline, semi-crystalline, amorphous polymeric and composite materials, a key physicochemical property that affects how the functionalization and applications possible. To collect XRD spectra (via a benchtop Miniflex 600 Rikagu, Japan) both un-oxidized commercial and oxidized samples were ground into fine powder and a very thin layer placed in the XRD sample holder. Optical devices were fixed with a soller slit at 2.5°. Data was collected from 9^0 to 90° with a 2° step at 5° per minute

4.3.9 *Quantification of chitosan crosslinking percentage of optimized Sago derivatives*

A method adapted from study by Ping He and peers (1998) was used to quantify chitosan crosslinking percentage via interactions between mucin and final oxidized (He *et al.,* 1998) and crosslinked derivative S_{ago}-millispheres. The absorbance of a 0.5M mucin solution was prepared and the absorbance of the solution measured at 280nm, this was recorded ta A_{muc}. $Sago_{NaIO4}$ (1g) was exposed to 1mL of the mucin solution for 15 minutes and the absorbance of the resultant mucin solution measured at 280nm. This was recorded at A_{syst} and the difference (A_{muc}-A_{sys}) between the 2 absorbance values ΔA was recorded as the fraction of chitosan that had not been crosslinked successfully. Thus, higher the ΔA correlates to low efficiency of the crosslinking method and vice versa.

4.3.10 *Maltose standard curve for quantification of amylase sensitivity*

To generate a standard curve for maltose, a maltose stock solution was prepared in a 0.02M Sodium phosphate buffer, pH 6.9. Serial dilutions of the stock solution were then prepared and exposed to the 3,5-dinitrosalicylic acid color reagent. The dinitrosalicylic acid color reagent was freshly prepared by dissolving 0.1%$^w/_v$ 3,5-dinitrosalicylic acid in 2M NaOH with 3%$^w/_v$ sodium potassium tartrate tetrahydrate added to the final solution. The color agents were then thoroughly mixed with the respective maltose in a 1:5 volume ratio and the absorbance at 540nm measured after the solution had been allowed to stand for exactly 5 minutes at room temperature.

4.3.11 *Optimized formulation amylase sensitivity analysis*

The α-Amylase enzyme 5µg/mL in a 0.02M sodium phosphate buffer, pH 6.9 and 0.006M sodium chloride was freshly prepared for each experiment. A 0.5mL aliquot of the enzyme solution was added to 4.1%$^{w}/_{v}$ Sago solution in sodium phosphate buffer. Aliquots were incubated at room temperature for 3 minutes and then an additional 5 minutes following the addition of add 1mL dinitrosalicylic acid reagent. The resulting reaction solution was then placed in the boiling water bath for 5 minutes, cooled and the absorbance at λ 540nm measured. The observed absorbance was then used to determine the liberated maltose equivalence using the maltose standard curve. The method was repeated in triplicate for both unmodified commercial sago and the optimized S_{ago}-millisphere formulations and the resulting data compared. To calculate the amount of starch hydrolyzed, the maltose content was multiplied by 0.9 (Rajan *et. al.,* 2006).

4.3.12 *In vitro drug release profiling: standard curve*

A standard solution of 20mg/mL of propranolol was prepared and the maximum wavelength determined as shown in Figure 2.1.1 was generated using the UV-Vis spectroscopy. Following the wave scan, the residual standard solution, not utilized in the wave scan, was diluted and the absorbance of the dilute samples measured at 290nm. This data was used to generate the standard curve on Figure 2.2.2

4.3.13 *In vitro drug Release Profiling: Dissolution*

Drug release was determined using capsules that were placed in 900mL USP simulated buffer at 37.5 ◦C for 24h and the absorbance measured using a UV/VIS spectrophotometer at 290nm. A 5mL sample was withdrawn and filtered through a 0.44µm Millipore Millex injection filter were placed within an Orbit Shaker Incubator (LM-530-2, MRC Laboratory Instruments Ltd, Hahistadrut, Holon, Israel) at 37°C at 50rpm. All samples collected were 5mL aliquots and were replaced with blank buffer. All buffers and samples collected or utilized were filtered through a 0.22µm Millipore Millex injection filter (Billerica, MA, USA) and kept at an equilibrated temperature.

4.4. Results and Discussion

4.4.1 *Standard curve*

Like other chromogenic substances, propranolol can absorb and emit UV light. As observed in Figure 4.1 the finger-print region for propranolol was identified at λ201-245nm as well as 290nm. The peak at λ 290nm was selected as the linear peak region consistent with the generally accepted region for propranolol (Venkatesh *et al.*, 2007). Based on Beer- Lamphert

law, an overall linear relationship was assumed to correlate light absorption and concentration via the equation: $A = \varepsilon l\,[C]$ (Reed *et al.*, 2007). The resulting standard curve in Figure 4.2 showing a linear correlation and allowing for further quantification of drug content in formulations through the derived equation: $y = 0.262554x + 0.0246$. This was utilized for propranolol quantification throughout the study.

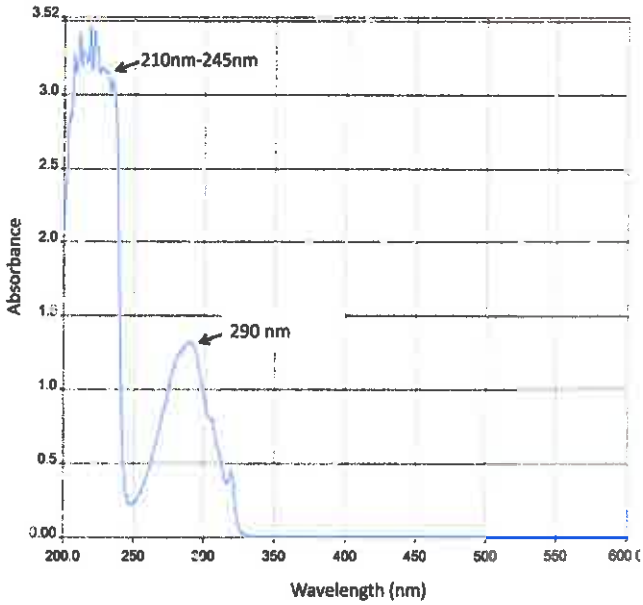

Figure 4.1: UV-VIS scan from λ 200-600nm to aid in confirmation of specific absorption unit peaks for propranolol solution at room temperature. The detection peak was confirmed at 290 nm.

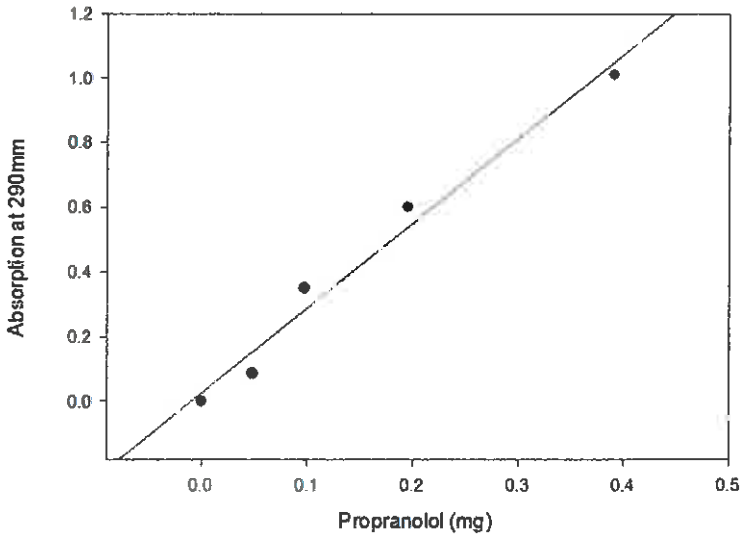

Figure 4.2: Standard curve generated using UV-VIS absorbance units for specified concentrations (mg) at ʎ 290nm. With Rsq = 0.977164 and equation: y=0.0246+0.262554x

4.4.2 *In vitro drug release characterization of S_{AGO}-millisphere designs*

Based on the nature of the devised delivery system, the predicted and expected drug release profile was a first order pharmaceutical kinetic profile. Mathematical predictions were based on an algorithmic Microsoft Excel add on; DDSolver. The drug release profiles for formulations with the lower chitosan percentages i.e. 0.1% and 1% $^{w}/_{v}$ showed an immediate/burst release formulation release profiles. Although in a few designs settings and with a select class of active agents, burst release is in fact selected for, it is not desired. Burst release is typically not predictable and associated with repeated dosages which can in turn affect patient compliance, cost escalation for patience and dosage related side effect (Huang and Brazel, 2001).

These results are consistent with initial the hypothesis as there is no matrix to allow for a more controlled/sustained release profile. In most cases matrix systems exhibit controlled release profile based on the pore size of the particular system (Balakrishnan, and Jayakrishnan, 2005). In this study, the reduced chitosan concentration has two possible impacts. Firstly, the reduction of available amine groups (Carbinatto *et al.*, 2012) which in turn reduces the quantity of crosslinked imine derivatives from the nucleophilic condensation reaction between the oxidized Sago derivatives and activated chitosan solution (Kato *et al.*, 2003). Although the secondary crosslinking method with GLA may increase the fraction of the chitosan crosslinking quantity it may also replace the amine groups which are donated by the activated chitosan groups (Brouillet *et al.*, 2008). Based on release profiles for formulations: 4-7, 9, 10 and 13 were eliminated as possible applicable formulations (see release profiles in Figure 4.3- 4.8).

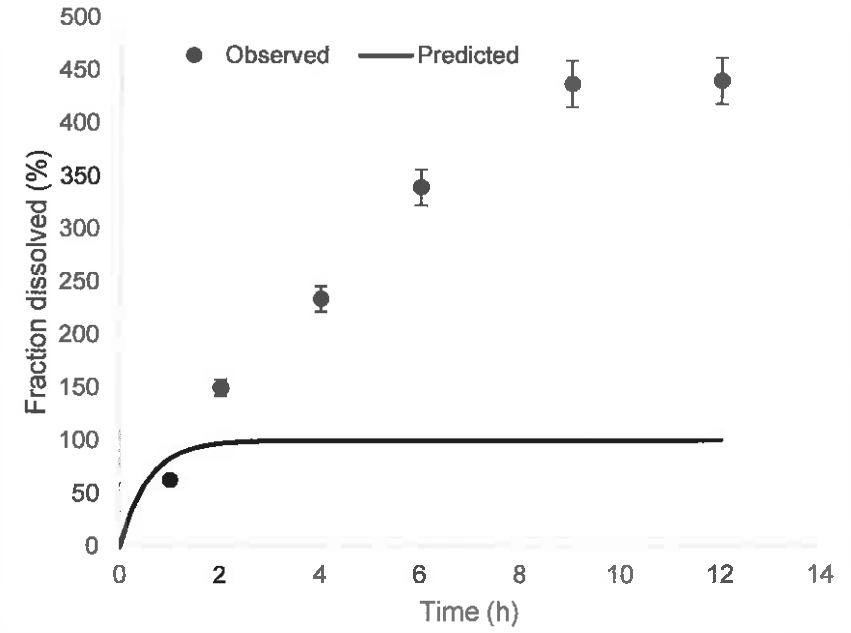

Figure 4.3: Release profiles for design formulation 4; with 90-minute oxidation and a 0.1%$^{w}/_{v}$ chitosan crosslinking solution at room temperature.

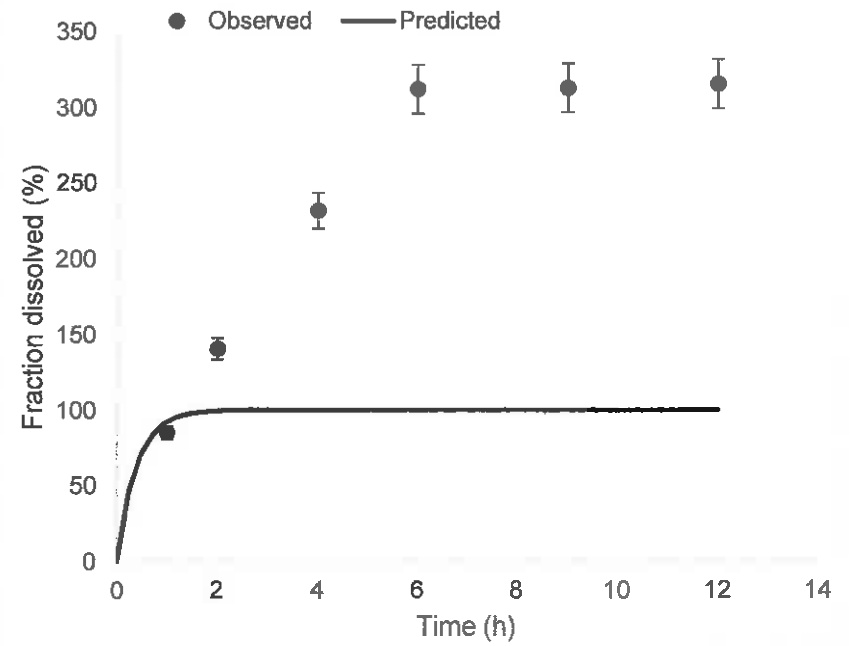

Figure 4.4: Release profiles for design formulation 7: with 60-minute oxidation period and crosslinked with a 0.1%$^{w}/_{v}$ chitosan solution at room temperature.

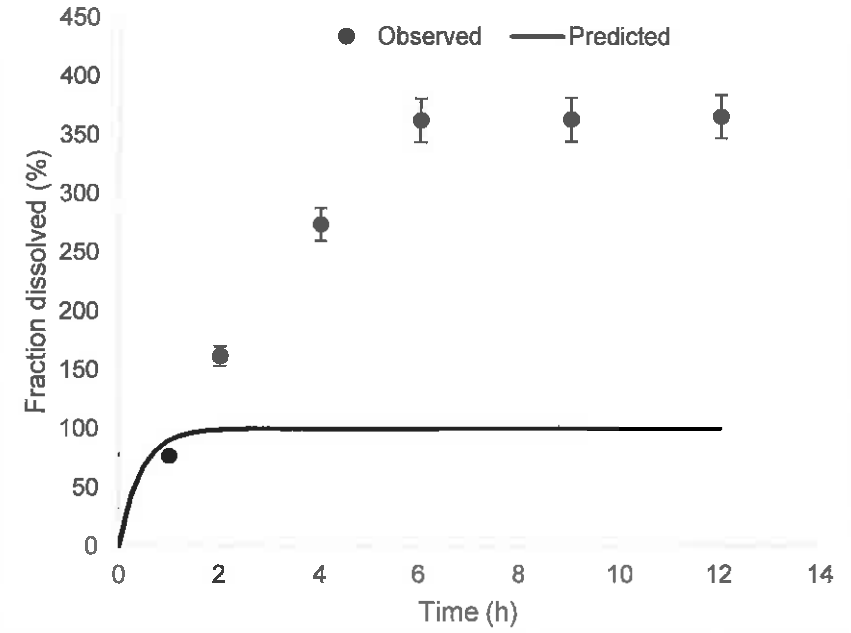

Figure 4.5: Release profiles for design formulation 9; with 30-minute oxidation period and crosslinked with a 0.1% $^{w}/_{v}$ chitosan solution at room temperature.

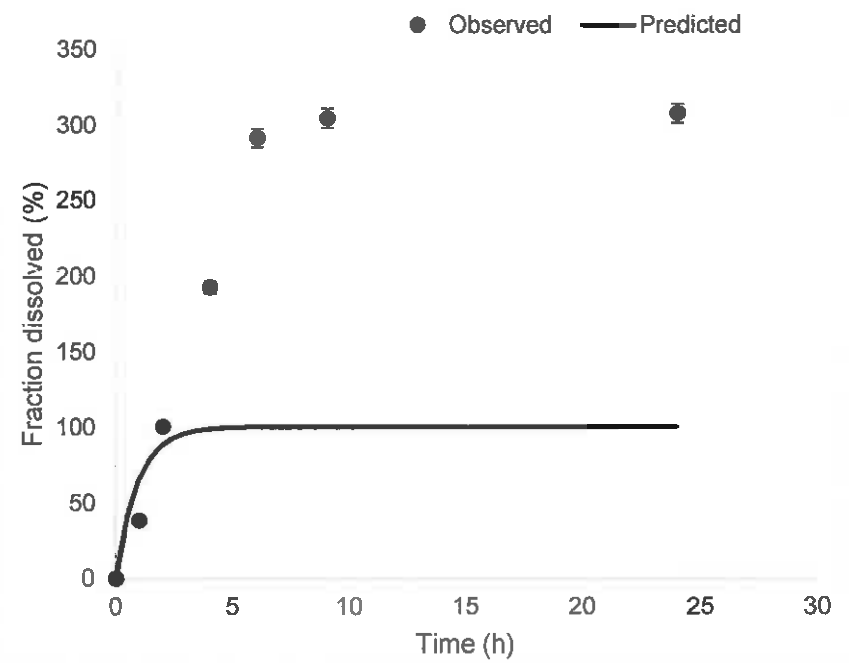

Figure 4.6: Release profiles for design formulation 10; with 90-minute oxidation period and crosslinked with a 1.05% $^{w}/_{v}$ chitosan solution at room temperature.

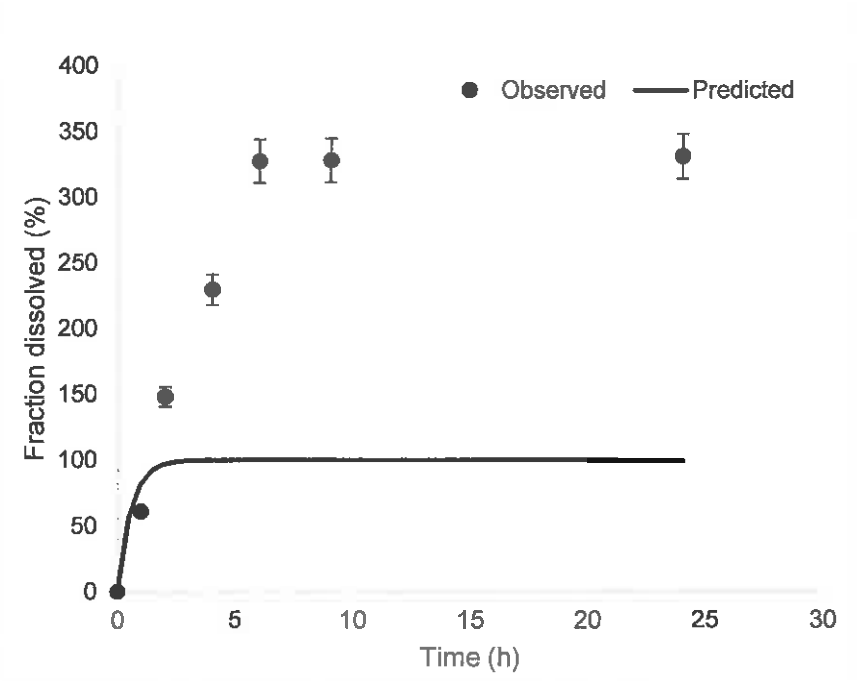

Figure 4.7: Release profile for design formulation 5 and 6 (average); with 60-minute oxidation period and crosslinked with a 1.05%$^{w}/_{v}$ chitosan solution at room temperature.

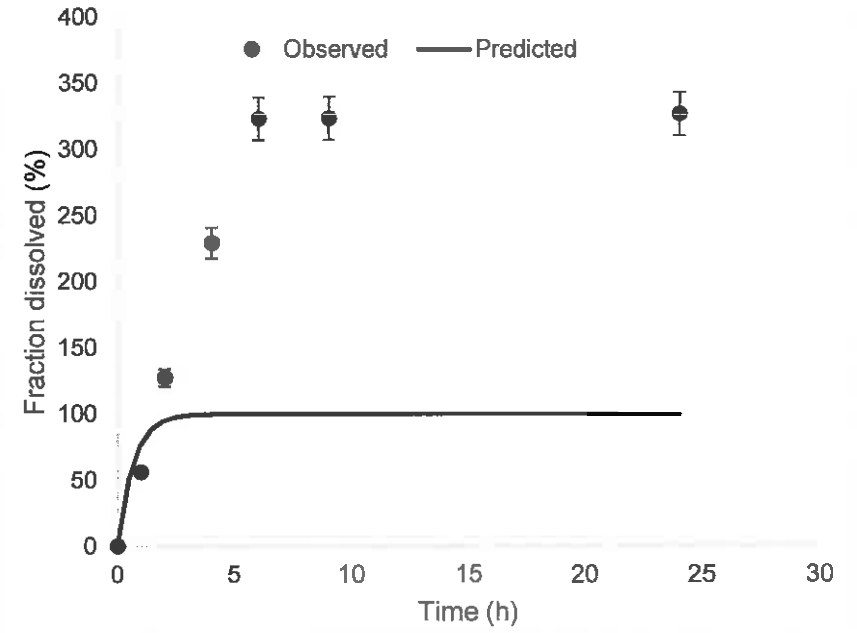

Figure 4.8: Release profiles for design formulation 13; with 30-minute oxidation period and crosslinked with a 1.05%$^{w}/_{v}$ chitosan solution at room temperature.

There is, however, a distinct difference in release profiles for formulations that have a higher chitosan percentage. As observed in figures 14.7 and 14.8, there is a clear first order release profile that is indeed expected for a matrix system of this nature and design. The increase in chitosan concentration provides an abundant increase in amine groups to allow for the

formation of a porous matrix lattice that allows for controlled and sustained release as shown in SEM micrographs previously. A noticeable variance in Figure 4.11 also proves that the aldehydes introduced via periodate oxidation influence the efficiency of crosslinking. Also evident is that that formulation 3 (Figure 4.9) outperforms formulation 1 (Figure 4.10) and thus the performance of the formulation is directly proportional to both the chitosan concentration as well as the quantity of aldehyde groups i.e. degree of substitution (DS). The free aldehyde groups provide reducing ends to facilitate the nucleophilic condensation reaction required for chitosan crosslinking (Hennink and van Nostrum 2012). The GLA usage in the sample preparation is thus a control measure; the main crosslinking is evidently due to spontaneous reaction between oxidized derivatives and activated chitosan.

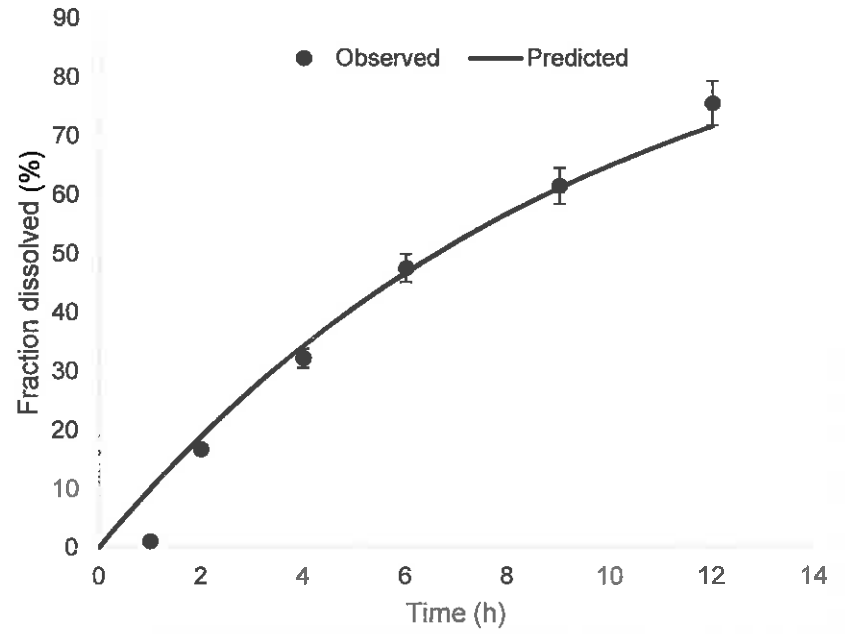

Figure 4.9: Release profiles for design formulation 3; with 90-minute oxidation period and crosslinked with a 2.00%$^{w}/_{v}$ chitosan solution at room temperature.

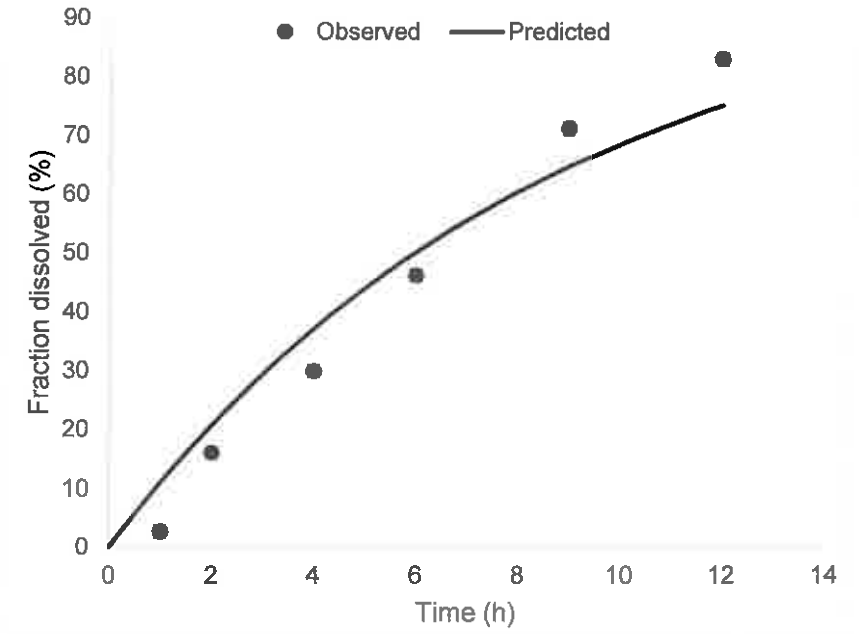

Figure 4.10: Release profiles for design formulation 1; with 60-minute oxidation period and crosslinked with a 2.00%$^{w}/_{v}$ chitosan solution at room temperature.

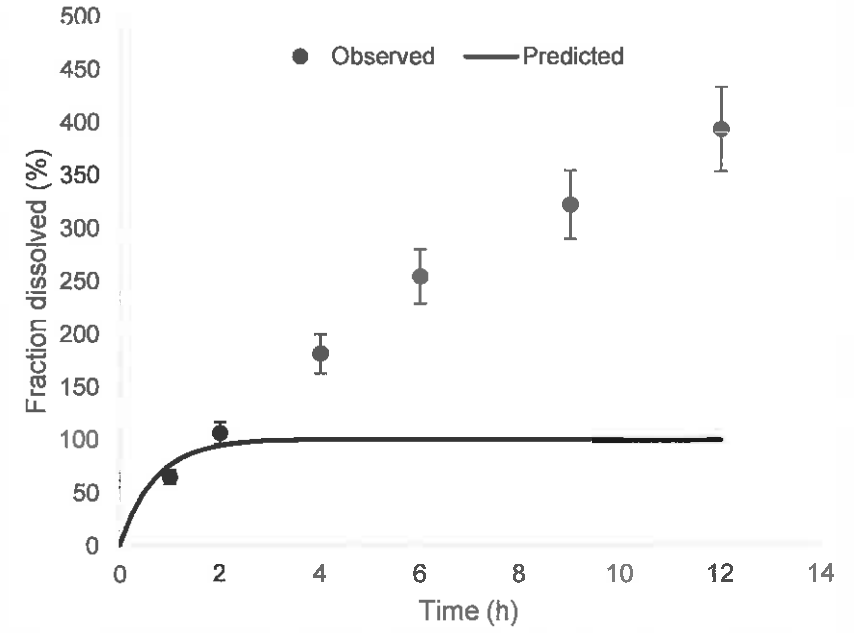

Figure 4.11: Release profiles for design formulation 2; with 30-minute oxidation period and crosslinked with a 2.00%$^{w}/_{v}$ chitosan solution at room temperature.

Data from DS determination (summarized on Table 4.1) confirms a successful oxidation method for the 30, 60 and 90-minute oxidation times. The derivatives showed 0.119, 0.267 and 0.311 respectively. The reproducibility of the DS result confirms a standard modification method; DS results of which can be reproduced. Furthermore, increased DS with increased oxidation time correlates with the increase of aldehyde groups and thus a reduced percentage

of carboxymethyl groups, as they are chemically transformed to aldehyde groups by the proposed nucleophilic reaction (Rinaudo, 2010). There is also a correlation between the efficiency of the formulations and aldehyde content as mentioned previously. Furthermore, the increase in oxidation efficiency has a positive impact on drug loading. There is an inflection point; however, in which if the oxidation efficiency is low combined with a low chitosan concentration, the drug loading efficiency also increases as observed in formulation 13. This is based on the increased access to the core of the Sago beads provided by the surface oxidation.

Table 4.1: Design study summary for all 13 face-centered central design formulations.

Formulation	Oxidation time (min)	Chitosan conc. (%w/v)	Drug loading efficiency (%)	DS
1	60	2.00	83.06	0.27
2	30	2.00	64.19	0.31
3	90	2.00	75.54	0.12
4	90	0.10	62.80	0.31
5	60	1.05	60.88	0.27
6	60	1.05	60.88	0.27
7	60	0.10	84.85	0.27
8	60	1.05	60.88	0.27
9	30	0.10	76.62	0.12
10	90	1.05	38.12	0.31
11	60	1.05	60.88	0.27
12	60	1.05	60.88	0.27
13	30	1.05	55.88	0.12

***Formulation variables: chitosan concentration (0.1, 1.05 and/or 2% weight per volume), Calc. MDT: Calculated Mean dissolution time and DS: Degree of substitution, face-centered central composite design for optimizing your formulation. There are 3 center points.

Based on the observed responses i.e. drug loading efficiency, dissolution efficiency and DS the ideal sample preparation was confirmed to be with 21.5428%$^{w}/_{v}$ chitosan concentration and with the best performing formulations at 73.0199-minute oxidation. All the responses were analyzed using the statistical analysis to predict with the highest precision possible, the optimal condition for a design formulation optimized for the required responses. The parameters as shown in Figure 4.12 (with 73.0199 seconds and 1.5428% w/v chitosan).

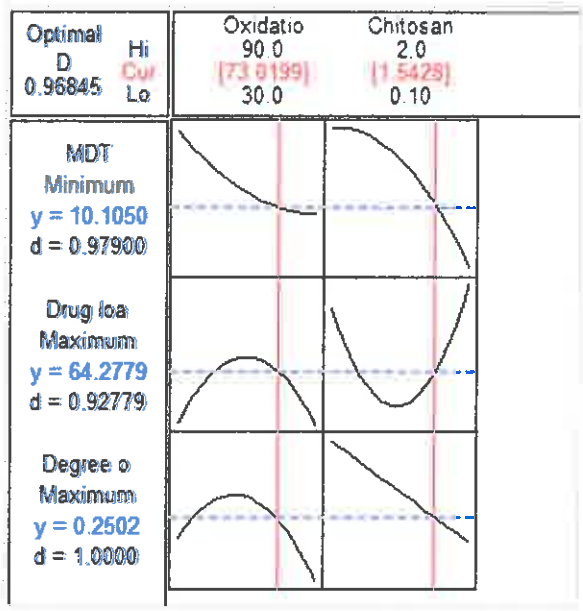

Figure 4.12: Optimized FCCCD statistical prediction for the optimized formulation.

4.4.3 *OPTIMIZED FORMULATION CHARACTERIZATION*

The design formulation was analyzed for performance through dissolution and released propranolol over a 24-hour period and showed a first-order-type release kinetics (see Figure 4.13). Furthermore, the derived beads did not dissolve in simulated dissolution media further confirming the chemical modification which interferes with generic amylase activity (Chen *et al.,* 2010). The chitosan crosslinking implicitly increased the gastro-retentive nature of the formulation, which when coupled with sustained release can prove quite superior for the delivery of propranolol and other NAW drugs alike. Typically, gastro-retentive formulations must be approximately 13mm in diameter to be retained within the gastric region for a desired period (Nayak *et al.*, 2010) which is more than the average diameter of the optimized formulation at 0.45mm.

Further confirmation of chemical alteration is evident on the TGA profile in Figure 4.14. From the two profiles, it is easy to mistake the derivative to be less stable when compared to unmodified bead. However, it should be noted that the profile has changed completely, like that of chitosan as seen in other references (Pradhan *et al.,* 2014). The observed profile is more indicative of a more crosslinked mesh that does not disintegrate easily and has rubber-like (Phillips and Blazey, 1991) behavior that allows for more molecular stretching which in-turn dissipates the heat across the organized metric mesh (Jeske *et al.*, 2012).

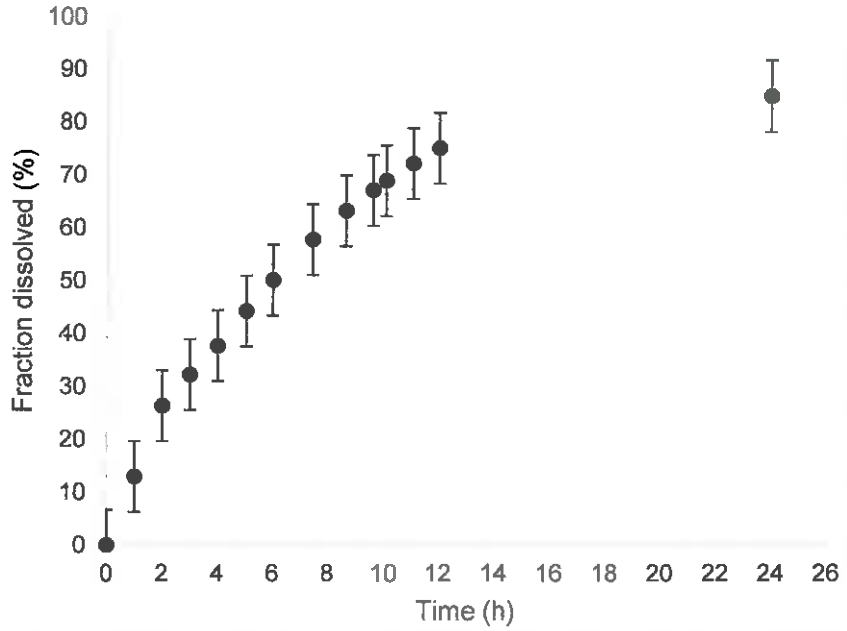

Figure 4.13: Release profile for optimized design formulation generated utilizing fractionalized released quantifiable by measuring absorption units at λ290nm over a 24-hour period with drug release values: AUC: 512.924, MRT: 9.836113, MDT: 10.222544, RD: 0.725516 and DE: 0.630385.

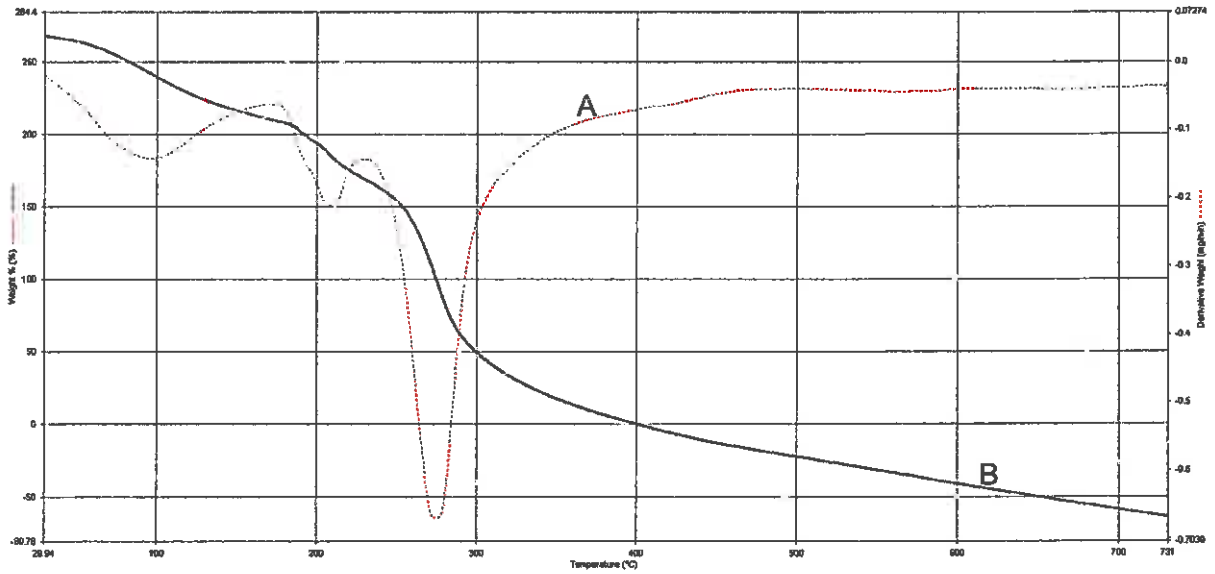

Figure 4.14: Thermogravitational Analysis (TGA) profiles for commercial Sago (A) and optimized formulation (B). Profiles generated under inert nitrogen conditions 25-700 ^{0}C at heating rate of 10 ^{0} minute $^{-1}$.

Physicochemical modifications are further confirmed by the ATR-FTIR spectra comparing optimized oxidation profiles to the commercial bead (see Figure 4.15). Oxidation results in the reduction of the O-H bond stretch within 3000-3500cm^{-1} correlating to a positive di-aldehyde introduction by periodate reaction (Pu *et al.*, 2011). Sodium *meta*-periodate ($NaIO_4$) is a mild and specific oxidant that can convert cis-glycol groups in carbohydrates to reactive aldehyde

groups. Unlike common oxidizing agents $NaIO_4$ is selective in its reaction and only targets the C2-C3 glycosidic link thus enabling the oxidation method to occur at a specific site (Rinaudo, 2010). It is for the same reason that the 1500-2000cm^{-1} region (Zhang *et al.,* 2011) becomes more characteristic as this is the classic footprint region for aldehyde groups as also evident in the octadecanal spectrum (see Figure 2.9 in Chapter 2). Similarly, aldehydes groups are also associated with aromatic stretching in the region 2500-3000cm^{-1}. This characterizes the hemiacetal aromatic structures that aldehydes can form when in high concentration.

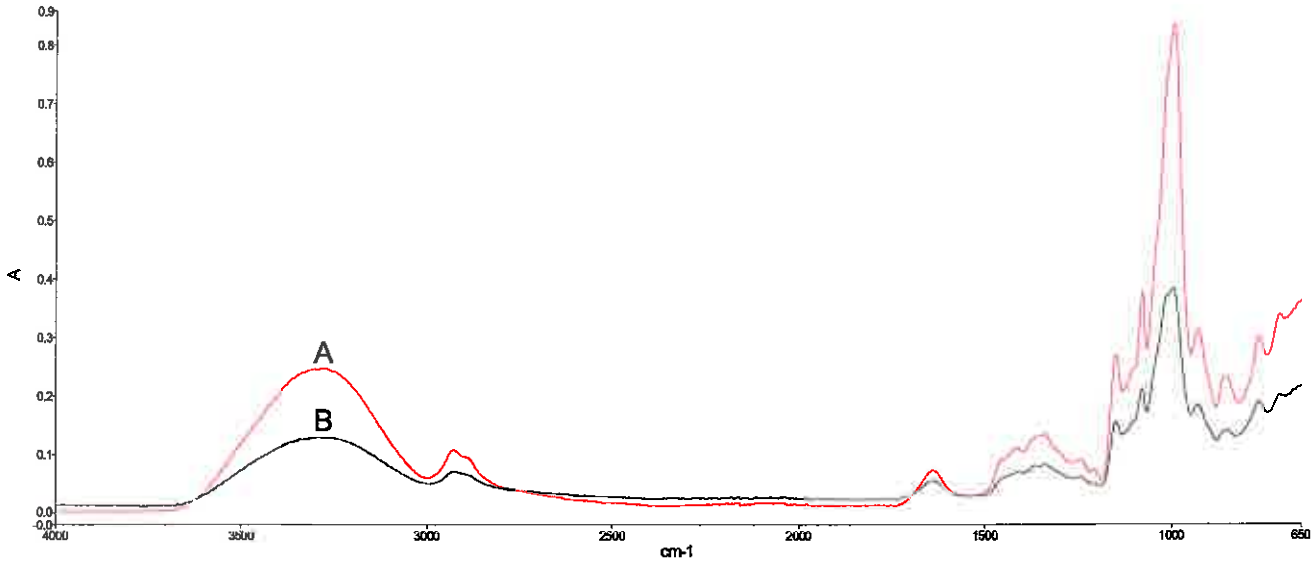

Figure 4.15: ATR-FTIR spectra of different the optimized oxidized derivatives (A) and unmodified bead. All ATR-FTIR profiles were obtained from 100 scans at a range of 4000-600cm^{-1} at a constant pressure of 130psi

Rheology results also correlated with TGA spectra. There was an evident increase in stability and linearity of the observed flow properties evident in the altered overall flow profile as seen on Figure 4.16. As previously discussed by Chen and co-workers, reducing sugars have a stabilizing role in polymers due to the reducing ends and can display the stabilizing effect of water aiding in the apparent linearized polymer flow (Chen *et al.,* 2010). There is an observable overall reduction of viscosity (G) see Figure 4.16 comparing unmodified with the optimized formulation and thus DS, resulting in the change in flow properties. When polymers chemically functionalized, the viscosity is altered which affects the dissolution, diffusion and ultimately the bioavailability of a drug in any delivery system.

The XRD (Figure 4.17) profiles show a complete transformation of an amorphous polymer to a more crystalline structure which supports data from preliminary tests confirming the introduction of aldehyde groups to the surface. When aldehydes are specifically introduced to the Sago at C2 and C3 carbons and, the dialdehydes introduced can interact to form a

hemiacetyl (Kim *et al.*, 2000). This results in a more crystal lattice-type morphology (Elfstrand *et al.*, 2007) that is more stable and much more organized as shown by analysis. XRD data correlates to rheology and FTIR data, confirming surface modification method that does not disrupt the structural integrity of the OTC food-grade Sago bead.

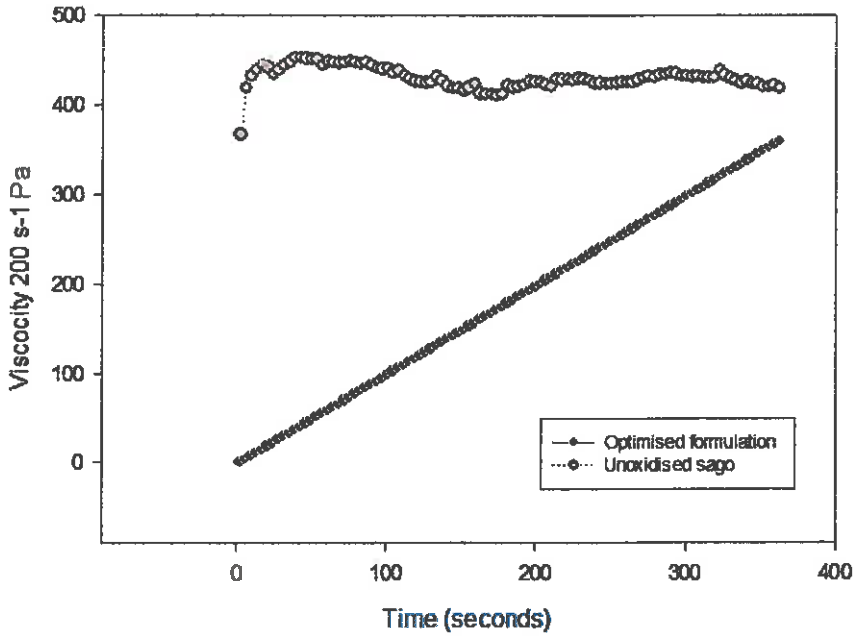

Figure 4.16: Rheology profiles of optimized formulation in comparison to unmodified OTC Sago beads.

As discussed previously, the absorbance-difference (ΔA) between the measured and theoretical values for the mixture of mucin/Sago system was calculated (see Table 4.2). The absence of any interaction is thus represented by a zero value for ΔA. The absorbance differences, measured between the pure mucin solution and the one that was exposed to the delivery system were close to zero. This result suggests that there was close to no interaction between chitosan and mucin (Deacon *et al.*, 1999). The absorbance in differences obtained from the mucin/Sago system were very precise as the calculated differences of the value for the individual solutions, ΔA≈0, see Table 4.1.

Based on this observation, it is correct to assume little interaction between mucin solution and chitosan-crosslinked beads suggesting that the crosslinking reaction for the designed system was a complete success. Successful crosslinking allows for future application in controlled and/or sustain drug release. Furthermore, chitosan inclusion on the surface of the Sago system makes is an ideal candidate for muco-adhesive functionalization for future application. This functionality would allow for array of application as disease states, food or drug administration may affect gastric motility thereby releasing the formulation prematurely into

the intestine where it may be ineffective (Sosnik *et al.*, 2014); cause premature gastric secretions and infer sub-optimal gastric conditions which may cause the delivery system to fail (Assaad and Mateescu, 2010).

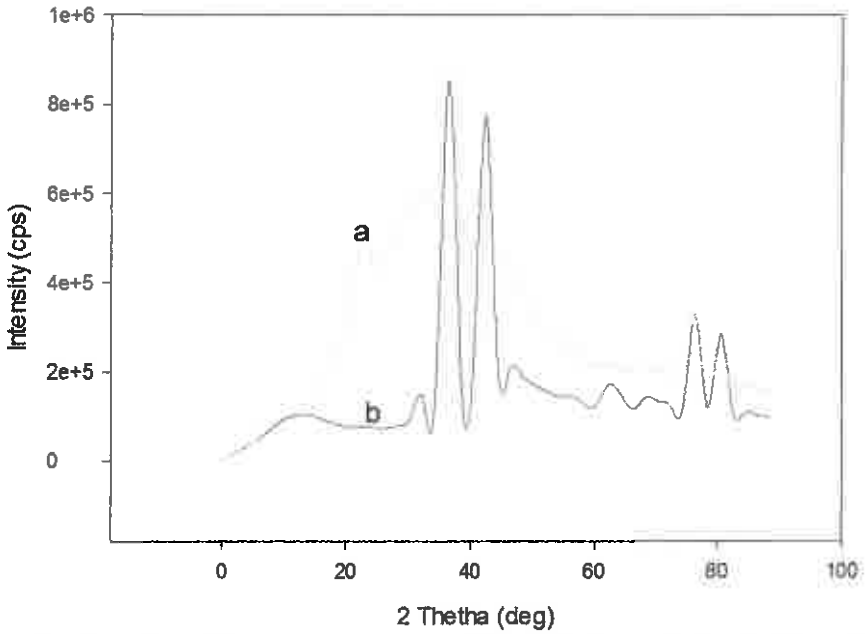

Figure 4.17: Powdered X-Ray Diffraction profiles of b: optimized formulation and a: unmodified formulations.

Table 4.1: Spectroscopic quantification of chitosan crosslinking efficiency of modified Sago beads

A_{muc}	A_{sys}	ΔA
0.207	0.205	0.002
0.206	0.203	0.003
0.205	0.203	0.002
0.205	0.203	0.002
0.205	0.203	0.00225

A_{syst} : Absorbance at λ 500 nm for the oxidized and crosslinked derivative
A_{muc}: Absorbance at λ 500 nm for the standard mucin solution
A_{muc}-A_{sys}: ΔA was recorded as the fraction of chitosan that had crosslinked unsuccessfully. Thus the higher the ΔA, the less efficient the crosslinking method and the vice versa also applies.

The maltose standard curve produced a linear curve that allows for quantification of maltose in solution, see Figure 4.18. The resulting equation $y = 0.4563x - 0.082$ was then utilized to quantify amylase sensitivity as summarized in Table 4.2. Evidently, amylase digestibility decreased by ~30% rendering the formulation suitable for sustained release as it can withstand harsh GIT environment for extended periods. As expected, due to the loss of the α-1-4 links with the derivative starch, the formulations are rendered less sensitive to amylase digestion. The reduced availability of the C α-1-4 links increases the hydrophobic character of the polymer (Cunha and Gandini, 2010) and in turn reduces gelatinization and thus reducing

groups exposed for hydrolysis (Delisle, *et al.*, 2012) further altering the flow property of the optimized starch derivative. This allows for a greater controlled release as the derived polymer exhibits a non-Newtonian flow. Furthermore, reduced amylase sensitivity coupled with the native muco-adhesive nature of mucin allow for increased GIT presence further enhancing formulation performance.

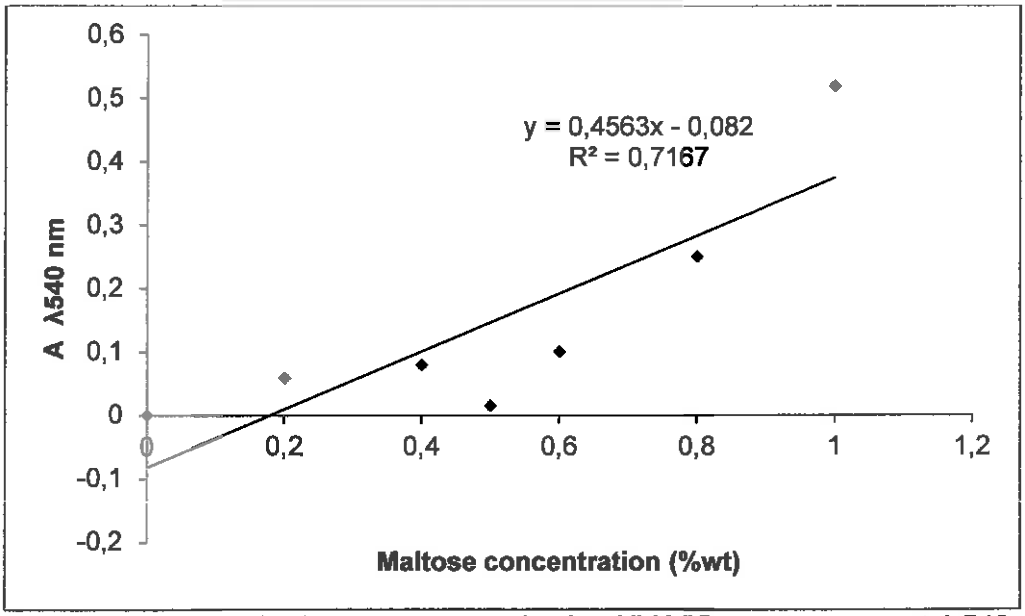

Figure 4.18: Maltose standard curve generated using UV-VIS spectroscopy at λ 540nm.

Table 4.2: Estimation of % α -amylase sensitivity of starch

Starch type	% α-Amylase Sensitivity
Control Sago starch (%)	76.9
Optimized form [1] (%)	45.4
Optimized form [2] (%)	45.3
Optimized form [3] (%)	45.1

4.5. CONCLUDING REMARKS

Functionalization of the beads was successful yielding a superior optimized formulation which showed great *in vitro* performance for a 24-hour period. The optimized formulation also shows superior physicochemical properties rendering it more superior that unmodified derivative. Furthermore, the optimized formulation as designed currently is a much cheaper alternative to what is currently on the market for propranolol delivery based on reagents used. The overall reduction in chemical-grade reagents in final optimized product possesses great potential in clinical applications as it may have a positive impact on patient compliance that are applicable across for hydrophilic active agents and potential protein/enzyme applications.

CHAPTER 5
IN VIVO PERFORMANCE ANALYSIS AND EVALUATION

5.1. INTRODUCTION

Human trial testing associated with biomedical inventions has a great deal of complexities with great financial and compliance implications. Thus, the use of animal models to prove *In vivo* performance is the first preference for optimized formulations. Although *in vitro* evaluations of the novel drug delivery system developed may provide valid information regarding the drug release characteristics however, they cannot completely simulate *in vivo* conditions. Thus *in vivo* studies need to be conducted to obtain significant performance efficacy and safety data for any novel delivery system. The large white pig model is generally preferred as a suitable animal model in oral drug delivery system assessment due to the dimensions (liver, kidney, heart, circulatory system, etc.) that are similar to the human body (Kaiser, *et al.*, 2006). Furthermore, pigs have body mass and a gastrointestinal tract very similar to that of human which allows for adequate investigation of the feasibility, safety and efficiency of the system before human usage (Grove *et al.*, 2007). The cost of maintaining pigs are minimal and present a low risk experiment potential.

Compared to guinea pigs, large white pigs have shown to have biotransformation processes similar to the human GI tract. This in conjunction with the similarities in GI cDNA renders the large white pig metabolism similar to that of humans. Such similarities in morphology also allow for correlations to be drawn in substrates, inducers, inhibitors, regulation, hepatic physiology and function. Despite tremendous advances in drug delivery systems within the past decade, the oral route remains the most preferred route for the administration of therapeutic agents mostly due to the ease and non-invasive nature of administration. This is particularly true for administration of hypertensive (high blood pressure) treatment regiments such as propranolol (Chobanian *et al.*, 2003). However, there are significant challenges associated with the oral route for propranolol delivery such as varied blood concentration due to natural detoxification processes before the drug can reach the site of action (Prisant and Elliott, 2003). Thus, more frequent doses are required to establish therapeutic effect which is typically associated with dosage related side-effects and reduced patient compliance amongst other challenges. The use of natural polymers as done in the novel Sago microsphere system has the potential to allow for controlled release formulations and to increase the efficiency of propranolol. This is due to prolonged gastrointestinal residence time reducing the dosages required to obtain therapeutic effect.

Ethical clearance (clearance certificate number: 2013/41/05) was awarded by the University of the Witwatersrand Animal Ethics Screening Committee (appendix 1). Two unique objectives were tested for during the study. Firstly, the toxicity of the formulation was established though dosage of a placebo formulation. Whilst the novel formulation was designed utilizing food-grade substrates, there was a level chemical modification that requires the safety confirmation. Furthermore, due to the unique combinations of modified derivatives we needed to note any adverse effect that could potentially skew the data giving either false positives or false negatives

Secondly, the determination of the performance of the chemically modified food-grade Sago system, the main objectives were:

- Assessment of *in vivo* drug release from the novel drug delivery system developed.
- Comparative analyses in relation propranolol 400mg in terms of the ability of the systems to provide superior control of drug concentration oscillation in plasma.
- Determination of unforeseen side-effects of the novel drug system that would not be able to be determined through investigative studies.

5.2. MATERIALS

Six healthy large female white pigs weighing 40 (±2)Kg were utilized for the study. All 5 animals were sourced locally. Sodium hydroxide (98 w/w), sodium chloride (≥98$^{w}/_{w}$), sodium dihydrogen phosphate monohydrate (≥99%$^{w}/_{v}$), sodium bicarbonate (≥99.5%$^{w}/_{w}$), ammonium persulfate (≥98%$^{w}/_{w}$), were purchased from Sigma-Aldrich (St. Louis, Missouri, USA) at reagent grade. Acetonitrile (≥99.9%$^{w}/_{v}$) and sodium oleate (≥99%$^{w}/_{v}$) were purchased from Sigma Aldrich at UPLC grade. Food-grade Sago starch beads were purchased over-the-counter (OTC), food-grade chitosan (Warren Chem Specialities, batch number: WA200703003), (99%$^{w}/_{w}$) sodium-meta-periodate (99%$^{w}/_{w}$), hydrochloric acid (HCL) 37%$^{w}/_{w}$, Glutaradehyde 50%$^{v}/_{v}$ solution, Dimethylfoxyde 50% $^{v}/_{v}$ were purchased from Sigma-Aldrich (St. Louis, Missouri, USA), acetic acid (99.99%$^{v}/_{v}$) and ethanol absolute (99.8%$^{w}/_{w}$) were purchased from Merck (Halfway House, Gauteng, South Africa) at reagent grade. Six sets of 7-gauge double lumen 35cm catheter (CS-28702) were purchased form Arrow Deutschland GmdH, Erding, Germany.

For the catheter implantation procedures, the following were supplied by the University of the Witwatersrand Central Animal Service (CAS) unit: ketamine HCL 11mg/Kg, midazolam 0.3mg/Kg, topical procaine HCL (0.5%), isoflurane gas (1-2%), Buprenorphine (0.05mg/Kg I.M.) and carpofen (4mg/Kg I.M.). For the maintenance of the catheter, 1000IU heparin in 1L

of 0.9% saline was utilized (also supplied by CAS). The pig feed was also supplied by CAS, food items used during acclimatization i.e. raisins, carrots, mixed vegetable and gelatinized jelly were purchased OTC from a local supermarket and were of food-grade.

5.3. METHODS

5.3.1 *CATHETER IMPLANTATION*

To aid in accuracy in sample collection and reduce overall physical discomfort of the study, catheters were implanted into the left jugular vein of all the pigs. All the pigs were weighed before the procedure to inform active agent dosage concentrations used during the procedures. Each pig was individually placed under anesthesia using intramuscular injection of ketamine HCL 11mg/Kg, midazolam 0.3mg/Kg, topical procaine HCL (0.5%), and maintained under medical oxygen and isoflurane gas (1-2%) for 30- 60 minutes described in further detail by Hodgson (2007) Linkenhoker *et al.* (2010). This facilitated the catheter implantation into the jugular vein with minimal stress to the pig.

The jugular vein was exposed by an incision on the dorsal jugular groove on the left lateral aspect of the neck. Following exposure, 10cm of the catheter was inserted into the lumen of the vein and fastened to the wall of the left jugular vein. The remaining 25cm of catheter was tunneled to an exit point cranial at the dorsal aspect of the scapula with the use of a trocar. The external injection ports of the catheter were sutured to the skin of the pig to prolong lifespan and prevent bleeding. Post-surgery blood samples were removed with heparinised saline to confirm surgery success and the catheter functionality. Buprenorphine (0.05mg/Kg I.M.) and carpofen (4mg/Kg I.M.) were administered post-surgery for analgesia and inflammation. Pigs were then numbered 1-6 based on the time of application of unaesthetic and subsequent surgery performed. All the pigs were allowed to recover for at least 10 days after the procedure to allow for enough recovery time (Kolawole *et al.*, 2010).

5.3.2 *MAINTENANCE OF CATHETER IMPLANT*

The intra-jugular catheter was maintained three times a day in which each catheter was flushed out with heparinised saline (1000IU heparin in 1L of 0.9% saline). Before and after the catheter was flushed with heparinised saline it was inspected to ensure the removal of any clots and clotting blood from the internal catheter compartment. There were careful inspections of the catheter before and after each heparinised flush such that any infections, if any, will be detected at an early stage. This was carried out during the recovery post-surgery of catheter implant and throughout the study.

5.3.3 *Sampling: Aspiration of blood samples via an intra-jugular CATHETER*

A blood sample volume of 3-5mL blood was withdrawn at predetermined time intervals through the catheterized jugular vein under strict aseptic techniques. The blood samples collected were placed in lithium heparin vials and centrifuged (5000rpm for 10 minutes) to allow collection of supernatant plasma. The collected supernatant was then transferred into sterile Eppendorf and frozen at -70°C until further analysis could be conducted (Hoogstraate, *et al.*, 1996; Claus *et al.*, 2007).

5.3.4 *SAGO DRUG DELIVERY SYSTEM SAMPLE PREPARATION UTILIZING OPTIMIZED MODIFICATION METHOD*

Dosage forms were prepared using the optimized method described in chapter 3 with an addition of a gelatin capsule as depicted in Figure 5.2. Both a placebo and an experimental formulation were prepared. Resulting Sago microspheres were then loaded onto a standard gelatin capsule with a final formulation of mass 0.74g with ~160mg of propranolol in each capsule for experimental formulations. Capsules were carefully coated with a generous layer of food grade olive oil to aid in easy dosing when formulations are passed through intragastric tubing.

5.3.5 *DOSAGE ADMINISTRATION FREQUENCY AND SAMPLING METHODOLOGY*

For all animals in the study, single dosage was administered via an intragastric tube (1.8cm outer diameter and 1.3cm inner diameter) and required the administration of local unaesthetic. The local applied unaesthetic was ketamine (11mg/Kg) and midazolam (0.3mg/Kg) which was directly injected into the jugular vein via the implanted catheter. After the dosing procedure, animals were allowed at least one hour of recovery time from the procedure before sample collection.

5.3.6 *PLACEBO DOSAGE: PLACEBO AND SAFETY CONFIRMATION*

All pigs were dosed with a placebo formulation on the eleventh day. This aided in the collection of blood to allow for correction of any baseline data errors that would have no association with the system to be tested. Dosage of the placebo also served as a confirmation for safety of the developed system. The study was conducted for 24 hours with blood (3mL) aspirated through the intra-jugular catheter at time intervals 0, 1, 2, 4, 6, 8, 10, 12, 18 and 24 hours.

5.3.7 *EXPERIMENTAL AND CONVENTIONAL DOSAGE*

On the thirtieth day of the study, all five pigs were dosed with the drug-loaded Sago-system in an identical intragastric method as performed for the placebo dosage. Samples of blood (3mL) were withdrawn at time intervals 0, 1, 2, 4, 6, 8, 10, 12, 18, 20 22 and 24 hours after having

allowed a lapse of an hour for recovery (before withdrawal of the first sample).

The conventional dosage form (non-sustained release) utilized a commercially available propranolol product donated by Wits Donald Gordon Pharmacy, Pur-bloka 40® (Pharmacare Ltd/Bpk) and was dosed on the ninetieth day of the animal trial. Dosage and sampling procedure procedures were identical to those of the placebo and experimental formulations. On completion of all experimental and conventional studies, all animals that were part of the study had the catheter removed of were flushed out xenobiotic substances and returned to stock. The dosage methodology and timeline is summarized on Figure 5.1.

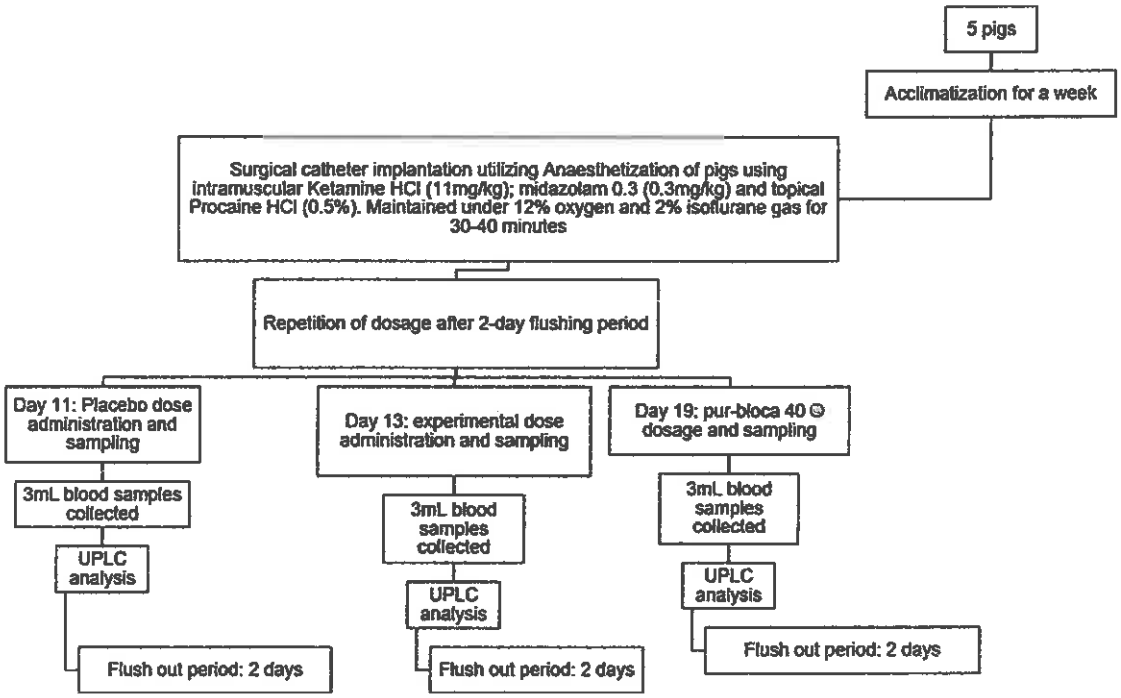

Figure 5.1: Schematic flow summarizing the sequence of the animal study.

5.3.8 *PLASMA SAMPLE AND STANDARD SOLUTION PREPARATION*

Stock solutions of propranolol (200µg/mL) and atenolol (200µg/mL), used as the internal standard, were prepared in methanol. The solutions were kept in dark containers protected from light and stored at 4°C. Working standard solutions of propranolol were prepared through dilutions of the stock solutions in methanol. The working standard solutions of propranolol were utilized with blank plasma standards for elucidation of a calibration curve for the model drug. This was done in batches of plasma standards prepared by adding 200µl of the working solutions to 2mL of blank plasma. For blank samples, only 1mL of blank plasma was used and kept under the same storage condition and later processed as the plasma standards. For the standards and experimental samples, the liberated model drugs were extracted with 3.5mL of the extraction solvents.

allowed a lapse of an hour for recovery (before withdrawal of the first sample).

The conventional dosage form (non-sustained release) utilized a commercially available propranolol product donated by Wits Donald Gordon Pharmacy, Pur-bloka 40® (Pharmacare Ltd/Bpk) and was dosed on the ninetieth day of the animal trial. Dosage and sampling procedure procedures were identical to those of the placebo and experimental formulations. On completion of all experimental and conventional studies, all animals that were part of the study had the catheter removed of were flushed out xenobiotic substances and returned to stock. The dosage methodology and timeline is summarized on Figure 5.1.

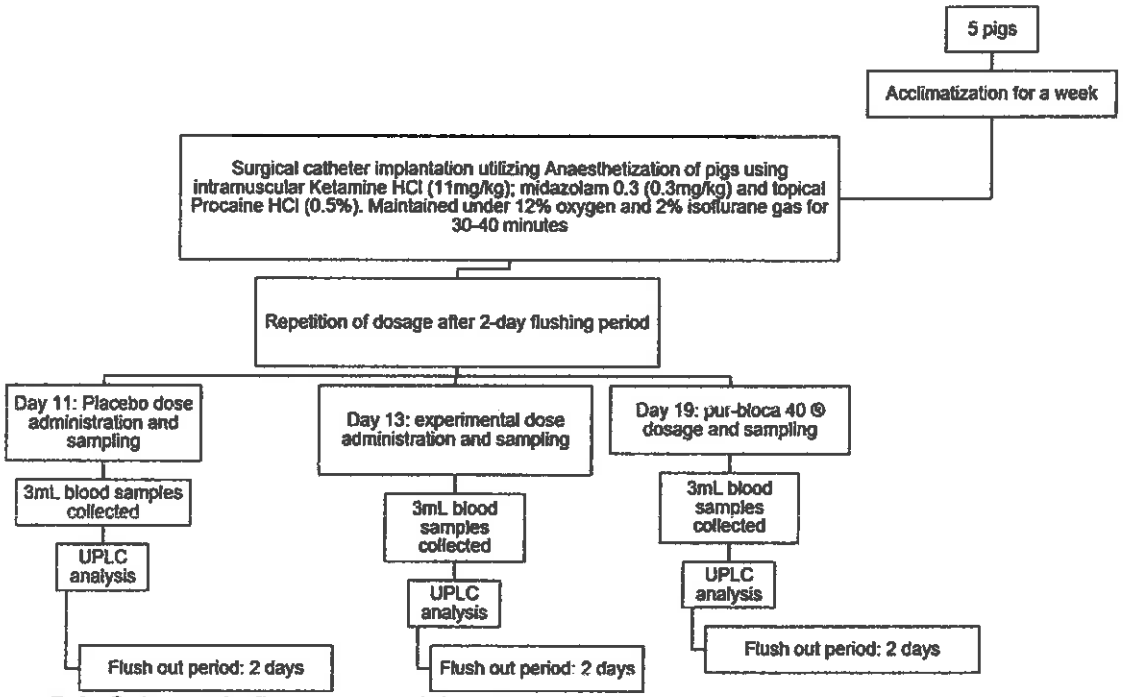

Figure 5.1: Schematic flow summarizing the sequence of the animal study.

5.3.8 *PLASMA SAMPLE AND STANDARD SOLUTION PREPARATION*

Stock solutions of propranolol (200µg/mL) and atenolol (200µg/mL), used as the internal standard, were prepared in methanol. The solutions were kept in dark containers protected from light and stored at 4°C. Working standard solutions of propranolol were prepared through dilutions of the stock solutions in methanol. The working standard solutions of propranolol were utilized with blank plasma standards for elucidation of a calibration curve for the model drug. This was done in batches of plasma standards prepared by adding 200µl of the working solutions to 2mL of blank plasma. For blank samples, only 1mL of blank plasma was used and kept under the same storage condition and later processed as the plasma standards. For the standards and experimental samples, the liberated model drugs were extracted with 3.5mL of the extraction solvents.

5.3.9 *Ultra-performance Liquid Chromatographic analysis for plasma samples*

UPLC refers to Ultra Performance Liquid Chromatography utilized in this study has been described in Zhong-Bo *et al.* (2011). UPLC was performed using an Acquity system from Waters and 100mm columns with an i.d. of 2.1mm packed with 1.7µm Acquity C_{18} BEH particles. Water was de-ionized using a Millipore system. Solvent A was 0.1%$^{v}/_{v}$% tri-fluoro acetic acid (TFA) in water and the solvent B solvent was 0.1%$^{v}/_{v}$TFA in acetonitrile. The mobile phase, pumped at a flow rate of 0.4mL min^{-1}, consisted of A (methanol) and B (0.1% formic acid in water). The initial mobile phase composed of 35% A/65% B. After sample injection, the mobile phase composition was changed linearly to 60% A/40% B over 0.5 minutes, held constant for an additional 2.0 minutes, and then returned to 35% A/65% B immediately for re-equilibration. The total analysis time was 3.5 minutes. The auto sampler was conditioned at 4C and the sample volume injected was 5mL.

5.4. Results and Discussion

5.4.1 *Surgery: catheter implant to left jugular vein*

All the animals recovered within 30 minutes' post-surgery, initially regaining movement of their upper body within 10 minutes of reversal of unaesthetic followed by dorsal body movement. There was an observed correlation with reduced body weight and extended recovery time post-unaesthetic reversal. The smallest pigs (numbered 5 and 6) took close to an hour and fifteen minutes on average to fully recover. The two were subsequently fed a bit more and observed carefully for the duration of the study. Observed data is summarized in Table 5.1 below indicating a clear inverse correlation between weight and in recovery time post-anesthesia application and removal thereof.

Table 5.1: Data summary for initial observation in intra-jugular catheter implant surgery showing weights pre-surgery and approximate recovery time post-surgery for six subjects involved in the trial.

Pig number	Weight (Kg) Pre-surgery	Post-surgery Recovery Time (minutes)
1	50.00	28
2	44.45	33
4	40.05	32
3	39.95	43
6	39.86	45
5	39.25	45

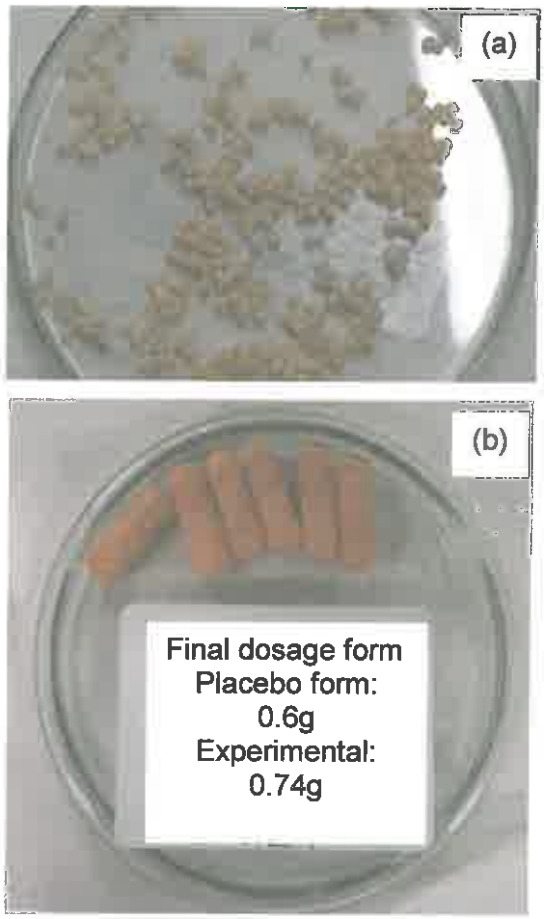

Figure 5.2: Sample preparation for S_{ago}-millisphere system prepared utilizing optimized method parameters with 73.0199 minutes oxidation and 1.5428%$^{w}/_{v}$ chitosan crosslinking in an aryl system with 3:1 glutaraldehyde: hydrochloric acid for every 3g of beads

All surgical procedures were successful. In all the animals, the anesthetic was administered with no complications. In each case the jugular vein was exposed by an incision on the dorsal jugular groove on the left of the neck. Following exposure, 10cm of the catheter was inserted into the lumen of the vein and fastened to the wall of the vein as seen on Figure 5.3.

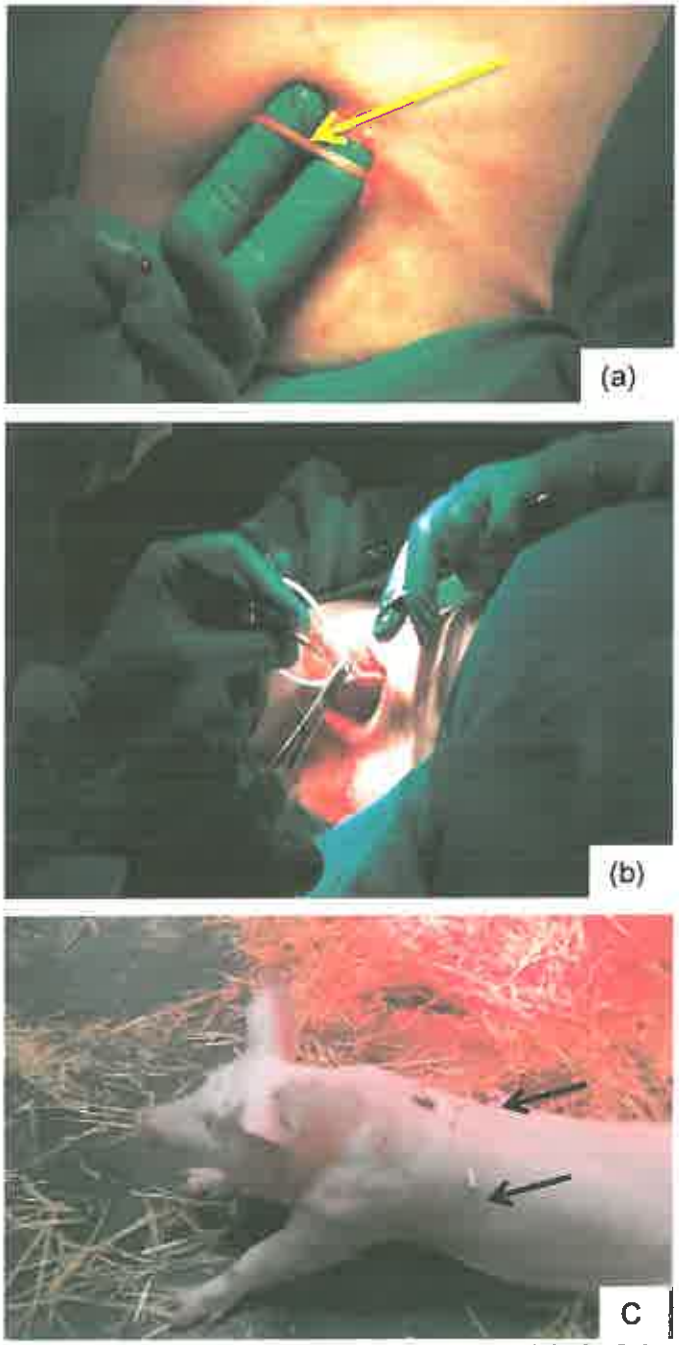

Figure 5.3: Catheter implantation procedure characterized. (a): Left jugular vein to which a (b): synthetic catheter is joined and looped back to yield two ports as highlighted on and (c) to allow for non-invasive sampling during study period.

5.4.2 *Optimized formulation dosage preparations and characterisation*

The final optimized placebo formulation had a mass of 0.6g on average and the experimental formulation weighed 0.74g on average. Bead structures were slightly opaque, compared to unmodified beads as seen on Figure 5.2. To allow for ease of dosage, beads were loaded onto a standard gelatin capsule. Sustained release over a 24-hour period was obtained due to the innovative designed discussed in previous chapters.

5.4.3 *Evaluation of dosage effects, formulation safety and physiological effects*

It should be noted that none of the animals in the trial experienced physiological or observable behavioral changes. All six females showed no adverse infection or physiological response to experimental procedures, placebo, experimental and conventional dosage forms. Although it is typically standard procedure to run a pilot study prior to full-scale animal trial, the food-grade based nature of the formulations was initially proposed as one of the main advantage of the formulation. This was confirmed by results from the placebo dosage with animals not showing any adverse responses to the placebo formulation. This further reinforces the hypothesis of the safety of the affordable Sago-based system. As observable in Table 5.2, the animals continued to grow post-placebo dosage and sample collection. Weight losses in such studies (amongst other physiological reactions) have been cited as a clear indicator of formulation failure (Kaiser *et al., 2006*).

Table 5.2: Weight tracker for all dosing procedures performed during the animal trial

Pig number	Weight at Placebo dosage	Weight (Kg) at Experimental dosing	Weight (Kg) at Conventional dosing
1	51.40	54.05	55.10
2	46.15	46.75	49.55
3	43.30	43.90	46.70
4	43.75	44.75	47.25
5	43.75	44.20	46.90
6	45.26	45.60	48.65

5.4.4 *Dosage methodology evaluation*

All dosing procedures were successful. The intragastric tube was inserted while on the surgical table whilst animals were under anesthetic and then the formulations allowed movement down using the natural GIT contractions.

5.4.5 *In vivo performance: Ultra Performance Liquid Chromatographic (UPLC) detection method evaluation*

To ascertain the speed at which propranolol was released. Drug concentrations were quantified in the collected plasma samples using a developed UPLC method as seen on Figure 5.4 below. Upon quantification of peaks for drug content in individual samples from each pig at specific time points, AUC and AUMC curves were generated utilizing individual peaks for time points and peaks as shown in Figure 5.5. The retention time for propranolol was found to be 0.832 minutes with the internal standard retention at 1.618 minutes.

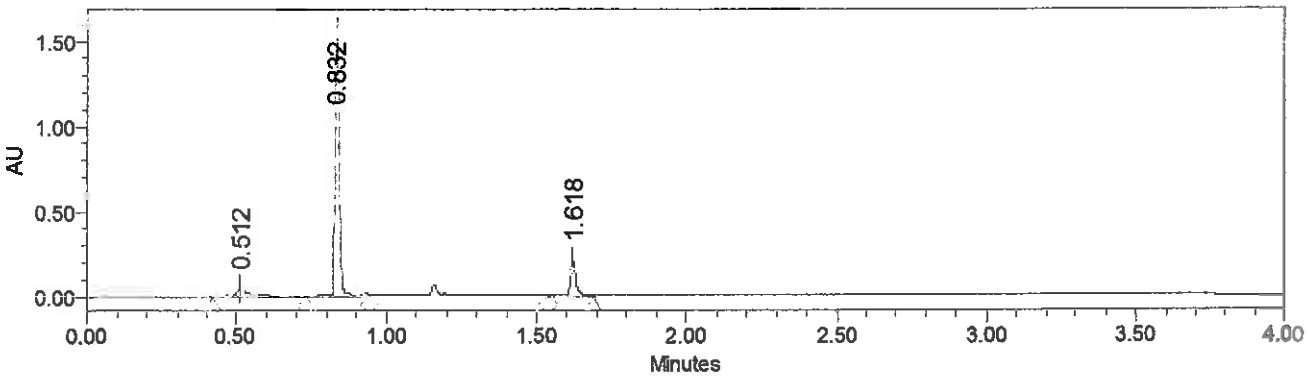

Figure 5.4: UPLC derived method parameters: The retention time was found to be 0.832 minutes

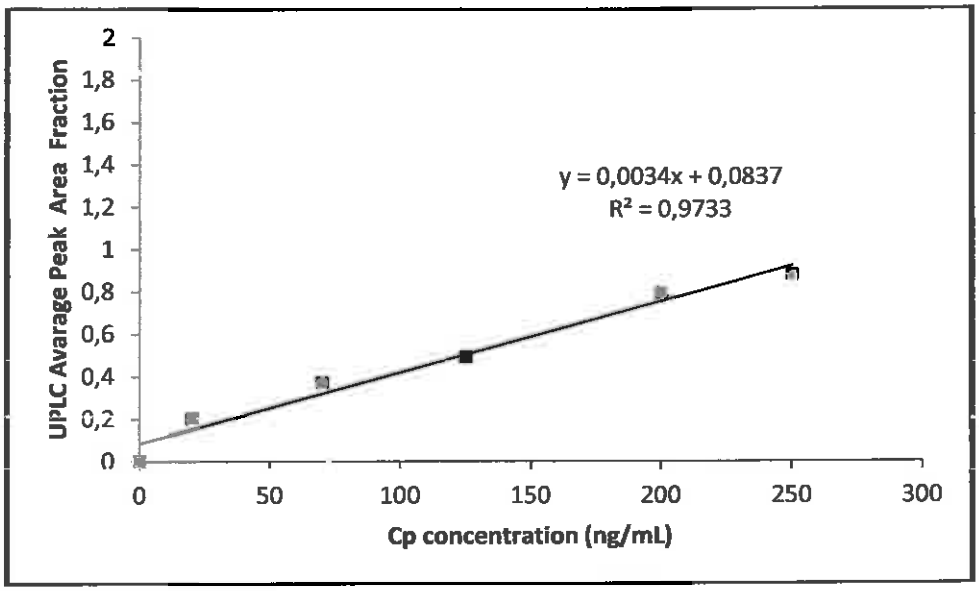

Figure 5.5: UPLC calibration curve indicating peak-time curve of plasma standards for C_p: Propranolol concentration detected via UPLC at λ 290nm for samples prepared from placebo plasma samples.

The use of AUC and AUMC calculations assumed a traditional trapezoid non-compartmentalized analysis of plasma propranolol pharmacodynamics. In such assumptions, it is generally accepted that each drug particle as can move independently across kinetic spaces and the time spent in the system by each particle is a random variable (Weerapol *et al.*, 2015). The AUC and AUMC were utilized within the non-compartmental analysis to determine the mean residence time (MRT). Utilizing the following equations:

$$AUC_{t_0}^{t_\infty} = \frac{Cp_{last}}{\lambda} \qquad \text{or} \qquad AUMC_{t_0}^{t_\infty} = \left(\frac{t_{last} \times Cp_{last}}{\lambda}\right) + \frac{Cp_{last}}{\lambda^2}$$

$$AUC_b^a = \int_a^b C(t)dt \qquad AUMC_b^a = \int_a^b C(t)tdt$$

$$MRT = \frac{AUMC}{AUC}$$

Where *MRT* is the mean residence time, *AUMC* is the area under the moment curve, *AUC* is the area under the curve and of λ is the elimination rate constant. The calculation of AUC and AUMC were used to process UPLC data for comparative analyses (Lou *et al., 2014)* performed for each pig utilized in the study. There was a notable variance in the profiles of the third pig to be dosed suggesting a weaker formulation compared to the other results. It should be noted that this animal had some adverse reaction to the anesthetic and took longer to recover post-dosage based on this and the variance, the results were subsequently disregarded and excluded from collective analyses. Furthermore, the pig was less than 50 Kg before the dosage procedures.

It should be noted however that all other profiles displayed a sustained release profile over a 24-hour period (see Figure 5.7). Experimental formulation showed an average MRT of 29.71, almost ten times that of the conventional formulation which peaked within 3 hours of dosage and then cleared off post thereafter. The sustained release was expected as prior studies confirmed successful chitosan crosslinkage. The expected MRT based on *in vitro* studies was lower that what was observed *in vivo* confirming an additional factor impacting the sustained release. Although not specifically tested within this study, chitosan has well documented muco-adhesive (Prabaharan et al 2008) properties which in this case implicitly aids not just in sustained release but secondarily reduces the chances of hepatic clearance of the drug from plasma as the concentration level are controlled with minimal oscillations.

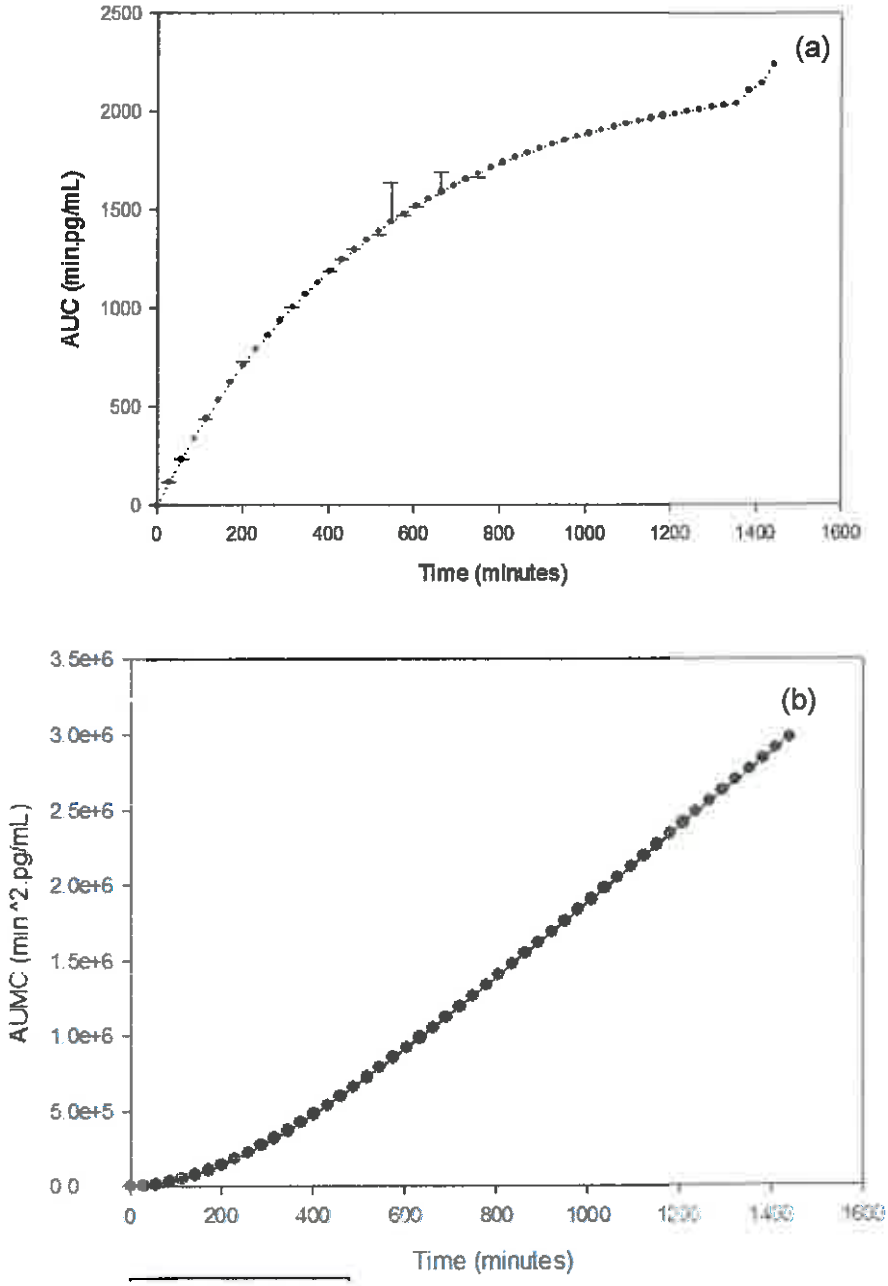

Figure 5.7: AUC and AUMC curves for experimental collated plasma data with final MRT averaged at and 29.71 hours.

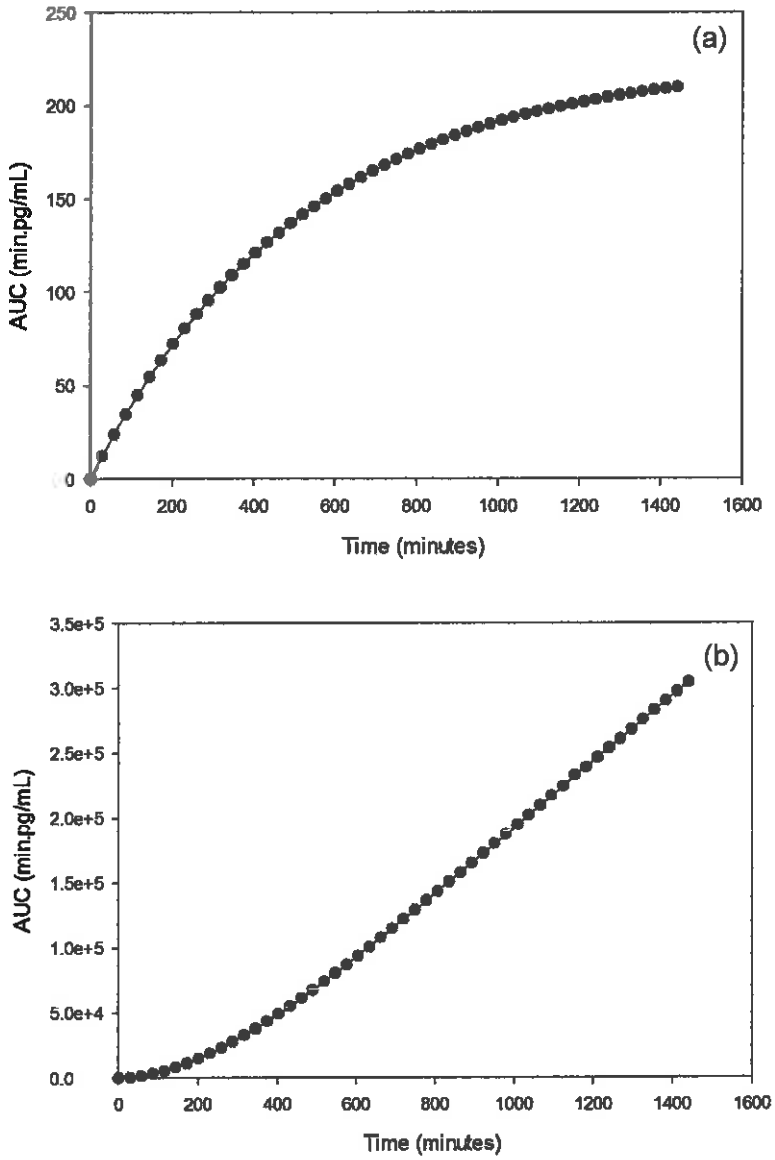

Figure 5.8: AUC (a) and AUMC (b) curves for conventional collated plasma data with final MRT averaged at 2.85 hours.

5.5. CONCLUDING REMARKS

The small-scale animal study confirmed both the safety and the superior performance of the Sago delivery system when compared to the current conventional pur-bloka® 40. The optimized Sago system design for propranolol delivery yielded an increase in the mean residence time by almost tenfold with physicochemical properties that aids in sustained delivery of propranolol. The reduced sensitivity toward amylase, by up to ~30%, activity may contribute to the observed superior performance observed. It is reasonable to expect the cost of production to be lower than traditional formulation production based on nature, grade and the associated costs of reagents used. Further trials need to be run to aid in the quantification and enhancement of the muco-adhesive potential of the system.

CHAPTER 6
CONCLUSION

The development of sustainable drug delivery systems continues to be an ongoing endeavor with a revitalized focus on biopolymers as patient compliance decreases due to increased information about reagent usage. There continues to be a growing demand for less expensive drug delivery systems for lifestyle and chronic diseases. The combination of the demand and patient perceptions presents the market with an exciting yet challenging reality and presents idealistic research opportunities that require a multidisciplinary approach to system development in drug delivery.

For the modification of food-grade Sago, periodate surface oxidation has been shown suitable method for oxidation of pre-formed starch particles. Furthermore, food-grade starch beads can be functionalized for application in pharmaceutical delivery of active agents. It is evident in this design is that of cost reduction for formulation, reduced chemical grade excipients that could have a positive effect on patient compliance as the use of "herbal" (more natural) formulations is the rise as patients become more informed about formulation composition. Furthermore, there is an increasing trend in the development of lifestyle diseases which must be treated most likely through orally administered formulations, as it continues to be the preferred route. This reality makes formulations such as the oxidized Sago potentially very lucrative. This system has potential to offer naturally occurring polymers and excipients benefits whilst maintaining optimal physicochemical properties essential in drug delivery.

Functionalization of the beads was successful yielding a superior optimized formulation which showed great *in vitro* performance over a 24-hour period correlating with *in vivo* findings. The optimized formulation also showed superior physicochemical properties rendering it superior to the unmodified derivative. Furthermore, the optimized formulation as designed currently is a much cheaper alternative to what is currently on the market for both overall starch derived solution and those specifically formulated for propranolol delivery. The overall reduction in chemical-grade reagents in final optimized product possesses great potential in clinical applications as it may have a positive impact on patient compliance a wide application for hydrophilic active agents and potential protein/enzyme applications.

RECOMMENDATIONS

Preliminary animal data results suggest that the proposed design for propranolol increases the mean residence time by almost tenfold. Whilst it can easily be deduced that the form is of improved quality of delivery system for an unprecedented extended period and reduced cost to production based on production procedure and excipients utilized.

For further optimization methods, the mucin interaction with the chitosan exterior layer can be optimised further by increased chitosan during the crosslinking method. More studies are required to quantify the behavior on the exterior layer in solution to clarify what the mucin-chitosan interaction looks like. For propranolol optimization, the addition of ascorbic acid as it has been document to increase the efficacy of propranolol. This should be investigated with caution if considered since ascorbic acid acts as an antioxidant. Its inclusion should be considered either after the crosslinking step or as nanoparticles onto the chitosan exterior layer.

The system currently caters to hydrophilic drugs, to further validate findings it should be trialed for the delivery of other hydrophilic drugs. It should be noted that the introduction of aldehydes may also render the system suitable for hydrophobic drugs as well and warrants further investigation.

REFERENCES

Ahmad, S., Tester, A. and Corbett A.,2006. Dextran and 5-aminosalicylic acid (5-ASA) conjugates: synthesis, characterisation and enzymic hydrolysis. *Carbohydrate Research*, 341(16), pp.2694–701.

Alves, C.M., Yang, Y., Carnes D.L., and Ong J.L., 2007. Modulating bone cells response onto starch-based biomaterials by surface plasma treatment and protein adsorption. *Biomaterials*, 28(2), pp.307–15.

Amass, W., Amass, A. and Tighe, B., 1998. A review of biodegradable polymers: uses, current developments in the synthesis and characterization of biodegradable polyesters, blends of biodegradable polymers and recent advances in biodegradation studies. *Polymer International*, 47(2), pp.89–144.

Assaad, E. *et al.*, 2011. Polyelectrolyte complex of carboxymethyl starch and chitosan as drug carrier for oral administration. *Carbohydrate Polymers*, 84(4), pp.1399–1407. Available at:

Assaad, E. and Mateescu, M.A., 2010. The influence of protonation ratio on properties of carboxymethyl starch excipient at various substitution degrees: Structural insights and drug release kinetics. *International Journal of Pharmaceutics*, 394(1-2), pp.75–84.

Balachandran, M., Devanathan, S., Muraleekrishnan, R., and Bhagawan, S.S., 2012. Optimizing properties of nanoclay–nitrile rubber (NBR) composites using Face Centred Central Composite Design. *Materials and Design*, 35, pp.854–862.

Balakrishnan, B. and Jayakrishnan, a, 2005. Self-cross-linking biopolymers as injectable in situ forming biodegradable scaffolds. *Biomaterials*, 26(18), pp.3941–51.

Basawaraj, P. and Feb, I., 2011. Comparative Evaluation of Tapioca Sago and Potato Page. *International Research Journal of Pharmacy*, 2(2), pp.134–140.

Bayazeed, A., Farag, S. and Shaarawy, S., 1998. Chemical Modification of Starch via Etherification with Methyl Methacrylate. *Starch - Stärke*, 32(2), pp.89–93.

Beneke, C.E., Viljoen, A.M. and Hamman, J.H., 2009. Polymeric plant-derived excipients in drug delivery. *Molecules*, 14(7), pp.2602–20.

Besheer, A. Hause, G., Kressler, J. and Mäder, K., 2007. Hydrophobically modified hydroxyethyl starch: synthesis, characterization, and aqueous self-assembly into nano-sized polymeric micelles and vesicles. *Biomacromolecules*, 8(2), pp.359–67.

Binh, D. et al., 2012. A study on size effect of carboxymethyl starch nanogel crosslinked by electron beam radiation. *Radiation Physics and Chemistry*, 81(7), pp.906–912.

Carbinatto, F.M. et al., 2012. Physical properties of pectin-high amylose starch mixtures cross-linked with sodium trimetaphosphate. *International Journal of Pharmaceutics*, 423(2), pp.281–8.

Carvalho, A., Curvelo, A. and Gandini, A., 2005. Surface chemical modification of thermoplastic starch: reactions with isocyanates, epoxy functions and stearoyl chloride. *Industrial Crops and Products*, 21(3), pp.331–336.

Chakraborty, S. Sahoo, B., Teraoka, I., Miller, L. M. and Gross, R.A.., 2005. Enzyme-Catalyzed Regioselective Modification of Starch Nanoparticles. *Macromolecules*, 38(1), pp.61–68.

Chen, L. Li, Xi.Li, L. and Guo, S. 2007. Acetylated starch-based biodegradable materials with potential biomedical applications as drug delivery systems. *Current Applied Physics*, 7, pp. 90–e93.

Chen, R., Ho, H., Yu, C. and Sheu, M., 2010. Development of swelling / floating gastroretentive drug delivery system based on a combination of hydroxyethyl cellulose and sodium carboxymethyl cellulose for Losartan and its clinical relevance in healthy volunteers. *European Journal of Pharmaceutical Sciences*, 39, pp.82–89.

Chen, Y. and Wang, G., 2006. Adsorption properties of oxidized carboxymethyl starch and cross-linked carboxymethyl starch for calcium ion. *Colloids and Surfaces*, 289, pp.75–83.

Cunha, A.G. and Gandini, A., 2010. Turning polysaccharides into hydrophobic materials: a critical review. Part 2. Hemicelluloses, chitin/chitosan, starch, pectin and alginates. *Cellulose*, 17(6), pp.1045–1065.

Cyras, V.P. et al., 2008. Physical and mechanical properties of thermoplastic starch/montmorillonite nanocomposite films. *Carbohydrate Polymers*, 73(1), pp.55–63.

Deacon, M.P. et al., 1999. Are chitosan–mucin interactions specific to different regions of the stomach? Velocity ultracentrifugation offers a clue. *Carbohydrate Polymers*, 38(3), pp.235–238.

Delisle, B., Calinescu, C., Mateescu, M., Fairbrother, J., and Nadeau, Éric 2012. Oral immunization with F4 fimbriae and CpG formulated with Carboxymethyl Starch enhances F4-specific mucosal immune response and modulates Th1 and Th2 cytokines in weaned pigs. *Journal of Pharmacy and Pharmaceutical Sciences*, 15(5), pp.642–656.

Demirgo, È., Elvira, C., Cunha, A., Piskin, E. and Reis, R., 2000. Chemical modification of starch based biodegradable polymeric blends: effects on water uptake, degradation behavior and mechanical properties. *Polymer Degradation and Stability*, 70, pp.161–170.

Dimantov, A., Greenberg, M., Kesselman, E. and Shimoni, E., 2004. Study of high amylose corn starch as food grade enteric coating in a microcapsule model system. *Innovative Food Science and Emerging Technologies*, 5(1), pp.93–100.

Dragan, E.S. and Apopei, D.F., 2011. Synthesis and swelling behavior of pH-sensitive semi-interpenetrating polymer network composite hydrogels based on native and modified potatoes starch as potential sorbent for cationic dyes. *Chemical Engineering Journal*, 178, pp.252–263

Dufresne, A., 2010. Processing of polymer nanocomposites reinforced with polysaccharide nanocrystals. *Molecules (Basel, Switzerland)*, 15(6), pp.4111–28.

Elfstrand, L., Eliasson, A., Jönsson, M. and Larsson, M., 2007. Recrystallization of waxy maize starch during manufacturing of starch microspheres for drug delivery: Influence of excipients. *Carbohydrate Polymers*, 69(4), pp.732–741.

Elomaa, M., 2004. Determination of the degree of substitution of acetylated starch by hydrolysis, 1H NMR and TGA/IR. *Carbohydrate Polymers*, 57(3), pp.261–267.

El-sherbiny, I.M., 2010. Enhanced pH-responsive carrier system based on alginate and chemically modified carboxymethyl chitosan for oral delivery of protein drugs: Preparation and in-vitro assessment. *Carbohydrate Polymers*, 80(4), pp.1125–1136.

Fahmy, T.M., Samstein, R., Harness, C. and Saltzman, W., 2005. Surface modification of biodegradable polyesters with fatty acid conjugates for improved drug targeting. *Biomaterials*, 26(28), pp.5727–36.

Fang, Y., Wang, L., Li, D., Li, B., Bhandari, B. and Mao, Z., 2008. Preparation of crosslinked starch microspheres and their drug loading and releasing properties. *Carbohydrate Polymers*, 74(3), pp.379–384.

Fukuoka, M., Ohta, K. and Watanabe, H., 2002. Determination of the terminal extent of starch gelatinization in a limited water system by DSC. *Journal of Food Engineering*, 53(1), pp.39–42.

Gao, C., Liu, M., Chen, S., Jin, S. and Chen, J., 2009. Preparation of oxidized sodium alginate-graft-poly ((2-dimethylamino) ethyl methacrylate) gel beads and in vitro controlled release behavior of BSA. *International Journal of Pharmaceutics*, 371(1-2), pp.16–24.

Gao, M. Gao, Mingyuan Kirstein, S., Mo, H., Chaussee, R., Berlin, D. and Rogach, A., Kornowski, A.,1998. Strongly Photoluminescent CdTe Nanocrystals by Proper Surface Modification. *Journal of Physical Chemistry B*, 5, pp.8360–8363.

Grove, M., Müllertz, A., Pedersen, G. and Nielsen, J., 2007. Bioavailability of seocalcitol III. Administration of lipid-based formulations to minipigs in the fasted and fed state. *European Journal of Pharmaceutical Sciences*, 31(1), pp.8–15.

He, P., Davis, S.S. and Illum, L., 1998. In vitro evaluation of the mucoadhesive properties of chitosan microspheres. *International Journal of Pharmaceutics*, 166, pp.75–88.

Hebeish, A., El-Rafie, M., El-Sisi, F., Abdel Hafiz, S., and Abdel-Rahman, A., 1994. Oxidation of maize and rice starches using potassium permanganate with various reductants. *Polymer Degradation and Stability*, 43(3), pp.363–371.

Heinze, T. and Koschella, A., 2005. Carboxymethyl Ethers of Cellulose and Starch - A Review. *Macromolecular Symposia*, 223(1), pp.13–40.

Heinze, T., Liebert, T., Heinze, U., Schwikal, K. and Jena, D., 2004. Starch derivatives of high degree of functionalization 9: carboxymethyl starches. *Cellulose*, 11, pp.239–245.

Hennink, W.E. and van Nostrum, C.F., 2012. Novel crosslinking methods to design hydrogels. *Advanced Drug Delivery Reviews*, 54.

Horchani, H., Chaâbouni, M., Gargouri, Y. and Sayari, A., 2010. Solvent-free lipase-catalyzed synthesis of long-chain starch esters using microwave heating: Optimization by response surface methodology. *Carbohydrate Polymers*, 79(2), pp.466–474.

Huang, X., Brazel, C.S., 2001. On the importance and mechanisms of burst release in matrix-controlled drug delivery systems. *Journal of Controlled Release*, 73, pp.121–136.

Huang, Y., Ding, S., Liu, M., Gao, C., Yang, J., Zhang, X. and Ding, Bin., 2013. Ultra-small and anionic starch nanospheres: formation and vitro thrombolytic behavior study. *Carbohydrate Polymers*, 96(2), pp.426–34.

Jacobs, H. and Delcour, J. a., 1998. Hydrothermal Modifications of Granular Starch, with Retention of the Granular Structure: A Review. *Journal of Agricultural and Food Chemistry*, 46(8), pp.2895–2905.

Jain, R., Dandekar, P., Loretz, B., Melero, A., Stauner, T. and Wenz, G., 2011. Enhanced cellular delivery of idarubicin by surface modification of propyl starch nanoparticles employing pteroic acid conjugated polyvinyl alcohol. *International Journal of Pharmaceutics*, 420(1), pp.147–55.

Jamzad, S., Tutunji, L. and Fassihi, R., 2005. Analysis of macromolecular changes and drug release from hydrophilic matrix systems. *International Journal of Pharmaceutics*, 292(1-2), pp.75–85.

Jeon, Y., Korea, I., Viswanathan, A., and Gross, R., 1999. Studies of Starch Esterification : Reactions with Alkenyl- succinates in Aqueous Slurry Systems. *Starch*, 51, pp.90–93.

Jeske, H., Schirp, A. and Cornelius, F., 2012. Development of a thermogravimetric analysis (TGA) method for quantitative analysis of wood flour and polypropylene in wood plastic composites (WPC). *Thermochimica Acta*, 543, pp.165–171.

Ju, B., Yan, D. and Zhang, S., 2012. Micelles self-assembled from thermoresponsive 2-hydroxy-3-butoxypropyl starches for drug delivery. *Carbohydrate Polymers*, 87(2), pp.1404–1409.

Kaiser, G.M., Heuer, M.M, Frühauf, N.R., Kühne, C.A and Broelsch, C.E., 2006. General handling and anesthesia for experimental surgery in pigs. *The Journal of Surgical Research*, 130(1), pp.73–79.

Karim A.A., Norziah, M H. and Seow, C.C., 2008. Dual Modification of Starch via Partial Enzymatic Hydroxypropylation. *Journal of Agricultural and Food Chemistry*, 56(1), 10901–10907.

Kato, Y., Onishi, H. and Machida, Y., 2003. Application of chitin and chitosan derivatives in the pharmaceutical field. *Current Pharmaceutical Biotechnology*, 4(5), pp.303–9.

Kaur, H., Ahuja, M., Kumar, S. and Dilbaghi, N., 2012. International Journal of Biological Macromolecules Carboxymethyl tamarind kernel polysaccharide nanoparticles for ophthalmic drug delivery. *Biological Macromolecules*, 50(3), pp.833–839.

Kenawy, E., Kamoun, E., Mohy Eldin., M. and El-Meligy, M., 2013. Physically crosslinked poly(vinyl alcohol)-hydroxyethyl starch blend hydrogel membranes: Synthesis and characterization for biomedical applications. *Arabian Journal of Chemistry*.

Khan, F. and Ahmad, S.R., 2013. Polysaccharides and their derivatives for versatile tissue engineering application. *Macromolecular Bioscience*, 13(4), pp.395–421.

Kim, B. and Lim, S., 1999. Removal of heavy metal ions from water by cross-linked carboxymethyl corn starch. *Carbohydrate Polymers*, 39(3), pp.217–223.

Kim, P., Olmstead, M., Nantz, M. and Kurth, M., 2000. Knoevenagel condensations of β-hemiacetyl esters. *Tetrahedron Letters*, 41(21), pp.4029–4032.

Kittipongpatana, O.S. and Kittipongpatana, N., 2013. Physicochemical, in vitro digestibility and functional properties of carboxymethyl rice starch cross-linked with epichlorohydrin. *Food Chemistry*, 141(2), pp.1438–44.

Kosan, B.,Meister, F.,Liebert, T. and Heinze, T.,2006. Hydrophobic modification of starch via grafting with an oxazoline-derivative. *Cellulose*, 13(1), pp.105–113.

Kumar, M.N., 2000. Nano and microparticles as controlled drug delivery devices. *Journal of Pharmacy and Pharmaceutical Sciences*, 3(2), pp.234–58.

Labet, M., Thielemans, W. and Dufresne, A., 2007. Polymer grafting onto starch nanocrystals. *Biomacromolecules*, 8(9), pp.2916–27.

Lawal, O.S., Storz, J., Storz, H., Lohmann, D., Lechner, D. and Kulicke, W.,2009. Hydrogels based on carboxymethyl cassava starch cross-linked with di- or polyfunctional carboxylic acids: Synthesis, water absorbent behavior and rheological characterizations. *European Polymer Journal*, 45(12), pp.3399–3408.

LeCorre, D., Bras, J. and Dufresne, A., 2012. Influence of native starch's properties on starch nanocrystals thermal properties. *Carbohydrate Polymers*, 87(1), pp.658–666.

Lee, S., Kim, S., Pant, B., Kwen, H., Song, H. and Lee, S., 2010. Carboxymethylation of corn starch and characterization using asymmetrical flow field-flow fractionation coupled with multiangle light scattering. *Journal of Chromatography. A*, 1217(27), pp.4623–4628.

Lemieux, M., Gosselin, P. and Mateescu, M.A., 2010. Influence of drying procedure and of low degree of substitution on the structural and drug release properties of carboxymethyl starch. *PharmSciTech*, 11(2), pp.775–85.

Li, C., Sun, P. and Yang, C., 2012. Emulsion stabilized by starch nanocrystals. *Starch – Stärke.*, pp. 497-502

Li, J. and Vasanthan, T., 2003. Hypochlorite oxidation of field pea starch and its suitability for noodle making using an extrusion cooker. *Food Research International*, 36(4), pp.381–386.

Li, J. and Vasanthan, T., 2003. Hypochlorite oxidation of field pea starch and its suitability for noodle making using an extrusion cooker. *Food Research International*, 36(4), pp.381–386.

Li, Y., Kadam, S., Abee, T., Slaghek, T., Timmermans, J., Cohen Stuart, M., Norde, W. and Kleijn, M., 2012. Antimicrobial lysozyme-containing starch microgel to target and inhibit amylase-producing microorganisms. *Food Hydrocolloids*, 28(1), pp.28–35.

Lin, N., Huang, J. and Dufresne, A., 2012. Preparation, properties and applications of polysaccharide nanocrystals in advanced functional nanomaterials: a review. *Nanoscale*, 4(11), pp.3274–94.

Liu, S. and Sun, G., 2008. Radical graft functional modification of cellulose with allyl monomers: Chemistry and structure characterization. *Carbohydrate Polymers*, 71(4), pp.614–625.

Lou, Y., Zheng, J., Wang, B., and Zhang, X., 2014. Metabolites characterization of chamaechromone in vivo and in vitro by using ultra-performance liquid chromatography/Xevo G2 quadrupole time-of-flight tandem mass spectrometry. *Journal of Ethnopharmacology*, 151(1), pp.242–52.

Mahkam, M., 2010. Starch-based polymeric carriers for oral-insulin delivery. *Journal of Biomedical Materials Research*, 92(4), pp.1392–7.

Malafaya, P. B, Elvira C., Gallardo A., 2001. Porous starch-based drug delivery systems processed by a microwave route. *Journal of Biomaterials Science*, 12(11), pp.1227–1241.

Molina-boisseau, S., Belgacem, M.N. and Dufresne, A., 2005. Surface Chemical Modification of Waxy Maize Starch. *Langmuir*, (22), pp.2425–2433.

Montazer, M., Alimohammadi, F., Shamei, A., Rahimi, M.K., 2012. In situ synthesis of nano silver on cotton using Tollens' reagent. *Carbohydrate Polymers*, 87(2), pp.1706–1712.

Mulhbacher, J., Ispas-Szabo, P. and Mateescu, M.A., 2004. Cross-linked high amylose starch derivatives for drug release. II. Swelling properties and mechanistic study. *International Journal of Pharmaceutics*, 278(2), pp.231–8.

Muljana M., Henky, P., Francesco, H., Hero J., Janssen, L., 2010. Green starch conversions: Studies on starch acetylation in densified CO2. *Carbohydrate Polymers*, 82(3), pp.653–662.

Nabais, T., Brouillet, F., Kyriacos, S., Mroueh, M., Amores da Silva, P., Bataille and Cartilier, L., 2007. High-amylose carboxymethyl starch matrices for oral sustained drug-release: in vitro and in vivo evaluation. *European Journal of Pharmaceutics and Biopharmaceutics*, 65(3), pp.371–8.

Namazi, H. and Dadkhah, A., 2010. Convenient method for preparation of hydrophobically modified starch nanocrystals with using fatty acids. *Carbohydrate Polymers*, 79(3), pp.731–737.

Nayak, A.K., Maji, R. and Das, B., 2010. Gastroretentive drug delivery systems: A review. *Asian Journal of Pharmaceutical and Clinical Research*, 3(1), pp.2–10.

Onishi, H. and Nagai, T., 1986. Characterization and evaluation of dialdehyde starch as an erodible medical polymer and a drug carrier. *International Journal of Pharmaceutics*, 30(2-3), pp.133–141.

Onofre, F., Wang, Y.-J. and Mauromoustakos, A., 2009. Effects of structure and modification on sustained release properties of starches. *Carbohydrate Polymers*, 76(4), pp.541–547.

Onofre, F.O. and Wang, Y.-J., 2010. Hydroxypropylated starches of varying amylose contents as sustained release matrices in tablets. *International journal of Pharmaceutics*, 385(1-2), pp.104–12.

Pabari, R.M. and Ramtoola, Z., 2012. Application of face centred central composite design to optimise compression force and tablet diameter for the formulation of mechanically strong and fast disintegrating orodispersible tablets. *International Journal of Pharmaceutics*, 430(1-2), pp.18–25

Pal, J., Singhal, R.S. and Kulkarni, P.R., 2002. Physicochemical properties of hydroxypropyl derivative from corn and amaranth starch. *Carbohydrate Polymers*, 48, pp.1–5.

Pashkuleva, I., Marques, A.P., Vaz, F. and Reis, R.L., 2010. Surface modification of starch based biomaterials by oxygen plasma or UV-irradiation. *Journal of Materials Science*, 21(1), pp.21–32.

Pashkuleva, I., Azevedo, H.S. and Reis, R.L., 2008. Surface structural investigation of starch-based biomaterials. *Macromolecular Bioscience*, 8(2), pp.210–219

Pashkuleva, I., Marques, A.P., Vaz, F., Reis, R L, 2005. Surface modification of starch based blends using potassium permanganate-nitric acid system and its effect on the adhesion and proliferation of osteoblast-like cells. *Journal of Materials Science*, 16(1), pp.81–92.

Phillips, E. and Blazey, S., 1991. Quantitative thermogravimetric analysis of starch contents in several polymer systems. *Thermochimica Acta*, 192, pp.191–197.

Pohja, S. et al., 2004. Starch acetate as a tablet matrix for sustained drug release. *Journal of Controlled Release*, 94(2-3), pp.293–302.

Pongstabodee, S., Monyanon, S. and Luengnaruemitchai, A., 2012. Applying a face-centered central composite design to optimize the preferential CO oxidation over a PtAu/CeO2–ZnO catalyst. *International Journal of Hydrogen Energy*, 37(6), pp.4749–4761.

Prabaharan, M. and Gong, S., 2008. Novel thiolated carboxymethyl chitosan-g-β-cyclodextrin as mucoadhesive hydrophobic drug delivery carriers. *Carbohydrate Polymers*, 73(1), pp.117–125.

Pradhan, G.C., Dash, S. and Swain, S.K., 2014. Effect of zirconium oxide nanopowder on the thermal, chemical and gas barrier properties of starch. *Materials Science in Semiconductor Processing*, 23, pp.115–121.

Prisant, L.M. and Elliott, W.J., 2003. Drug delivery systems for treatment of systemic hypertension. *Clinical Pharmacokinetics*, 42(11), pp.931–40.

Pu, H., Chen, L., Li, X., Xie, F., Yu, L., and Li, L.., 2011. An oral colon-targeting controlled release system based on resistant starch acetate: synthetization, characterization, and

preparation of film-coating pellets. *Journal of Agricultural and Food Chemistry*, 59(10), pp.5738–45.

Raatikainen, P., Korhonen, O., Peltonen, S. and Parone, P., 2002. Acetylation enhances the tabletting properties of starch. *Drug Development and Industrial Pharmacy*, 28(2), pp.165–75.

Rajan, A., Prasad, V.S. and Abraham, T.E., 2006. Enzymatic esterification of starch using recovered coconut oil. *International Journal of Biological Macromolecules*, 39(4-5), pp.265–72.

Ražem, D. and Katušin-Ražem, B., 2008. The effects of irradiation on controlled drug delivery/controlled drug release systems. *Radiation Physics and Chemistry*, 77(3), pp.288–344.

Rinaudo, M., 2010. Periodate Oxidation of Methylcellulose: Characterization and Properties of Oxidized Derivatives. *Polymers*, 2(4), pp.505–521.

Sánchez-Rivera, M., García-Suárez, F., Velázquez del Valle, M., Gutierrez-Meraz, F. and Bello-Pérez, L., 2005. Partial characterization of banana starches oxidized by different levels of sodium hypochlorite. *Carbohydrate Polymers*, 62(1), pp.50–56.

Sangseethong, K., Ketsilp, S. and Sriroth, K., 2005. The Role of Reaction Parameters on the Preparation and Properties of Carboxymethyl Cassava Starch. *Starch - St*[illegible]*Rke*, 57(2), pp.84–93.

Sangseethong, K., Termvejsayanon, N. and Sriroth, K., 2010. Characterization of physicochemical properties of hypochlorite- and peroxide-oxidized cassava starches. *Carbohydrate Polymers*, 82(2), pp.446–453.

Sangsuk, S., 2010. Preparation of high surface area silver powder via Tollens process under sonication. *Materials Letters*, 64(6), pp.775–777.

Shalviri, A., Liu, Q., Abdekhodaie, M. and Wu, X., 2010. Novel modified starch–xanthan gum hydrogels for controlled drug delivery: Synthesis and characterization. *Carbohydrate Polymers*, 79(4), pp.898–907.

Shirwaikar, A., Prabu, S. and Kumar, G.,et al., 2008. Herbal excipients in novel drug delivery systems. *Indian journal of Pharmaceutical Sciences*, 70(4), pp.415–22.

Singh, J., Kaur, L. and McCarthy, O.J., 2007. Factors influencing the physico-chemical, morphological, thermal and rheological properties of some chemically modified starches for food applications—A review. *Food Hydrocolloids*, 21(1), pp.1–22.

Sosnik, A., das Neves, J. and Sarmento, B., 2014. Mucoadhesive polymers in the design of nano-drug delivery systems for administration by non-parenteral routes: A review. *Progress in Polymer Science*, 39(12), pp.2030–2075.

Sui, Z. and BeMiller, J.N., 2013. Relationship of the channels of normal maize starch to the properties of its modified products. *Carbohydrate Polymers*, 92(1), pp.894–904.

Te Wierik G., Eissens, A., Bergsma, J., Arends-Scholte, A. and Bolhuis, G., 1997. A new generation starch product as excipient in pharmaceutical tablets. III. Parameters affecting controlled drug release from tablets based on high surface area retrograded pregelatinized potato starch. *InternationalJjournal of Pharmaceutics*, 157(2), pp.181–187.

Thakur, K., Ahuja, M. and Kumar, A., 2013. Carboxymethyl functionalization of amylopectin and its evaluation as a nanometric drug carrier. *International Journal of Biological Macromolecules*, 62, pp.25–9.

Tharanathan, R.N., 2005. Starch--value addition by modification. *Critical Reviews in Food Science and Nutrition*, 45(5), pp.371–84.

Thielemans, W., Belgacem, M.N. and Dufresne, A., 2006. Starch nanocrystals with large chain surface modifications. *Langmuir*, 22(10), pp.4804–10.

Tuovinen, L., Peltonen, S. and Järvinen, K., 2004. Drug release from starch-acetate microparticles and films with and without incorporated alpha-amylase. *Biomaterials*, 25(18), pp.4355–62.

Tuovinen, L., Peltonen, S. and Järvinen, K., 2003. Drug release from starch-acetate films. *Journal of Controlled Release*, 91(3), pp.345–54.

Venkatesh, G., Ramanathan, S., Mansor, S. M., Nair, N., Sattar, Munavvar and Croft, S., 2007. Development and validation of RP-HPLC-UV method for simultaneous determination of buparvaquone, atenolol, propranolol, quinidine and verapamil: A tool for the standardization of rat in situ intestinal permeability studies. *Journal of Pharmaceutical and Biomedical Analysis*, 43(4), pp.1546–1551.

Vieira, A., Ferreira, P., Coelho, J. and Gil, M., 2008. Photocrosslinkable starch-based polymers for ophthalmologic drug delivery. *International Journal of Biological Macromolecules*, 43(4), pp.325–32.

Wang, J., Zhai, W. and Zheng, W., 2011. Preparation of granular cold-water-soluble corn starch by surface modification with poly(ethylene glycol). *Starch - Stärke*, 63(10), pp.625–631.

Wang, S., Cui, W. and Bei, J., 2005. Bulk and surface modifications of polylactide. *Analytical and Bioanalytical Chemistry*, 381(3), pp.547–56.

Wang, Y.J. et al., 2011. NMR imaging of chitosan and carboxymethyl starch tablets: swelling and hydration of the polyelectrolyte complex. *International Journal of Pharmaceutics*, 419(1-2), pp.215–21.

Wang, Y.-J. and Wang, L., 2003. Physicochemical properties of common and waxy corn starches oxidized by different levels of sodium hypochlorite. *Carbohydrate Polymers*, 52(3), pp.207–217.

Weerapol, Y., Limmatvapirat, S., Jansakul, C.,Takeuchi, H. and Sriamornsak P., 2015. Enhanced dissolution and oral bioavailability of nifedipine by spontaneous emulsifying

powders: Effect of solid carriers and dietary state. *European Journal of Pharmaceutics and Biopharmaceutics*, 91, pp.25–34.

Wolf, B.W., Bauer, L.L. and Fahey, G.C., 1999. Effects of chemical modification on in vitro rate and extent of food starch digestion: an attempt to discover a slowly digested starch. *Journal of Agricultural and Food Chemistry*, 47(10), pp.4178–83.

Xiao, C., 2012. Current advances of chemical and physical starch-based hydrogels. *Starch - Stärke*, 00(00), pp.1–7.

Xiao, S., Liu, X., Tong, C., Zhao, L., Liu, X. and Zhou, A., 2012. Dialdehyde starch nanoparticles as antitumor drug delivery system: An in vitro, in vivo, and immunohistological evaluation. *Chinese Science Bulletin*, 57(24), pp.3226–3232.

Yaacob, B., 2011. Optimization of reaction conditions for carboxymethylated sago starch., 20(3), pp.195–204.

Yu, J., Chang, P.R. and Ma, X., 2010. The preparation and properties of dialdehyde starch and thermoplastic dialdehyde starch. *Carbohydrate Polymers*, 79(2), pp.296–300.

Zahirul, M. and Khan, I., 1996. Dissolution testing for sustained or controlled release oral dosage forms and correlation with in vivo data: Challenges and opportunities. *International Journal of Pharmaceutics*, 140(2), pp.131–143.

Zhang, L., Liu, P., Wang, Y. and Gao, W., 2011. Study on physico-chemical properties of dialdehyde yam starch with different aldehyde group contents. *Thermochimica Acta*, 512(1-2), pp.196–201.

Zhang, Y. and Zhang, J., 2008. Optimization of headspace solid-phase microextraction for analysis of ethyl carbamate in alcoholic beverages using a face-centered cube central composite design. *Analytica Chimica Acta*, 627(2), pp.212–8.

Zhang, Y., Wang, X., Zhao, G. and Wang, Y., 2012. Preparation and properties of oxidized starch with high degree of oxidation. *Carbohydrate Polymers*, 87(4), pp.2554–2562.

APPENDIX 1

STRICTLY CONFIDENTIAL

ANIMAL ETHICS SCREENING COMMITTEE (AESC)

CLEARANCE CERTIFICATE NO. 2013/41/05

APPLICANT: Ms N Masina

SCHOOL: Medical School
DEPARTMENT: Pharmacy & Pharmacology
LOCATION: Faculty of Health Sciences

PROJECT TITLE: *In vivo evaluation of food-grade Sago-based oral drug delivery systems in Large White pigs*

Number and Species

5 Pigs

Approval was given for to the use of animals for the project described above at an AESC meeting held on 20 August 2013. This approval remains valid until 19 August 2015.

The use of these animals is subject to AESC guidelines for the use and care of animals, is limited to the procedures described in the application form and is subject to any additional conditions listed below:

None.

Signed: _____ (Chairperson, AESC) Date: 10/9/2013.

I am satisfied that the persons listed in this application are competent to perform the procedures therein, in terms of Section 23 (1) (c) of the Veterinary and Para-Veterinary Professions Act (19 of 1982)

Signed: _____ (Registered Veterinarian) Date: 10/9/2013

cc: Supervisor: Prof V Pillay
Director: CAS

Works 2000/fain0015/AESCCert.wps

APPENDIX 2

A review of the chemical modification techniques of starchNonhlanhla Masina, Yahya E. Choonara, Pradeep Kumar, Lisa C. du Toit,Mershen Govender, Sunaina Indermun, Viness Pillay

Wits Advanced Drug Delivery Platform Research Unit, Department of Pharmacy and Pharmacology, School of Therapeutic Sciences, Faculty of Health Sciences, University of the Witwatersrand, Johannesburg, 7 York Road, Parktown, 2193, South Africa

Abstract

Starch is a naturally occurring storage copolymer with unique physicochemical properties. There are, however, some key structural properties of starch that can be modified in order to functionalize the copolymer to meet specific requirements. Specifically, the chemical modification of starch provides a variety of physicochemical benefits, some of which have been used previously to functionalize preformed drug delivery systems. Of the three main chemical modification methods reviewed (namely: oxidation, esterification and etherification), surface chemical oxidation introduces more pertinent physicochemical properties that increase overall drug delivery system efficacy and applicability. Surface oxidation evidently is the more preferable chemical modification method of pre-formed starch particles and has the greatest potential for further development when compared to the other reviewed chemical modification methods. The use of modified starch in clinical trials as well as the potential future implications of these systems is also included in this review.

APPENDIX 3

PERIODATE OXIDATION OF FOOD-GRADE-PRE-FORMED SAGO BEADS FOR APPLICATION IN DRUG DELIVERY

Nonhlanhla Masina, Yahya E Choonara, Pradeep Kumar, Lisa C du Toit and Viness Pillay
Wits Advanced Drug Delivery Platform Research Unit, Department of Pharmacy and Pharmacology, School of Therapeutic Sciences, Faculty of Health Sciences, University of the Witwatersrand, Johannesburg, 7 York Road, Parktown, 2193, South Africa.

Abstract
This study involved the development and optimization of a surface oxidation method for food-grade Sago starch beads utilizing sodium-meta-periodate ($NaIO_4$) as an oxidizing agent. Resulting derivatives were characterized using a chemical measure of the degree of substitution (DS). Ammoniacal silver nitrate test was used to confirm aldehyde introduction and tested positive on the traditional Tollen's test. The flow properties observed through rheology are indicative of a reduced viscosity and Newtonian flow properties. Fourier Transform Inferred Spectroscopy (FTIR) and Scanning Electron Microscopy (SEM) further confirm altered physicochemical properties. X-ray diffraction (XRD) profiles also confirmed

surface modification resulted in derivatives with more crystalline physicochemical observed in oxidized derivatives. Crystalline profiles of oxidized derivatives with physicochemical techniques confirm the introduction of di-aldehyde groups via the nucleophilic attack by the periodate group as described by Pashkuleva and co-workers in 2005. The reducing ends produced as part of this oxidation method further facilitates crosslinking and thus enabling the development of systems that can have a controlled drug release profile with a potential of functionalization of drug delivery systems post-production. Successful surface modification in such mild reaction conditions render the oxidized derivatives as high potential candidates for application in the delivery of water soluble drugs and can allow for controlled release due to usage of food-grade chitosan as a crosslinking polymer.